MODIFIED MULTI EFFECT DESALINATION SYSTEMS WITH MECHANICAL VAPOR COMPRESSION

BY

SADDAM ELTAYIB AJIB JABER

A Thesis Presented to the
DEANSHIP OF GRADUATE STUDIES

KING FAHD UNIVERSITY OF PETROLEUM & MINERALS

DHAHRAN, SAUDI ARABIA

In Partial Fulfillment of the
Requirements for the Degree of

MASTER OF SCIENCE

In

MECHANICAL ENGINEERING

December 2016

KING FAHD UNIVERSITY OF PETROLEUM & MINERALS

DHAHRAN- 31261, SAUDI ARABIA

DEANSHIP OF GRADUATE STUDIES

This thesis, written by **SADDAM ELTAYIB AJIB JABER** under the direction of his thesis advisor and approved by his thesis committee, has been presented and accepted by the Dean of Graduate Studies, in partial fulfillment of the requirements for the degree of **MASTER OF SCIENCE IN MECHANICAL ENGINEERING.**

Dr. Mohamed A. Antar
(Advisor)

Dr. Zuhair M. Gasem
Department Chairman

Dr. Syed M. Zubair
(Member)

Dr. Salam A. Zummo
Dean of Graduate Studies

Dr. Atia E. khalifa
(Member)

2/2/17
Date

This Work is dedicated to my beloved family

ACKNOWLEDGMENTS

No task of this magnitude is accomplished alone, and therefore I would like to acknowledge all those who helped me succeed. I would like to thank my supervisor Dr. Mohamed A. Antar at Mechanical Engineering Department for his guidance, support and time during different research stages.

My thanks also extend to Dr. Syed M. Zubair, and for his flexibility and advice. Equally, I also would like to thank Dr. Atia E. khalifa.

I am grateful to the Dean and colleagues at the Faculty of Engineering, FKUPM.

In addition, I would like to thank the people supported me outside the academia, my dear parents, Future wife and all my family for their patience, support and understanding throughout my Master life, I will be forever grateful. Allah blesses you all.

TABLE OF CONTENTS

LIST OF TABLES

LIST OF FIGURES

LIST OF ABBREVIATIONS

$\dot{D}$	Distillate flow rate, kg/s
$\dot{B}$	Brine Flow rate, kg/s
X	Brine concentration, ppm
T	Temperature, ^{o}C
$\dot{m}_d$	Total distillate flow rate, kg/s
mv_1	Mass vapor flow rate in first effect, kg/s
mv_n	Mass vapor flow rate in last effect, kg/s
$\dot{Q}$	The thermal load, kW
h_{fg}	The latent heat, kJ/kg
$h_{fg,s}$	The latent heat at T_s, kJ/kg
U	Overall heat transfer coefficient, KJ/s.m^2. ^{o}C
BPE	Boiling point elevation, ^{o}C
c_p	The specific heat at constant pressure, kJ/kg.k
c_v	The specific heat at constant volume, kJ/kg.k
w	Consumed power, kW.h/m^3
w_k	Consumed power for first compressor, kW.h/m^3

w_s Consumed power for second compressor, kW.h/m^3

P Pressure, kPa

S Entropy, kW/k

$S_{gen.i}$ Entropy generation at effect (i) , kW/k

$s_{T_{vi}}$ Specific entropy of the vapor at T_{vi}, kJ/kg.k

s_{T_i} Specific entropy of the liquid at T_i, kJ/kg.k

$s_{T_{fi}}$ Specific entropy of the liquid at T_{fi}, kJ/kg.k

s The specific entropy, kJ/kg.k

w_{rev} Consumed power at $\eta = 1$, kW.h/m^3

xx Extraction

$\dot{D}_f$ Distillate in flashing box

$\dot{D}_{n(i-1)}$ Flow rate of vapor formed by brine flashing inside the effect

Greek symbols

γ The compression ratio

η The compressor efficiency

Subscripts

s Steam

i	Effect
f	Feed
v	Formed vapor
d	Distillate
n	Last effect
cw	Cooling water
b	Brine

ABSTRACT

Full Name : Saddam Eltayib Ajib Jaber

Thesis Title : Modify Multi Effect Desalination Systems with Mechanical Vapor Compression

Major Field : Mechanical Engineering

Date of Degree : [December 2016]

In this thesis, we concentrate on the multi effect desalination system with mechanical vapor compression (MED-MVC). Mechanical vapor compression desalination is a very competitive and attractive technology for medium and small scale water production. Unlike thermal desalination systems that operate with thermal vapor compression, MVC systems have the advantage of being compact and independent of an external steam sources; e.g. a power plant or a boiler. This work presents a mathematical model of forward feed, parallel feed, and parallel cross MED-MVC systems with a secondary, small mechanical compressor that provides improved system performance. In the suction side of the secondary compressor, vapor is extracted from one of the effects' formed vapor flow. Operation of the system is based on a unit product (distillate water) flow rate of 1 kg/s. In the MVC system, the mass and energy balance equations are solved. The system performance is evaluated under different locations of vapor extraction. Results indicate that the specific power consumption and heat transfer area decrease by increasing the rate of vapor extraction. It is also found that the minimum value of the consumed power corresponds to a higher value of vapor extraction that occurs in the effect (n/2). Furthermore, the minimum value of the specific heat transfer area is obtained when a high rate of vapor extraction occurs in the first effect.

ملخص الرسالة

الاسم الكامل: صدام الطيب عاجب جابر

عنوان الرسالة: تعديل تأثير أنظمة تحلية المياة مع ضغط البخار الميكانيكي

التخصص: الهندسة الميكانيكية

تاريخ الدرجة العلمية:ديسمبر 2016

تحلية المياة عن طريق ضغط البخار الميكانيكي هي تقنية جذابة وتنافسية لانتاج كمية صغيرة أو متوسط من المياه الصالحة للشرب. وخلافا لأنظمة التحلية الحرارية للمياه التي تعمل مع ضغط البخار، فإن هذا النظام لدية ميزتين وهما صغر الحجم وعدم الحاجة لوجود مصدر بخار خارجي. وأقدم في هذا البحث نموذج رياضي لمنظومة ذات تغذية أمامية وتغذية موازية، وتغذية عبر موازية لوحدة التحلية متعددة تأثير التقطير وذلك مع اضافة ضاغط ثانوي صغير لتحسين اداء المنظومة. ويستند تشغيل المنظومة علي انتاج وحدة بمعدل تقطير ا كجم/ث. ويتم تقييم أداء النظام في أمكان مختلفة لاستخراج البخار وإمداده للضاغط الثانوي. وتشير النتائج الي أن معدل استهلاك الطاقة ومساحة سطح الأنابيب اللازمة لانتقال الحرارة انخفضا مع زيادة معدل استخراج البخار. وأن الحد الأدني لمعدل أستهلاك الطاقة يحدث عند أعلي استخراج عند وسط المنظومة. وأن الحد الأدني للمساحة اللازمة لانتقال الحرارة يحدث عند أعلي أستخراج عند الأثر الأول.

CHAPTER 1

INTRODUCTION

1.1 Introduction

Desalination of seawater involves dividing a body of salty water into two different components, one of which is salt-free and the other contains high salt concentration (brine). Although in theory, this process requires very little power, in practice it requires considerably more power with regard to actual performance and efficiency of the thermodynamic cycle and rotary machines. Among many methods that have been proposed for desalting seawater, only a few have actually progressed away from the drawing board. On the market, there are two main techniques for desalination seawater: Membrane (Reverse Osmosis, Forward Osmosis and Electro Dialysis) and thermal (multi-stage Flash, Single Effect Evaporation, Freezing, Humidification-Dehumidification, Solar Stills, Multi-Effect (ME) Evaporation, Thermal (VC) or Mechanical Vapor Compression).

The thermal desalination process contains an evaporating and a condensing process. The heat required for evaporation can be partly recovered during the condensing phase. MED desalination is a type of evaporation with many economic and technical advantages and can be regarded presently as providing the best solution to the problem of sea-water desalting.

Seawater accounts for 70% of desalinated water worldwide, i. e., a total of 14 million m^3/day and the remaining 30% being supplied from of brackish water. Thermal desalination process require water heating up to 120 °C in some cases, which can be supplied from solar energy, waste heat or fossil fuels.

1.2 Classification of Desalination Technologies

There are many systems of desalination of seawater that have been tested and developed. Some of these processes have been neglected, due to their uneconomical applications [3]. Currently, desalination processes focus on the following three treatment processes:

(1) Distillation.

(2) Membrane techniques.

(3) Crystallization.

Desalination technologies are categorized based on the phase produced (e. g. remains unchanged: liquid to liquid, liquid to solid, or liquid to vapor). The desalination technologies have been utilized for a long time for seawater desalination purposes. The general concept of the thermal desalination processes is that vapor is produced by heating salty water, generating vapor which is free from minerals. Vapor is then condensed to produce fresh water [2]. The main distillation techniques utilized in the thermal desalination processes are multi stage flash distillation (MSF) and multi effect distillation (MED). Table 1.1 summarizes the pros and cons of several desalination methods.

Table 1.1 Pros & cons of each desalination technique. [2]

Method	Pros	Cons
Multi effect Distillation (MED)	High product purity. The capital cost is lower compared to other techniques. The production is high capacity.	Hard to monitor water quality. Conversion of feed water between (30 – 40%). Long construction period.
Reverse Osmosis (RO)	Appropriate for both brackish and seawater. Simple operation. Flexibility in site location.	High pressure requirements. Requires high quality fed water. Low quality production (250-500 ppm).
Multi stage flash Distillation (MSF)	The production is of high purity. High capacity production. Low skills required for maintenance.	High operating cost. Requires pretreatment of feed water. Low conversion of Feed water.
Vapor Compression (VC)	High water quality. Operation and production flexibility. Small space requirements. High operational load.	The consumed power is high. High operational cost.

1.3 Multiple-Effect Distillation

MED plants are progressively being used when thermal evaporation is favored to membrane separation. The production rate of multi effect distillation (MED) plants is comparatively less than multi stage flash distillation (MSF) plants. MSF has lower power consumption and a superior thermal performance than MED. The problems with scaling on the heat transfer tubes create the drawbacks to MED; however newer plants are designed to limit problems related to scaling by operating at lower temperatures [3].

Similar to MSF, the consecutive chambers used in the MED are run with lower pressure than atmospheric and temperature raising the feed temperature closer to boiling point. A thin film of feed-water is sprayed onto surface of the evaporator tubes in the first chamber. As steam passes, it encourages rapid boiling and evaporation at one part of the tube and condensation on the other. The condensate steam from the boiler is sent back to the boiler for use again. Fresh water is the product of the condensed vapor, which also provides additional heat for vaporization in the next chamber [4].

The MED plant can run at high or low temperatures. Thus an advantage of this process is its ability to reduce the effects of corrosion and scaling by running at low temperatures. However, this raises the requirement for a further heat transfer (H.T) area in the form of tubes and therefore increasing the capital and operating expenditure of the plant [5].

1.4 Developments in Multi effect distillate

The multi-effect desalination system contains a series of single effect desalination units, where the vapor generated in one effect is used in the next effect. The vapor used again in the multi-effect system allows a decrease of the temperature of the brine to minimum values and reduces the energy losses to the surrounding. There are three kinds of the multi effect distillate forward, parallel, or backward.

The multi effect distillate process can be in Forward Feed (FF), Backward Feed (BF), and Parallel Feed (PF); Figure1.1 shows the difference in the flow directions of the evaporating brine, the heating steam, and the distillate flow rate for each one of them.

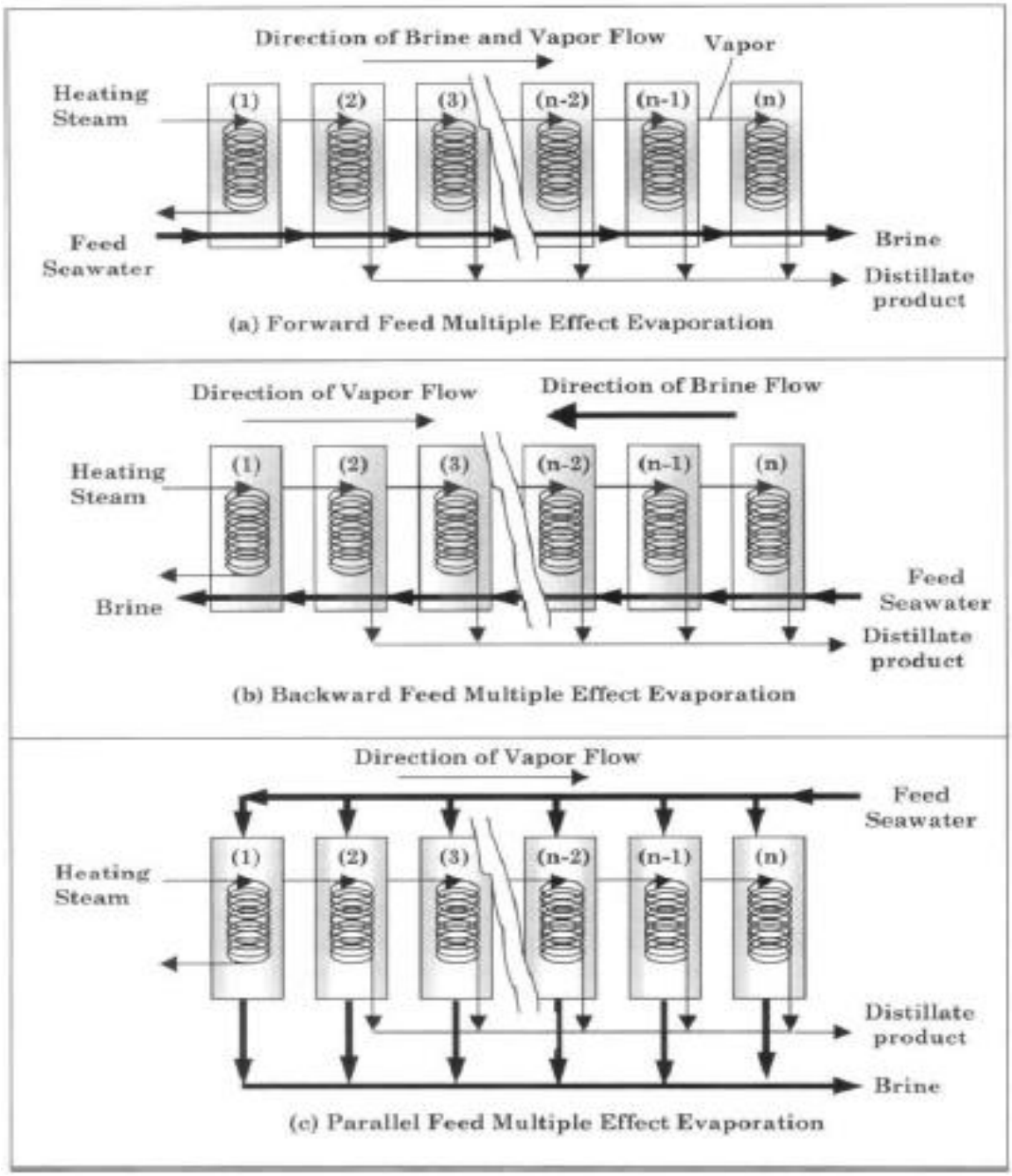

Figure 1.1 Multi-effect distillate (a) Forward Feed (FF) (b) Backward Feed (BF) (c) Parallel Feed (PF) [4].

1.5 Objectives

Based on the previous studies and literature, no studies are available in the open literatures that have investigated the effect of extracting a certain amount of formed vapor from an effect other than the last effect. Accordingly, the objectives of this work are to:

- To develop a model to simulate the MED-MVC system performance. To be accurate and using recent seawater properties in literature.
- To modify the existing layout of MED-MVC by adding a secondary compressor that extracts vapor at various locations and study its effect on performance improvement.
- To estimate the performance through evaluating

    1- The specific power consumption.

    2- The specific heat transfer area.

    3- The entropy generation.
- To compare the perfect of MED-MVC systems with extraction, for Forward Feed, parallel and parallel cross flow.

CHAPTER 2

LITERATURE REVIEW

2.1 Literature review

2.1.1 Single effect MVC

MVC units are likely to be used where cooling water and low-cost steam are expensive or complex to use. This is the reason why the process primarily used in small and medium scale water desalination plants [4]. Hamed et al. [6] study was focused on exergy analysis for MVC and TVC desalination systems for a system made of four effects, based on the second law of thermodynamic. It was found the TVC system is more efficient than MVC system. Al-Juwayhel et al. [7] studied and analyzed single-effect desalination systems with vapor compression, both thermal (TVC), and mechanical (MVC). The analysis was based on comparison of the performance ratio (PR) and the consumed power (w). It was found that the PR for TVC system increased as the pressure of motive steam and boiling temperature decreased. In MVC system, the power (w) increases with the decrease of boiling temperature. Aybar [8] developed a mathematical model for MVC at low temperature with the tube length of 9 m, and the tube diameter of 0.025m.The MVC system includes a compressor, evaporators, condenser, and heat exchangers. It was found that the consumed power is 11.47 kWh/t of water with the tube length equal to 9m. Aly et al. [9] studied theoretically and experimentally the MVC systems to investigate the effect of evaporator temperature on the performance. Both theoretical and experimental results showed that the rate of production depends on the operating temperature. MVC system includes evaporator, heat exchanger, compressor, pumps. It was also found that

the evaporator temperature should be increased to get a higher heat transfer coefficient. El-Khatib et al. [10] investigated multi-output, multi-input control of a single effect desalination with MVC with two controls (one for distillate while the other is for evaporation temperature). The (MVC) system includes compressor, evaporator/condenser heat exchanger, preheater, pumps, venting system. It was developed to characterize the dynamics of a vapor compression (VC) desalination system by using the Matlab program. The PID controllers for evaporation and distillate temperature were developed to attain good performance. Ettouney [11] studied design model of the SED-MVC processes. The main features included in this study were all major element dimensions. He discussed the performance as a function of the length of the evaporator tube, distillate flow rate, and brine boiling temperature. The MVC system includes the evaporator/condenser, mechanical compressor, non-condensable gases ejector, preheater, pumps, and venting system. It was found that the diameter of the evaporator, the difference in temperature between the boiling brine and saturated compressed vapor, evaporator tube length, and the brine boiling temperature are the main parameters. It was also found that both of the demister width and tube length are a function of the distillate flow rate and brine boiling temperature. Mussat et al. [12] developed a mathematical model for the optimal design of single effect mechanical vapor compression (SE-MVC) desalination, by using general algebraic modeling systems (GAMS) and NLP solver. The model included real-physical constraints for the evaporation process. MVC system includes mechanical vapor compressor, evaporators, condenser, preheaters, and pumps. Results showed that the consumed power as well as the streams flow rate rise with the water demands and the consumed power decrease as the brine flow-rate decreases. It was also found that the total

cost of the system depends on fresh water demands. Marian et al. [14] developed a mathematical model for the optimal design of single effect mechanical vapor compression desalination to minimize the consumed power in order to fulfill the given fresh water demand, by using the ME-D algorithm developed earlier by M. Marcovecchio [13]. The model includes real physical constraints for the evaporation process. The obtained results show that the consumed power as well as the streams flow rate increase with the sweet water demands. Alasfour al. [15] theoretically studied the effect of stage temperature drop on MED-MVC. Result showed the consumed power decreases as MVC brine temperature increase, and volume flow rate is decreased as MVC brine temperature increase. The brine temperature increases, the ratio between Feed to distillate (F/D) decrease, and the MVC effect temperature drop decrease. Han et al. [16] developed a mathematical model to study zero-emission desalination systems, including single effect and the multi-effect systems, based on the technology of mechanical vapor compression (ZED-MVC). The suggested desalination system is possible when the final seawater concentration exceeds 25% to realize the objective of zero-emission. It was found that the compressor power consumption of the (ZED-MVC) system increases with the rise of the seawater concentration because of the increase in boiling point elevation BPE.

2.1.2 MED-MVC

MED plants are progressively being used when thermal evaporation is favored to membrane separation. This is because multi-effect distillation (MED) plants consume comparatively less energy than multi-stage flash distillation (MSF) plants. The problems with scaling on the heat transfer tubes create a drawback to MED. Thus, newer plants are

designed to limit problems related to scaling by operating at low top brine temperature, TBT of 65^{o}C [1]. Madani [17] studied desalination process from an economical point of view for different plant sizes, 100 m^3/d (small capacity), between 100 – 200 m^3/d (medium capacity) and above 200 m^3/d (large capacity). It was found that the MVC system is the most economical for medium capacity, and MSF is the most economical for large capacity. El-Dessouky et al. [18] theoretically studied the MED-MVC Parallel and Parallel cross feed. Results showed the consumed power for MED-MVC parallel cross is lower than MED-MVC parallel feed, and the specific heat transfer area for MED-MVC parallel cross is lower than MED-MVC parallel feed. Kronenberg et al. [19] developed a MED-MVC desalination process for single-dual purpose plants (electricity & water production) at low temperature. It was found The main factor in increasing MVC capacities is by develop compressors with higher head and volumetric flow, and increasing the number of evaporators that would also provide more specific heat transfer area and reduce the average mean effective BPE in the plant. Another experiment was conducted by Bahar et al. [20]. This experiment used two effect (MVC) unit to evaluate performance under difference operating conditions (compressor speed and feed recirculation rate). Results showed that the brine concentration rate affects the distillate flow rate. It has minor effect on the performance ratio. It was also found that compressor speed affects distillate and performance ratio. Al-Sahali et al. [21] studied the MVC distillate, and compared the process with MSF; the unit cost for MSF system is similar to MED. It was found the MED-MVC desalination is process highly competitive to the MSF. Ophir et al. [22] studied the MED with turbo-compressor at low temperature. Thermo-compressor of lower efficiency than a compressor and auxiliary turbine results in

considerable energy savings, thus lowering the desalination costs. Cardona et al. [23] studied the performance evaluation of thermal desalination system (MED-SWRO) using a reciprocated engine with heat recovery, which supplies power and heat for a RO and MED units. The (MED-SWRO) system was simulated and the environmental, energetic and economical results calculated and compared with parallel RO system. Producing the same freshwater flow rate, 30% decrease in CO_2 emissions and 8% decrease in unit cost of freshwater were reported. Mabrouk et al. [24] analyzed a new design of a multi-stage flash - mechanical vapor compression (MSF-MVC) desalination process base on exergy, energy, and thermo-economic methodologies. The (MSF-MVC) system was investigated by using a developed design and simulation software. It was compared with MSF desalination process. Results showed that the best TBT is 110^{o} C and the perfect operating suction pressure for the compressor is 8kPa. It was also found that performance ratio (PR) for MSF-MED was equal 2.4 times the PR for MSF system. The exergetic efficiency for MSF system was lower than MSF-MVC system, and the unit product cost of system is 25% less than MSF system.

Lara et al. [25] studied a MVC system operating at 172^{o}C, and investigated the pros of MED at high operating temperature: latent heat transfer area is small and low compression work. They used a small compressor to reduce the capital cost. The disadvantages of MED at high operating temperature are corrosion and fouling in the preheaters. Nafey et al. [26] study was on thermo-economic design for MED-MVC desalination processes, for the normal operation (without external steam) and with external steam for 1500 m^3/day production. It was found that the performance ratio (PR = $\dot{m}_d * h_{lat.}$ / $[\dot{m}_{steam} * h_{lat.,steam} + \dot{W}_{comp.}$ / $Efficiey_{carnot}]$) for the system with

external steam is 8% less than that the normal operation. Results showed the normal operation, by reducing the pressure ratio of the VC from 1.35 to 1.15, the consumed power is also reduced by 50 %, and the unit product costs reduced from 1.7 – 1.24 $/m^3. The unit product cost decreases with increasing the capacity required. Sharaf et al. [27] studied solar collectors use in MED-PF-MVC. In this study, he used solar organic rankine cycle to generate electrical power to operate the compressor. It was found that the consumed power and required area for placing the solar collectors decrease with reduced compression ratio and increased number of evaporators. Labib et al. [28] studied MED–MVC system where the MVC is a major element that governs the performance of the system numerically by (CFD). They studied the effect of changing inlet skew angle of the impeller on the performance. Results showed detailed effect of flow pattern on reducing the secondary flow because of incidence angle at the impeller passage and impeller eye affect on the flow rate, the consumed power. The distillate increased with increasing compressor speed. Wu et al. [29] conducted an experimental study on MED mechanical vapor compression that separates the condenser element from the evaporator element by using a rotating disk evaporator. The separated evaporator element is designed to provide enhanced heat transfer, antiscaling and descaling. The performance was studied under various values of evaporating temperature and compressor frequency. It was found that the main parameters are pressure, evaporating temperature, flow rate of the vapor in the compressor, and the temperature difference as function of the compressor frequency. They also reported that the coefficient of performance increases with rising evaporating temperature. Mistry et al. [30] theoretically studied an improved MED system. An itemized model for MED is developed that is simple, flexible to implement, and

appropriate for use in optimization of power and water co-generation systems. The improvement of Forward MED was studied with minimum code duplication, and compared with: existing models in the literature. It was found easier to implement (by adopting fewer assumptions), and it is virtually more detailed to calculate the temperature profiles. Shen et al. [31] theoretically studied the MED-MVC system by using a water-injected screw compressor, and investigated the operating characteristics of the water-injected twin screw compressor. MED-MVC system contains five elements, which include a water-injected twin screw compressor, evaporator/condenser, preheaters, pipelines and pumps, and non-condensable gases ejector. It was found that the pressure ratio and compressor inlet mass flow rate principally depend on the difference in temperature between the boiling vapor and the saturated compressed vapor in addition to the brine boiling temperature. It was found that the mass fraction of injected-water decreases with the brine boiling temperature. It was also found that the a slight amount of water injection has negligible effect on the compressor volume flow rate. However, it substantially reduced the compressor power consumption and lowered the compressed steam temperature. Then Shen et al. [32] conducted an experimental study on a water-injected mechanical vapor compression desalination system. A prototype is improved and applied in a double-effect MVC system. They studied the effect of important parameters including velocity and inlet temperature of the compressor, and water injection flow rate on the compressor performance. Experimental results showed that water injection and velocity of the compressor had a major effect on the performance, while effect of inlet temperature of the compressor was relatively small. Results showed also that the flow rate of the compressor increases linearly with its speed. It was also found that consumed

power increases with the compressor speed, and the compressor inlet temperature only affects the consumed power of the compressor.

2.1.3 Utilization of solar or wind energy to run the systems

Karameldin et al. [33] studied the MVC desalination system driven by a wind turbine in Red sea area. The evaporator was operating at 50^{o} C with a difference in temperature through the evaporator tubes of 3^{o} C, and with an average wind speed of about 7 m/s. The main drawback for wind driven units is the variable wind speed. Garcia et al. [34] studied and reviewed seawater desalination driven by renewable energies. Renewable energy sources availability and seasonal changes. Results have shown that renewable energy has limited capacity. Lourdes Garcia et al. [35] study was focused on desalination process driven by Renewable energy. It was found that the solar PV has high cost, and wind power is lower than PV energy. The best selection was driven RO and ED by using wind turbine. Geothermal energy is appropriated for all desalination process, and the main pros is that there is no energy storage required. Forstmeiera et al. [36] conducted feasibility studies on MVC and RO desalination driven by wind-power. It was found that a RO system is lower in consumed energy, and the MVC system is suitable for desalination process because of its variability in operation. The wind-power is dependent on local conditions for the production of freshwater. Fernandez-Lopez et al. [37] analyzed an integrated multi-effect distillation (MED) mechanical vapor compression system based on evaporator equipment operated by renewable energy. The multi-effect distillation MVC system includes compressor, evaporators, condenser, preheaters, pumps, wind turbine, and thermal solar collector. The energy is obtained by several thermal solar collectors and wind turbines. Energy needed for the (MED) unit is supplied by thermal

solar collectors, and (MVC) unit is operated by wind turbines. It is environmentally friendly and no brine is flowing into the sea. Zejli et al. [38] theoretically studied the optimization of the MVC system driven by a PV/wind turbine hybrid system with a storage unit, to evaluate its feasibility and efficiency. A mathematical model was developed for monitoring the energy flows exchanged among the system to satisfy the water demand in Morocco. Results showed that the water demands are met at any time period with a feasibly economic cost compared to the current average cost of water in Morocco.

2.2 Vapor-compression distillation (VC)

To drive evaporation, vapor compression (VC) processes rely on reduced pressure in consecutive effects, which reduces the boiling point. As seen in MSF and MED, the heat used for evaporating water comes from the VC, rather than steam produced from a power plant turbine or through direct exchange with steam formed in a boiler.

VC units are likely to be used where cooling water and low-cost steam are expensive or complex to use. This is a reason why the process is primarily used in small and medium scale water desalination plants [4].

Two main processes are used to the steam that condenses so as to produce heat to evaporate coming seawater: a steam jet (ejector, or TVC) or a mechanical compressor. The MVC is usually electrically device, allowing the unit to use electrical energy to produce fresh water by distillation (Figure 2.1).

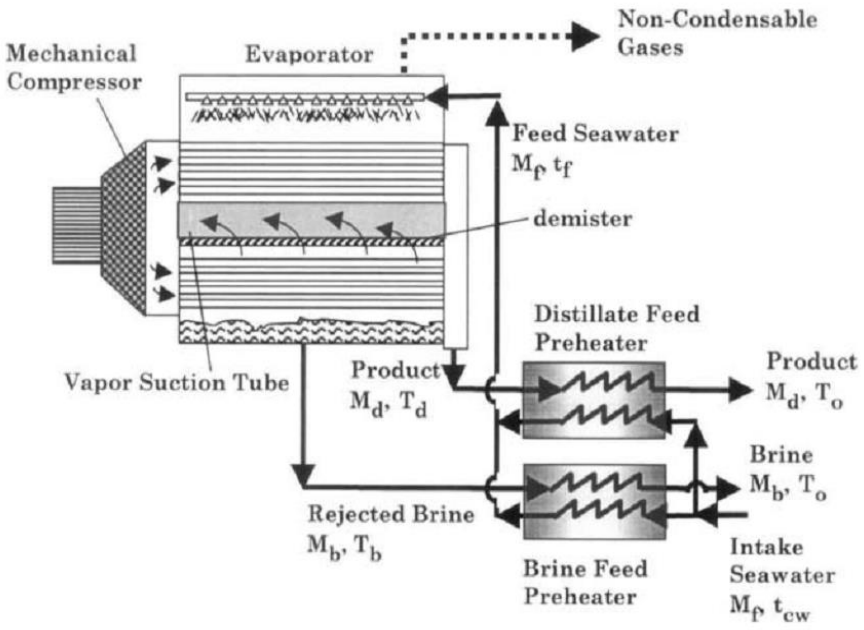

Figure 2.1 Mechanical vapor compression for Single effect [4]

2.3 MED-MVC

MED-MVC is a thermal desalination process as shown in Figure 2.2, where the saline water (Feed water) is sprinkled or otherwise spread onto the surface area of the effect (Evaporator) surface (Ordinarily tubes). The effect tubes in the first evaporator are gaining heated by Steam extracted from mechanical vapor compressor. The vapor produced at the first effect is condensed inside tubes of the second effect, where again vapor is generated. The other effects gain heated by vapor created in each previous effect. Each effect has a lower temperature than previous one.

The vapor in the final effects enters to the compressor where it's compressed to the desirable super-heated temperature and pressure.

It is needful to take into consideration the change of the vapor flow rate that is generated in each effect.

The inlet seawater ($\dot{m}_{cw}$) is passed through two preheaters where it's heated by transferring the heat from the distillate ($\dot{m}_d$) and brine ($\dot{m}_b$) streams into it, the heat exchangers are used to improvement thermal efficiency [4].

This is needful to take into consideration the comparison between the amounts of vapor in the first effect with that the amount of vapor formed in the final effect.

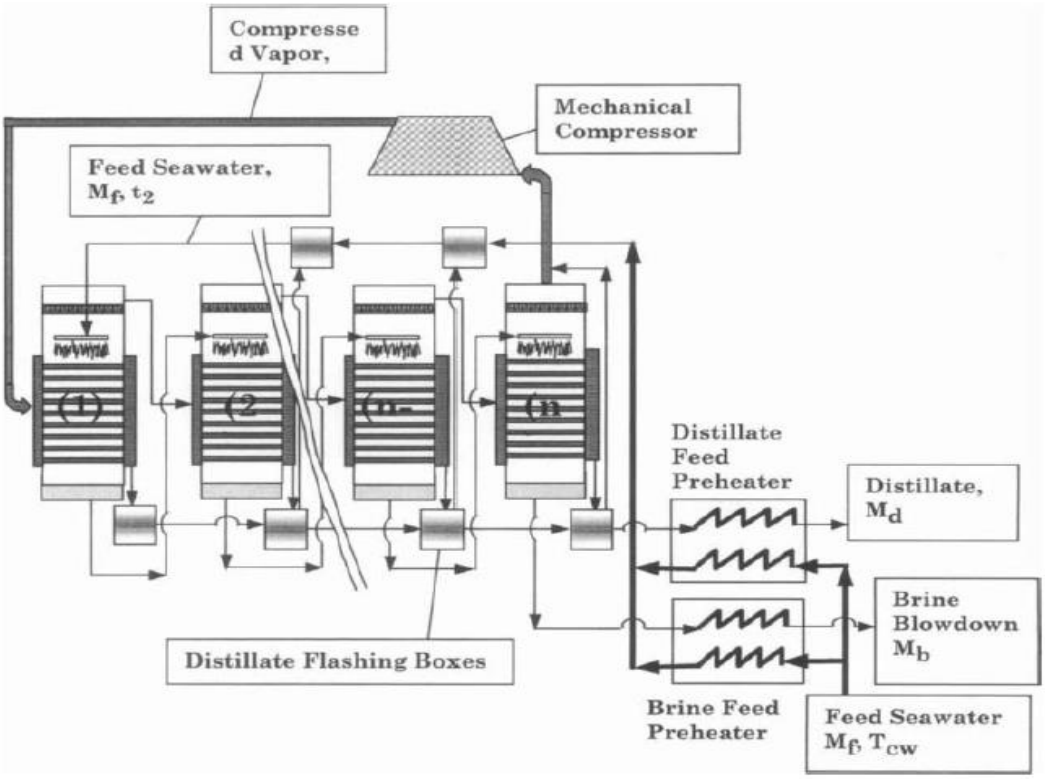

Figure 2.2 forward feed MED-Mechanical vapor compression [4]

CHAPTER 3

Forward feed Multi-Effect Distillation with Mechanical Vapor Compression

In this chapter, a modification in the forward feed multi effect distillation MED-FF system with mechanical vapor compression is investigated. It includes adding a second mechanical compressor that extracts a part of the vapor from one of the effects to mix with steam entering into the first effect. The MVC-FF system includes two compressors, evaporators, heat exchangers, preheaters, and pumps.

3.1 Forward feed Multi-Effect Distillation with two Mechanical Vapor Compressors:

Figure 3.1 shows the original layout of a forward feed MED-MVC system. Vapor that forms at the last effect is directed to the suction side of the mechanical compressor where it is compressed into superheated vapor that is used to heat the sprayed seawater in the first effect and eventually generating some vapor. The generated vapor in the first effect is used as the source of heat for the second effect and so on. The modification to the original layout of the forward feed MED-MVC system is shown in Figure 3.2. It includes adding a smaller (or secondary) compressor that extracts a portion of the vapor from one of the other effects (2 to N), compresses it to the state of the vapor entering to the first effect, mixing it with the inlet vapor to the first effect to enhance the heat transfer (and accordingly, evaporation rate) in the first effect. The MED mechanical vapor compression system is different from the other MED arrangement (simple arrangement

without vapor compression or the MED-TVC systems) in some aspects. It is equipped with two additional heat exchangers used as feed preheaters; the down condenser is eliminated since the whole vapor in the final effect is drawn to the suction side of the main compressor.

The inlet seawater ($\dot{m}_{cw}$) is passed through two preheaters after being splitted into two streams where it gains heat by transferring it from the distillate ($\dot{m}_d$) stream in one exchanger and the brine ($\dot{m}_b$) stream in the other. Both are contributing to energy recovery that improves the system performance.

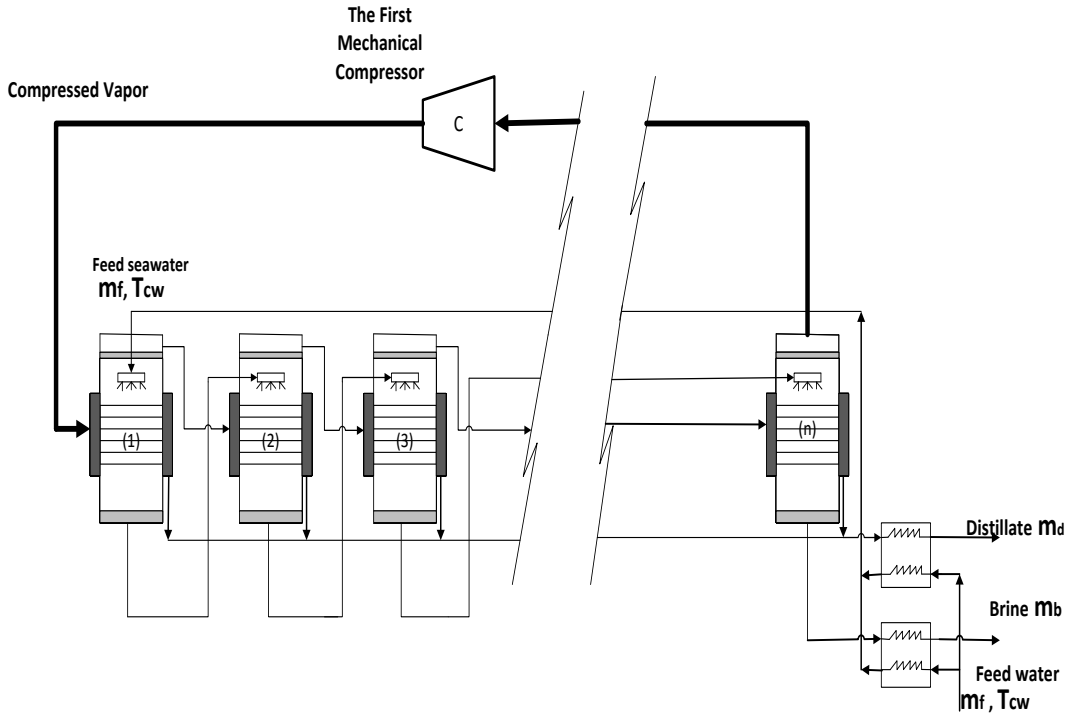

Figure 3.1 Forward feed MED Mechanical vapor compression

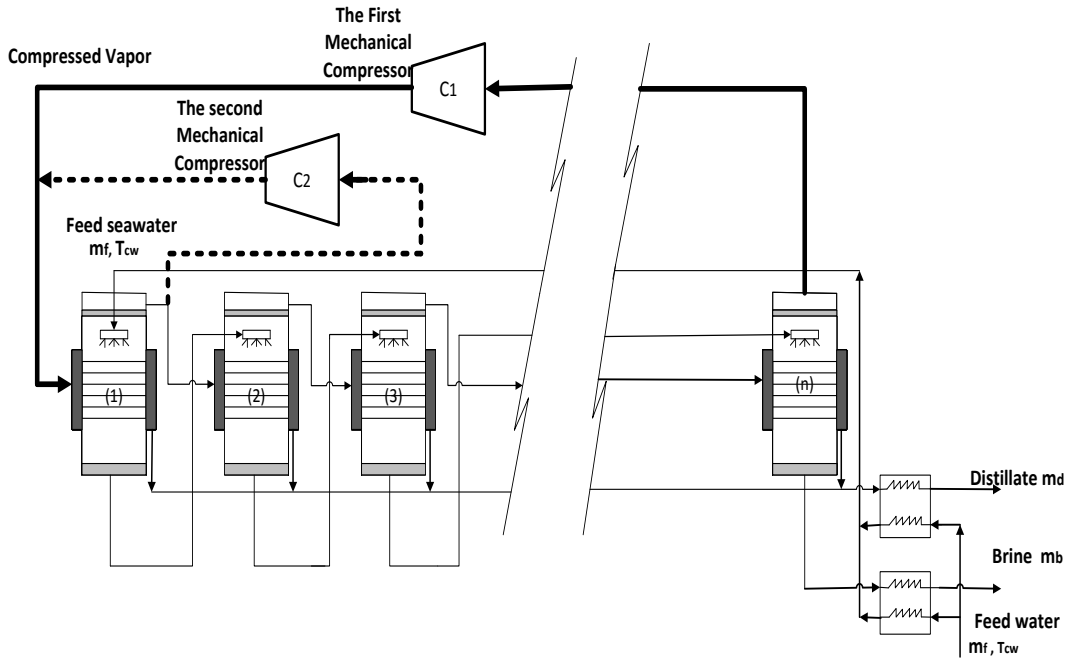

Figure 3.2 Forward feed MED with Two Mechanical vapor compression

3.2 Mathematical model of MED-MVC Forward Feed:

The mathematical model for effect (i), includes the mass, energy and material balances, and heat transfer (H.T) equation per effect.

Data generated are related to:

- Distillate flow rate ($\dot{m}_d$).
- Brine flow rate ($\dot{B}_n$).
- Concentration of the brine.
- Heat transfer area.

Material and heat balances for flash boxes and preheaters are excluded in this model.

Assumption:

- Thermodynamic losses are constant.
- Negligible energy losses to surroundings.
- Thermal load is the same in all effects.
- Zero vapor flashing inside effect.

The number of mass, energy and material balance equations (Seawater mixture between salt water and fresh).

There are (n) equations for H.T in any effect, which relate the effect thermal load to the overall the coefficient of heat transfer, the area, and driving force by temperature.

Brine Flow rate, $\dot{B}_1, \dot{B}_2, \dots, \dot{B}_{n-1}, \dot{B}_n$ (n unknown)

Distillate flow rate, $\dot{D}_1, \dot{D}_2, \dots, \dot{D}_{n-1}, \dot{D}_n$ (n unknown)

Brine concentration, $X_1, X_2, \dots, X_{n-1}$ (n-1 unknown)

Effect temperature, $T_1, T_2, \dots, T_{n-1}$ (n-1 unknown)

Heat transfer (H.T) area (1 unknown)

Flow rate of steam (1 unknown)

Total = (4n) unknowns

Parameters to be specified before solution:

- Motive steam temperature, T_s.
- The last effect (n) Temperature, T_n.

- Salt concentration leaving last effect (n), X_n.
- Distillate flow rate ($\dot{m}_d$).
- Salt concentration of feed (X_f).

3.2.1 Model equations

Mass balance:

$$\dot{m}_f = \dot{m}_d + \dot{B}_n \quad (1)$$

$$X_f \dot{m}_f = X_n \dot{B}_n \quad (2)$$

From equation (1) & (2) we can write:

$$\dot{B}_n = \left(\frac{X_f}{X_n - X_f}\right) * \dot{m}_d \quad (3)$$

The thermal load,

$$\dot{Q}_2 = \dot{Q}_3 = \ \ldots\ldots\ = \dot{Q}_{n-1} = \dot{Q}_n \quad (4)$$

For first effect: $$\dot{Q}_1 = \dot{m}_s * h_{fg,s} \quad (5)$$

$$\dot{Q}_1 = \dot{D}_1 * h_{fg,v1}$$

$$\dot{D}_1 = xx * m_{v1} + m_{vn}$$

Mass flow rate of vapor at first effect (mv_1):

$$m_{v1} = \frac{\dot{D}_1 * h_{fg,v1}}{h_{fg,v2}}$$

Distillate flow rate that condenses in the second effect after the extraction (xx) in the first effect:

$$\dot{D}_2 = (1 - xx) * m_{v1}$$

Where:

m_{v1} = mass vapor for the first effect.

For effects 2 to n: $$\dot{Q}_i = \dot{D}_i * h_{fg,vi} \quad (6)$$

Also: $$\dot{Q}_i = A_i * U_i * \Delta T_{loss} \quad (7)$$

Remember that the heat transfer rate and the area are equal in each effect, then

$$\frac{\dot{Q}_1}{A_1} = \frac{\dot{Q}_2}{A_2} = \cdots = \frac{\dot{Q}_{n-1}}{A_{n-1}} = \frac{\dot{Q}_n}{A_n} \quad (8)$$

$$U_1\Delta T_1 = U_2\Delta T_2 = \cdots = U_{n-1}\Delta T_{n-1} = U_n\Delta T_n \quad (9)$$

Temperature drop:

$$\Delta T = T_s - T_n \quad (10)$$

This drop is equal for each effect;

$$\Delta T = \Delta T_1 + \Delta T_2 + \cdots + \Delta T_{n-1} + \Delta T_n \quad (11)$$

From above equations Find:

$$\Delta T_1 = \frac{\Delta T}{U_1 \sum_{i=1}^{n} \frac{1}{U_i}} \quad (12)$$

Temperature profile

For first effect:

$$T_1 = T_s - \Delta T_1 \quad (13)$$

For effects (2 to n):

$$T_i = T_{i-1} - \Delta T_1 \frac{U_1}{U_i} \quad (14)$$

Temperatures drop (2 to n):

$$\Delta T_i = \Delta T_1 \frac{U_1}{U_i} \quad (15)$$

For effects (2 to n):

$$T_i = T_{i-1} - \Delta T_1 \frac{U_1}{U_i} \quad (16)$$

Distillate flow rate:

$$\dot{m}_d = \dot{D}_1 + \dot{D}_2 + \ldots\ldots + \dot{D}_{n-1} + \dot{D}_n \quad (17)$$

$$\dot{D}_i = \dot{D}_2 * h_{fg,v2} / h_{fg,vi} \qquad (i= 3\ldots n) \quad (18)$$

Flow rate of brine in first effect:

$$\dot{B}_1 = \dot{m}_f - \dot{D}_1 \quad (19)$$

$$\dot{B}_i = \dot{B}_{i-1} - \dot{D}_i \quad (i= 2\ldots n) \quad (20)$$

Salt concentration profile:

$$X_1 = X_f * (\dot{m}_f / \dot{B}_1) \quad (21)$$

$$X_i = X_{i-1} * (\dot{B}_{i-1} / \dot{B}_i) \quad (22)$$

Heat Transfer Area:

In First effect: $$A_1 = \left(\dot{D}_1 * h_{fg,v1}\right) / (U_1(T_s - T_1)) \quad (23)$$

$$A_i = \left(\dot{D}_i * h_{fg,vi}\right) / \left(U_i(T_s - \Delta T_{loss})\right) \quad \text{(i= 1... n)} \qquad (24)$$

ΔT_{loss} = Temperature drop.

$$T_{vi} = T_i - BPE \qquad (25)$$

Specific heat transfer area (sA):

$$sA = \frac{\sum_{i=1}^{n} A_i}{\dot{m}_d} \qquad (26)$$

Heat exchangers thermal load $\dot{Q}_h$:

$$\dot{Q}_h = \dot{m}_d * c_p * (T_d - T_o) + \dot{B}_n * c_p * (T_b - T_o) \qquad (27)$$

Where:

$$T_o = \left(T_{cw} - T_f\right) + \left(\frac{X_f}{X_b}\right) * T_b + \left(\frac{X_b - X_f}{X_b}\right) * T_d \qquad (28)$$

The specific power consumption:

Total power consumption:

$$w = w_k + w_s$$

The consumed power for first (main) compressor w_k

$$w_s = (m_{vn}) \frac{\gamma}{\eta(\gamma-1)} P_{vn} v_{vn} \left[\left(\frac{P_s}{P_{vn}}\right)^{\frac{\gamma-1}{\gamma}} - 1\right] \qquad (29)$$

Where: $\gamma = \frac{C_p}{C_v}$

The consumed power for second compressor w_s

$$w_k = (xx * m_{v1}) \frac{\gamma}{\eta(\gamma-1)} P_{v1} v_{v1} \left[\left(\frac{P_s}{P_{v1}} \right)^{\frac{\gamma-1}{\gamma}} - 1 \right] \quad (30)$$

The Entropy Generation

The second law leads to the definition of a new property called entropy. Irreversible process ($\int \frac{\delta Q}{T} = 0$).

In general the entropy generation for any process,

$$S_{gen} = \sum \dot{m}_e s_e - \sum \dot{m}_i s_i \quad (31)$$

Where:

$\dot{m}_e$ = the exit mass flow rate, s_e = the entropy at exit, kJ/kg.k

$\dot{m}_i$ = the enter mass flow rate, s_i = the entropy at enter, kJ/kg.k

The entropy generation for second compressor, $S_{gen.c1}$:

$$S_{gen.c1} = xx * m_{v1} * (s_{T_s} - s_{T_{v1}}) \quad (32)$$

The entropy generation for first compressor, $S_{gen.c2}$:

$$S_{gen.c2} = m_{vn} * (s_{T_s} - s_{T_{vn}}) \quad (33)$$

For first effect:

$$S_{gen.1} = \left[m_{v1} * s_{T_{v1}} + \dot{D}_1 * s_{T_1} + \dot{B}_1 * s_{T_1} \right] - [\dot{m}_s * s_{T_s} + \dot{m}_f * s_{T_{f1}}] \quad (34)$$

Second Effect:

$$S_{gen.2} = \left[\dot{D}_3 * s_{T_{v2}} + \dot{D}_2 * s_{T_2} + \dot{B}_2 * s_{T_2} \right] - \left[(1 - xx) m_{v1} * s_{T_{v1}} + \dot{B}_1 * s_{T_1} \right] \quad (35)$$

For effects 3 to (n-1):

$$S_{gen.i} = \left[\dot{D}_{i+1} * s_{T_{vi}} + \dot{D}_i * \ s_{T_i} + \dot{B}_i * s_{T_i} \right] - \left[\dot{B}_{i-1} * s_{T_{(i-1)}} + \ \dot{D}_i * s_{T_{v(i-1)}} \right] \quad (36)$$

For the last Effect:

$$S_{gen.n} = \left[\ m_{vn} * s_{T_{vn}} + \dot{D}_n * \ s_{T_n} + \dot{B}_n * s_{T_n} \right] - \left[\dot{B}_{n-1} * s_{T_{(n-1)}} + \ \dot{D}_n * s_{T_{v(n-1)}} \right] \quad (37)$$

Then the total entropy generation $S_{gen.total}$:

$$S_{gen.total} = S_{gen.c1} + \ S_{gen.c1} + \sum_{i=1}^{n} S_{gen.i} \quad (38)$$

Where:

$S_{gen.i}$= the entropy generation at effect i. (i= 1….n)

Exergy Efficiency

Exergy Efficiency is a measure of the performance of the system that shows the components of the system where more losses are associated. It gives an indication to system designers of the locations that require further enhancements for better system performance. The exergy balance of the vapor compressor is developed as follows:

The exergy efficiency η_{II}

$$\eta_{II} = \frac{\dot{E}_{vapor\ ,out} - \dot{E}_{vapor\ ,in}}{w_{rev}} \quad (39)$$

$\dot{E}_{vapor\ ,out} = \dot{m}_v(h_v - h_o - T_o(s_v - s_o))$

The exergy efficiency η_{II} first (main) compressor w_k

$$\eta_{II,n} = \frac{\dot{m}_{vn}(h_{g,n} - h_{g,s} - T_o(s_{g,n} - s_{g,s}))}{w_{rev}}$$

The exergy efficiency η_{II} second compressor w_k

$$\eta_{II,1} = \frac{xx*\dot{m}_{v1}(h_{g,1}-h_{g,s}-T_o(s_{g,1}-s_{g,s}))}{w_{rev}}$$

The exergy efficiency

$$\eta_{II} =$$

$$\frac{\dot{m}_{vn}\left(h_{g,n}-h_{g,s}-T_o\left(s_{g,n}-s_{g,s}\right)\right)+\text{xx}*\dot{m}_{v1}\left(h_{g,1}-h_{g,s}-T_o\left(s_{g,1}-s_{g,s}\right)\right)}{w_{rev}}$$

Input Conditions

- Numbers of effects (n) are 4 and 6, 8.
- X_{cw}, and T_{cw}, are 42000 ppm and 25^o C.
- The salinity of rejected brine, X_b = 70000 ppm.
- T_s = 60^o C & T_n = 40^o C.
- The feed water temperature, T_f = 35^o C.
- The flow rate of distillate, m_d = 1 kg/s.
- The overall heat transfer (H.T) coefficient in the preheater, U_d = 1.8 kJ/s.m^2.^{o}C.
- The compressor efficiency, η = 76 %.

3.3 Validation for MED-MVC forward feed

A very good agreement with the published work of El-Dessouky and Ettouney [4] is observed in Figure 3.3. The figure shows that the increase in the temperature difference across the compressor results in an increase in the work consumed by the compressor. Moreover, increasing the operating temperature results in a decrease of the consumed power due to the decrease in the vapor specific volume at higher operating temperature.

Furthermore, a higher temperature difference between the saturation temperature of the brine blow down in the last effect and the compressed vapor (Delivery side of the compressor) results in an increase of the consumed power, and an increase the compression ratio.

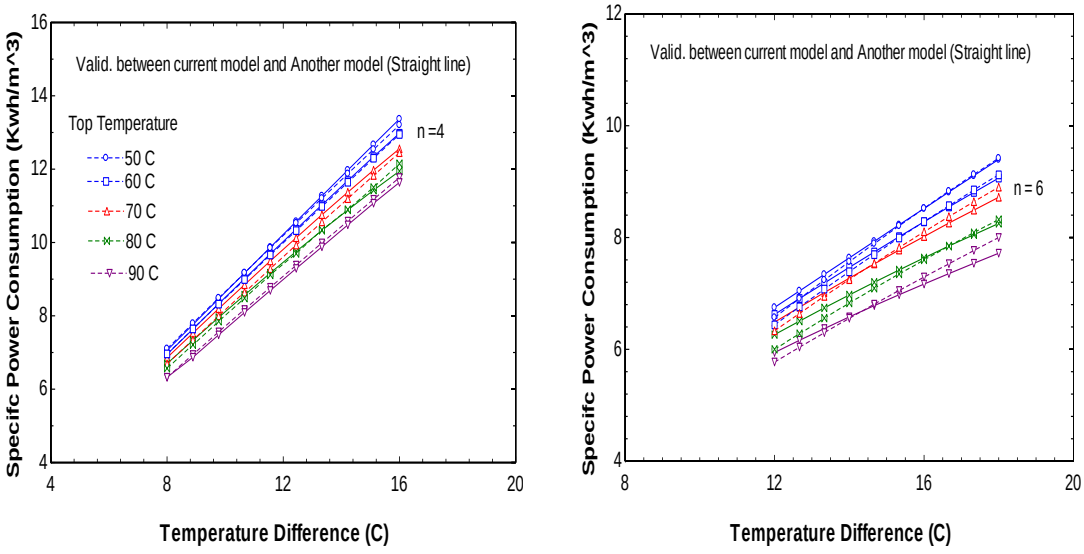

(a) (b)

Figure 3.3 the specific power Consumption with the Temperature difference across the compressor (a) n = 4 effects (b) n = 6 effects. Applied by current model and another model [4].

The assumed values used for the validation of the results are

- The salinity of rejected brine, X_b = 70000 ppm
- X_{cw}, and T_{cw}, are 42000 ppm and 25^o C.
- The compressor efficiency, η = 76 %.
- The overall heat transfer (H.T) coefficient in the first effect, U_1 = 2.4 kJ/s.m^2.^{o}C and decreases 5%.
- The overall heat transfer (H.T) coefficient in the preheater, U_d = 1.8 kJ/s.m^2.^{o}C.
- The flow rate of distillate, m_d = 1 kg/s.

3.4 Results and Discussion

3.4.1 The consumed specific power

The consumed specific power is the power consumption required for separating saline water into a unit mass flow rate of pure water and concentrated brine. It is dependent on the salt concentration of the Feed water. The consumed power depends also on steam pressure, vapor pressure, specific volume, pressure ratio, and the number of effects.

Furthermore, the consumed power in MED-MVC-FF depends on the rate of extracted vapor leaving any effect to enter the secondary compressor as well as the steam entering to the first effect, the compression ratio (since its temperature increases as a result of the change in its pressure) , and the number of effects. Figure 3.4 (a), (b), (c) show the variation of the specific power of the system with the extracted vapor entering the secondary compressor compared with the original case of no secondary compressor for systems of 4-effects (Fig. 3.4a), 6 effects (Fig. 3.4b) and 8 effects (Fig.3.4c). As shown in Fig 3.4 (a), the specific power decreases with the increase in extraction rate due to the increase in the rate of steam that enters the first effect as a result of combined flow rates from both compressors. This, in turn, results in an increased rate of evaporation of sprayed seawater in the first effect and results in more formed vapor. Also it is obvious that the relation between the consumed specific power and the extracted vapor in each effect is not linear due to the nonlinear decrease in the compression ratio of the second mechanical compressor. It is important to note that the specific power also depends on the location of the effect where extraction of formed vapor takes place. The specific power is always lower when extraction is made for the formed vapor in effect number 2 (compared to the case of extraction from effects 1 and 3). This is believed to be a result

of the changes in compression ratio of the secondary compressor. Too low compression ratio (extraction from effect number 1) will not bring considerable vapor to join the main stream leaving the primary compressor and entering the first effect. On the other hand, extraction from effect (3) results in higher pressure ratio that results in higher power consumption.

Fig 3.4 (b) shows that the specific power decreases with increased extraction percentage for a system made of 6 effects. It is obvious that there is a relation between the consumed power with the change in the point of extraction. It can be noticed that lower consumed power occurs when vapor is extracted at the middle location of the extraction (n = 3) with neither high nor low pressure ratio across the secondary compressor. Fig 3.4 (c) shows similar trend of specific power dependence on the system with the percentage of vapor extracted and the location where the secondary flow (extracted vapor) takes place for an 8-effects system. It is also shown that extracting the vapor at effect (4) resulted in the lowest specific power, and hence better system performance.

Another important observation from these figures is the decrease in the specific power with the increased formed vapor flow rate extracted to the secondary compressor. This amount goes through compression in the secondary compressor to P_s (accordingly at T_s) where the compression ratio and hence the power is less compared to the primary compressor that has to compress the vapor form the last effect (lowest pressure) to the first effect (highest pressure of the system). Early extraction decreases the rate of vapor formed in the last effect and accordingly decreases its associated compressor power and higher rate of vapor flows into the secondary compressor where lower power is needed due to the decreased compression ratio. Thus, a general observation is made here that

lower values of the specific power correspond to a higher value of extraction that occurs in the effect (n/2). The vapor extracted after the first effect has the lowest pressure ratio as shown in Fig. 3.6 whereas its vapor flow rate entering the second compressor is the highest with the extraction percentage (see Fig. 3.7), and the vapor extracted at effect

(n-1) has the highest pressure ratio whereas its mass vapor is the lowest. Therefore, the optimal case is to extract the vapor after the effect (n/2).

Comparing the specific power in Figures 3.4 (a), (b), (c), we notice that the increase in the consumed power corresponds to systems of lower number of effects. It is important to mention that the systems are modeled based on a unit production of desalinated water. Therefore, the formed vapor flow rate for each effect is less as the number of effects increase and accordingly, lower specific power consumption is observed. The decrease in the vapor specific volume at higher operating temperature also contributes to reduction in the specific power for vapor compression. Figure 3.5 (a), (b), (c) show the variation of the work ratio (w_k/w_s) of the system with the extraction.

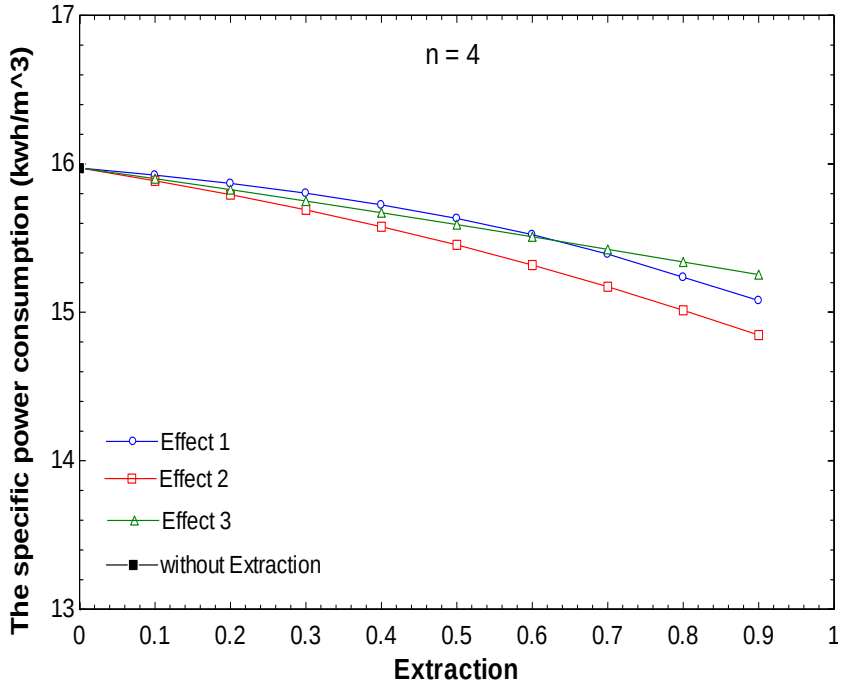
n = 4
The specific power consumption (kwh/m^3)
Extraction
Effect 1
Effect 2
Effect 3
without Extraction
17
16
15
14
13
0
0.1
0.2
0.3
0.4
0.5
0.6
0.7
0.8
0.9
1

(a)

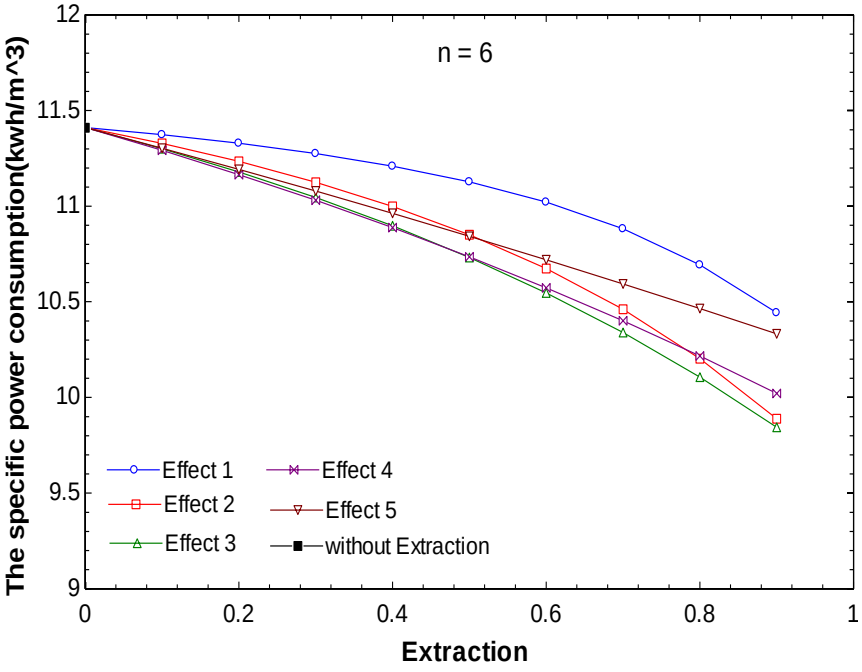
n = 6
The specific power consumption(kwh/m^3)
Extraction
Effect 1
Effect 2
Effect 3
Effect 4
Effect 5
without Extraction
12
11.5
11
10.5
10
9.5
9
0
0.2
0.4
0.6
0.8
1

(b)

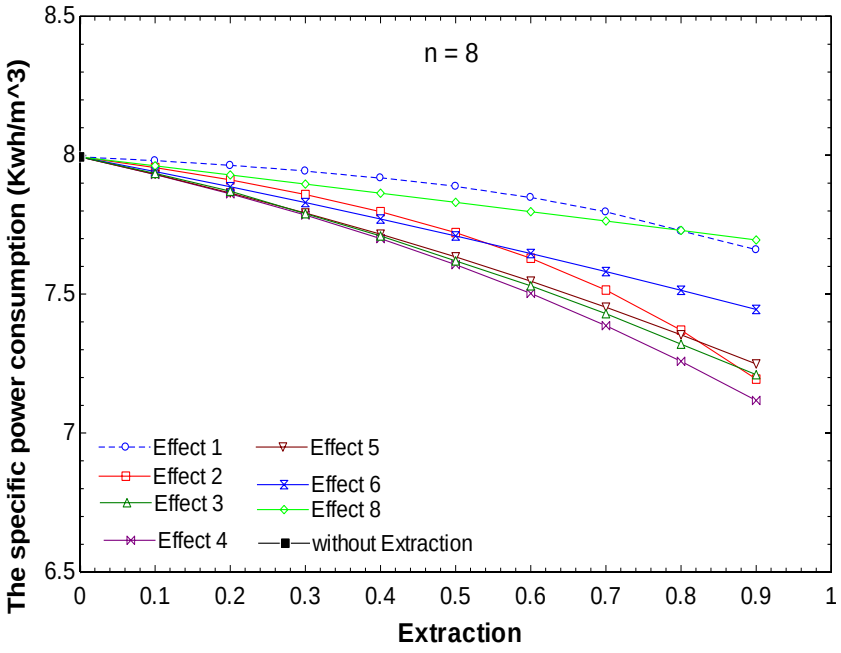

(c)

Figure 3.4 Change in the consumed power for the forward feed (MED-MVC) with Extraction for (a) n = 4 Effects (b) n = 6 Effects (c) n = 8 Effects.

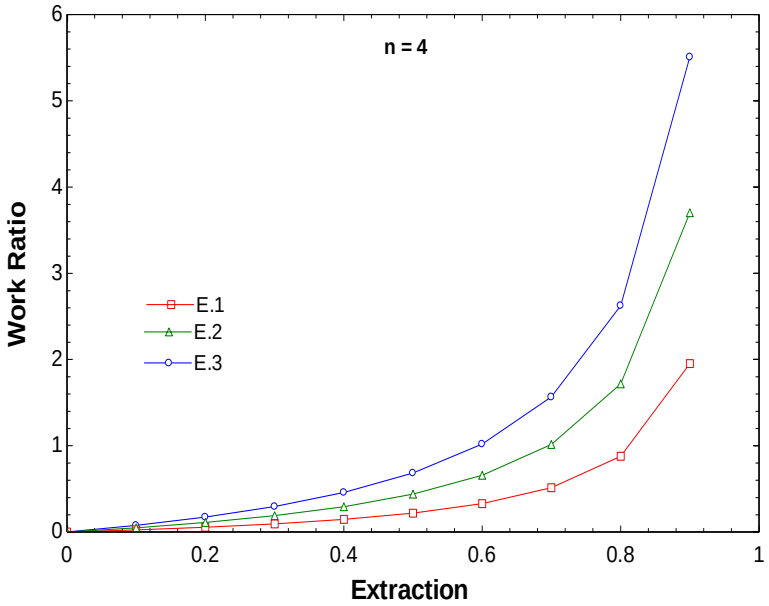

(a)

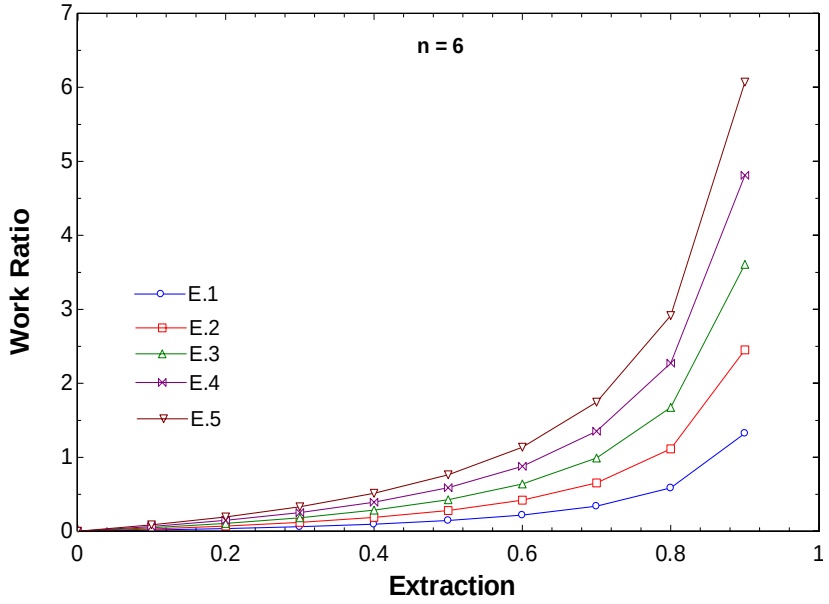

(b)

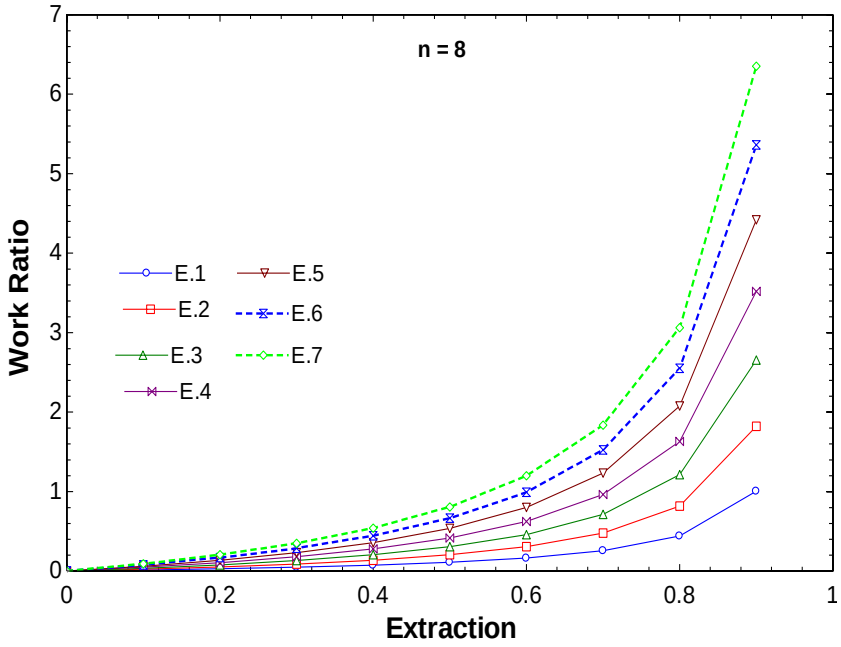

(c)

Figure 3.5 Change in the work ratio of the forward feed MED-MVC with Extraction for (a) n = 4 Effects (b) n = 6 Effects (c) n = 8 Effects

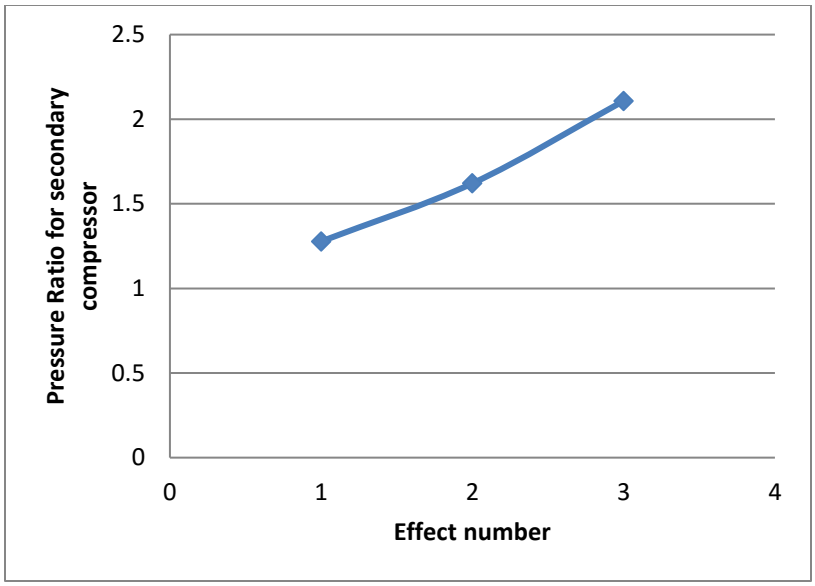

Figure 3.6 Change of the pressure ratio for secondary compressor with effect number for n = 4 effects.

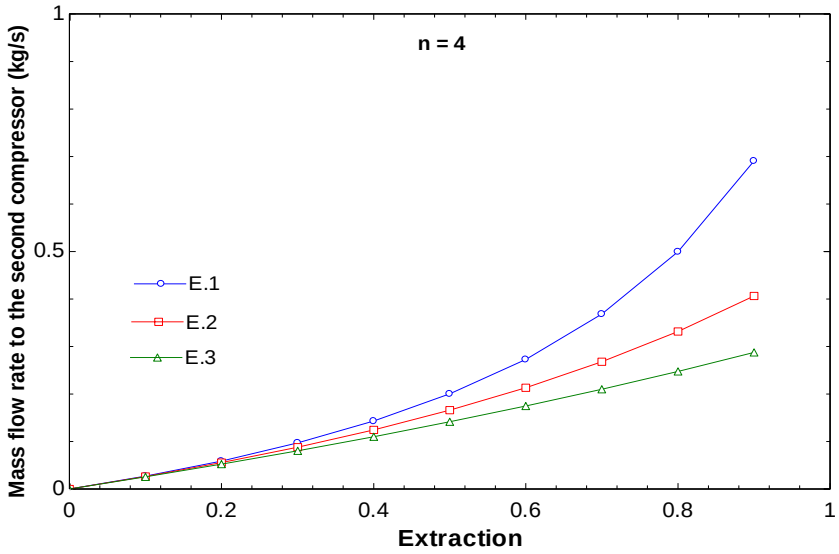

Figure 3.7 Change the mass flow rate enter the second compressor with Extraction for n = 4 effects.

3.4.2 Specific heat transfer area

Specific heat transfer area is the sum of the total area of the system per distillate flow rate. The specific heat transfer area in MED-MVC-FF is dependent on distillate rate per effect. It also depends on the latent heat of condensation at the temperature at which the

vapor leaves the effect as well as the number of effects. Fig 3.8 (a) shows the specific heat transfer area decrease with the extraction at the effect (1, 2 or 3) because of the decrease in the vapor flow rate that flows to subsequent effects. When the extraction of formed vapor to the secondary compressors occurs at effect (1), the specific heat transfer area is minimum due to the low latent heat (corresponding to maximum temperature) as well as the decrease of the distillate flow rate that flows to the next effects. Moreover, the rate of vapor formed in the first effect is higher than other effects. High extraction for the first effect means higher vapor flow rate to the secondary compressor and higher total flow rate to the vapor side of the first effect (inside the tubes) where vapor condenses. Since it occurs at the first effect (highest temperature among all effects), a higher overall heat transfer coefficient is expected leading to lower heat transfer area. Fig 3.8 (b), (c) similarly show that the specific heat transfer (sA) decrease with the increase in the percentage extraction. The specific heat transfer rate is minimum when extraction occurs at effect (1) at high rates of extraction as explained earlier. Generally speaking, it is observed in Figs. 3.8 (a), (b), (c) that the heat transfer area decreases as the extraction increases. It obvious that the specific heat transfer area for an effect is higher than its previous effect at the same extraction because of the decrease in the temperature of the vapor formed in the effect where extraction of vapor occurs. On the other hand, increasing extraction results in higher rate of vapor leaving both compressors (mainly due to flow rate across the secondary compressor), generating more formed vapor and hence the specific area $\left(\frac{A}{\dot{m}_d}\right)$ decreases.

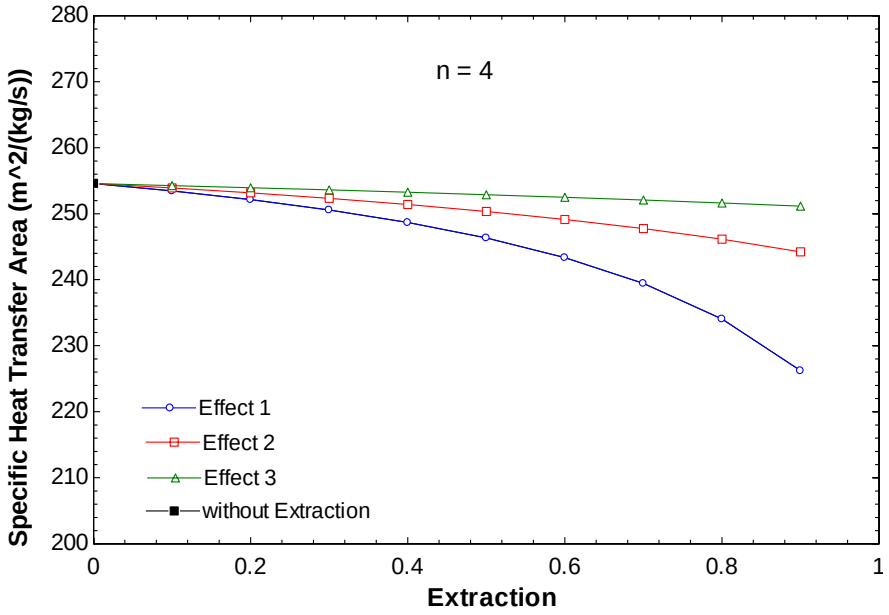
n = 4
Specific Heat Transfer Area (m^2/(kg/s))
Extraction
Effect 1
Effect 2
Effect 3
without Extraction
280
270
260
250
240
230
220
210
200
0
0.2
0.4
0.6
0.8
1

(a)

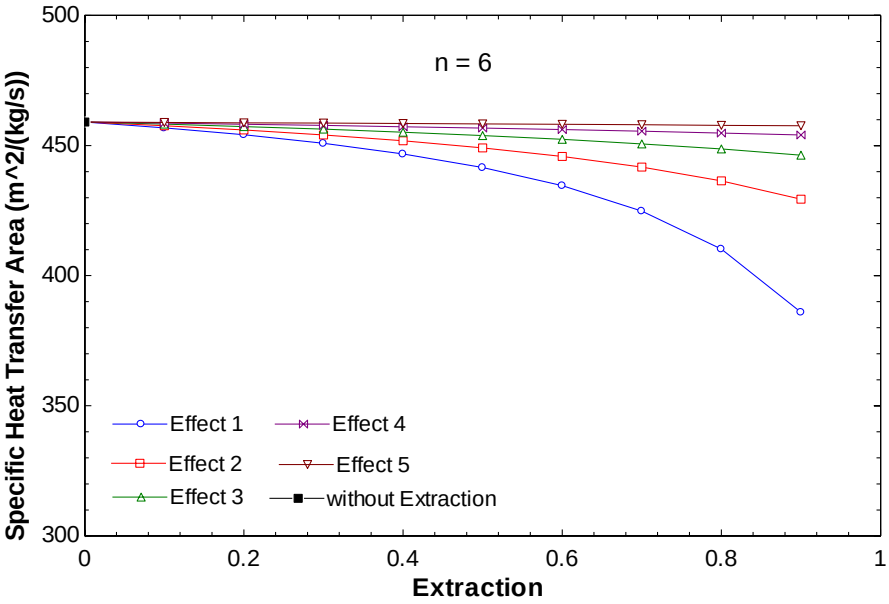
n = 6
Specific Heat Transfer Area (m^2/(kg/s))
Extraction
Effect 1
Effect 2
Effect 3
Effect 4
Effect 5
without Extraction
500
450
400
350
300
0
0.2
0.4
0.6
0.8
1

(b)

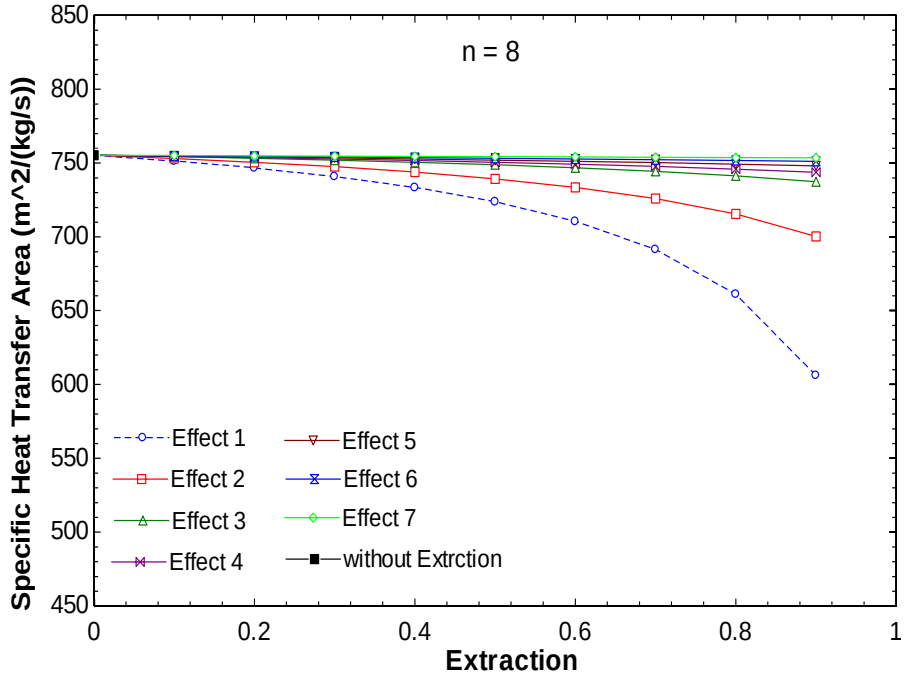

(c)

Figure 3.8 Change in the heat transfer area of the forward feed MED-MVC with Extraction for (a) n = 4 Effects (b) n = 6 Effects (c) n = 8 Effects.

3.4.3 Entropy generation

Entropy generation is a measure of the performance of the system as it shows the components of the system where more losses are associated. It gives an indication to system designers of the locations that require further enhancements for better system performance. The net entropy change of the effects and the entropy change of the compressors are balanced by the Entropy generation. The entropy change for the effects depends on the Extraction rate, the flow rate and the temperature of the distillate, the temperature of the brine, the vapor temperature of the effect, and the number of effects.

Fig. 3.8 (a) shows the total entropy generation change with the rate of extraction. Entropy generation of the compression increases due to the addition of a secondary compressor.

Also, it is obvious that the relation between the entropy generation and the extracted vapor in each effect is nonlinear for effect 1, 2 and 3 because the decrease in the distillate and the brine per stage are nonlinear. Fig. 3.9 (b), (c) also show that the entropy generation increases with the rate extraction due to increased vapor flow rate to the secondary compressor. Comparing Figures 3.9 (a), (b), (c) shows that the Total entropy generation increases with the increase in the number of effects due to the increase in the entropy generation in each effect. The entropy generation after effect (n/2) approximately linear due to the change of the mass flow rate with extraction percentage is linear, the higher value of the entropy change occurs in location of the effect where extractions of form vapor.

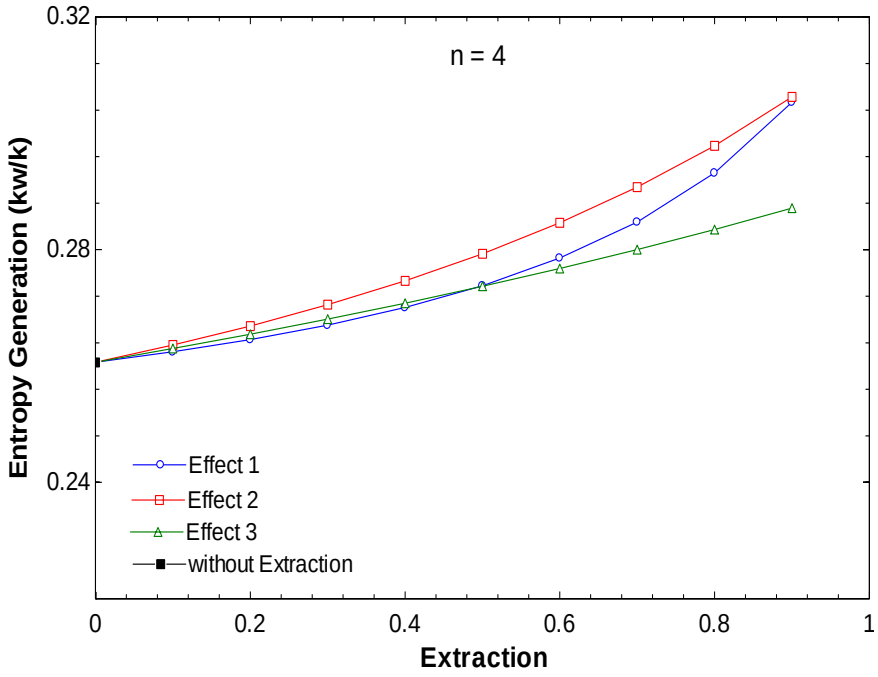

(a)

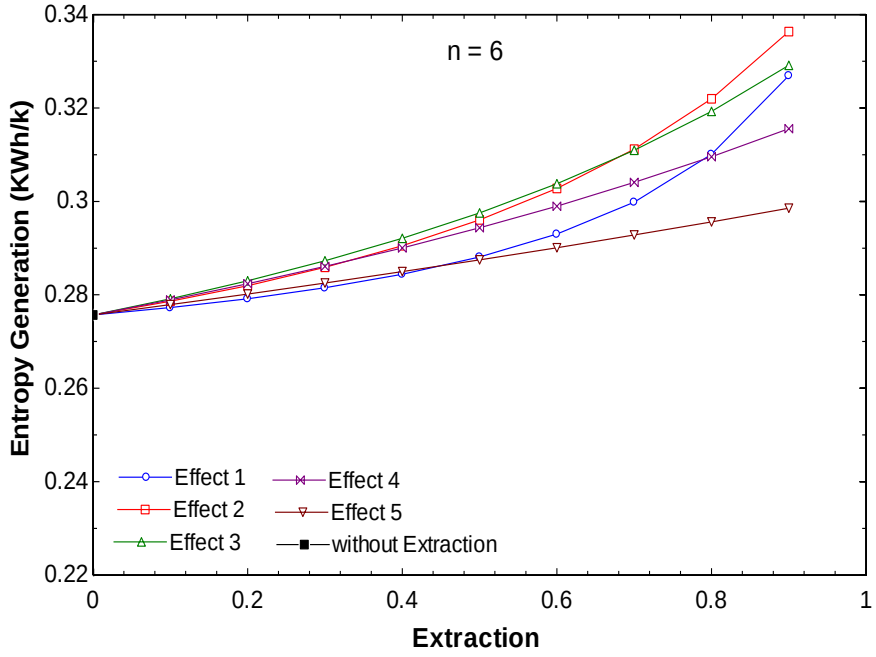

(b)

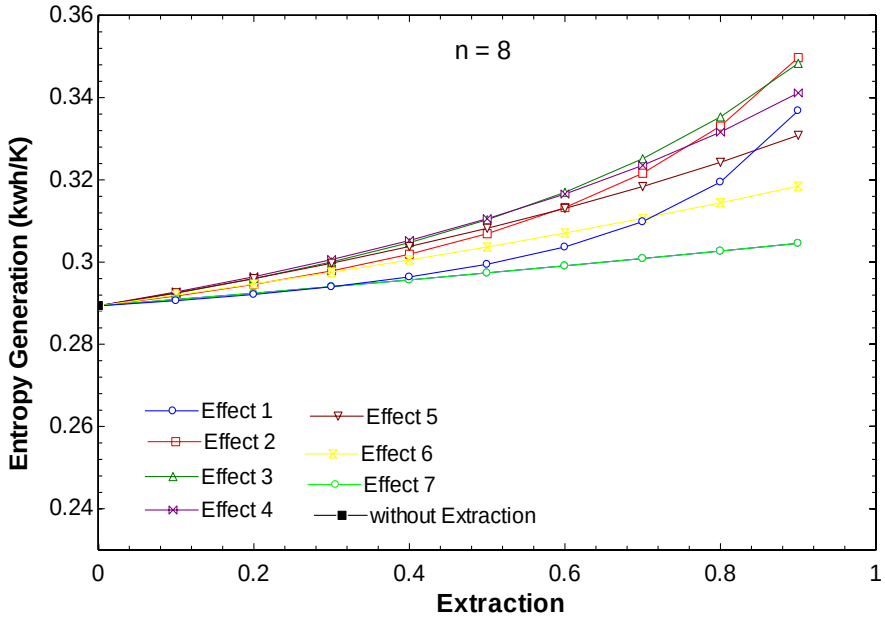

(c)

Figure 3.9 Entropy generation of the forward feed MED-MVC with Extraction for (a) n = 4 Effects (b) n = 6 Effects (c) n = 8 Effects

3.4.4 Exergy Efficiency

Exergy efficiency is a measure of the performance of the system. Figs. 3.10 (a), (b), (c) show the variation of the exergy efficiency of the system with the extracted vapor entering the secondary compressor compared with the original case of no secondary compressor for systems of 4 effects (Fig. 3.10 a), 6 effects (Fig. 3.10 b) and 8 effects (Fig. 3.10 c). The exergy efficiency increases with the increase in extraction rate.

The exergy efficiency at Fig 3.10 (a), (b), (c) increases with the decrease the consumed power. (η_{II}) increases with the Extraction due to decrease the total specific power consumption. Thus, a general observation is made here that higher values of the exergy efficiency correspond to a higher value of extraction that occurs in the effect (n/2).

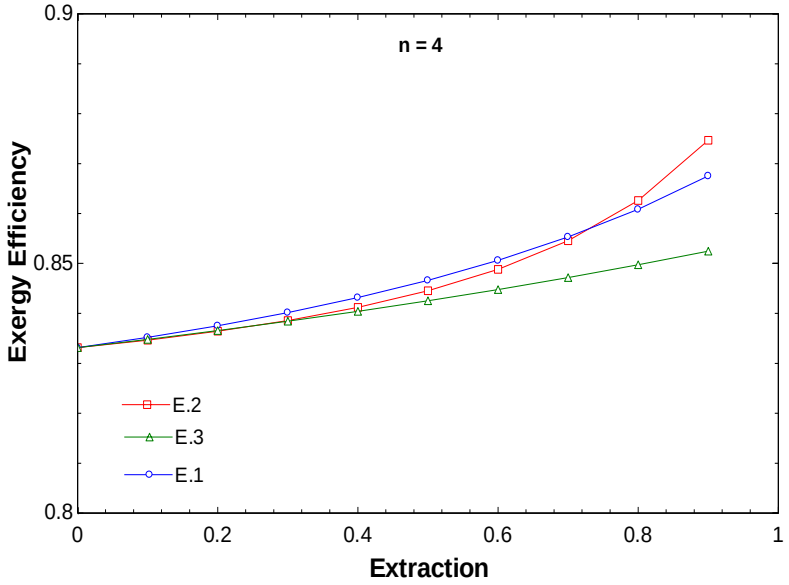

(a)

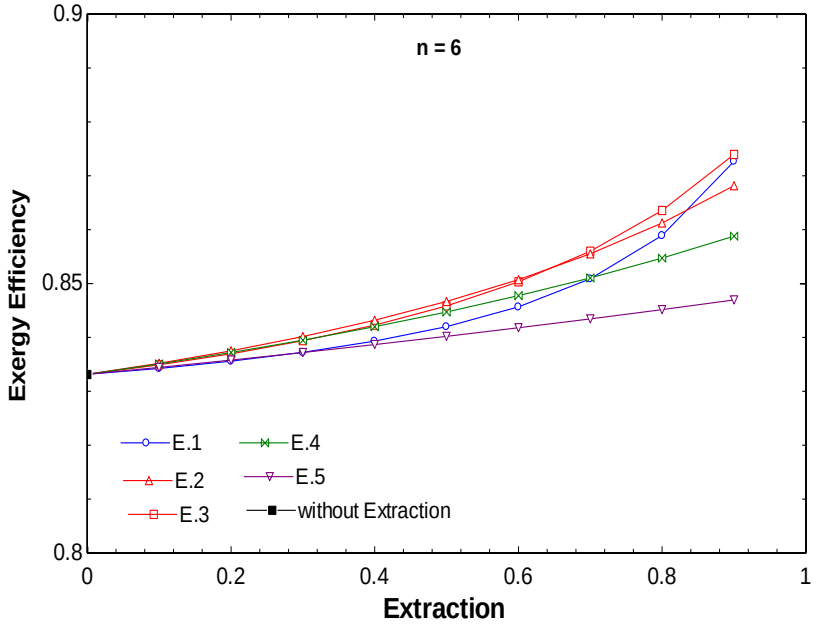

(b)

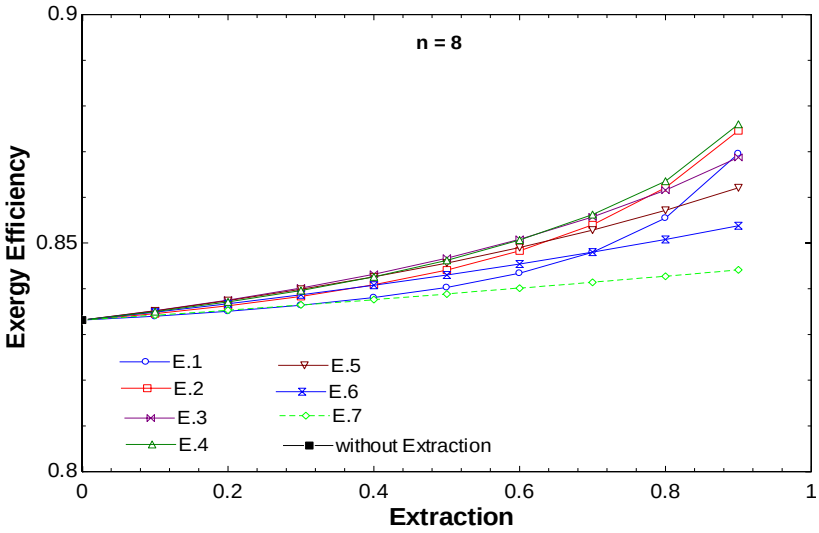

(c)

Figure 3.10 change in the exergy efficiency of the forward feed MED-MVC with Extraction for (a) n = 4 Effects (b) n = 6 Effects (c) n = 8 Effects.

3.4.5 The effect of the number of compressors

This section addresses the selection of the appropriate number of secondary compressors to the system. In order to analyze this case, a system of 4 effects is selected and the addition of more compressors associated with various effects is studied. Cases include using two compressors associates with effects 1 and 2, effects 1 and 3, effects 2 and 3 and finally, attaching a secondary compressor to each effect and for each of these cases, the extraction rate is changed. Figure 3.11 shows that although all of these options results in an increases water desalination rate, the power increases due to the addition of more compressors. The best performance is associated with using a single "secondary" compressor that extracts formed vapor in the second effect. To generalize, using an additional "secondary" compressor located at the exit of the vapor formed in the effect "N/2" yields the best results in terms of specific power consumption.

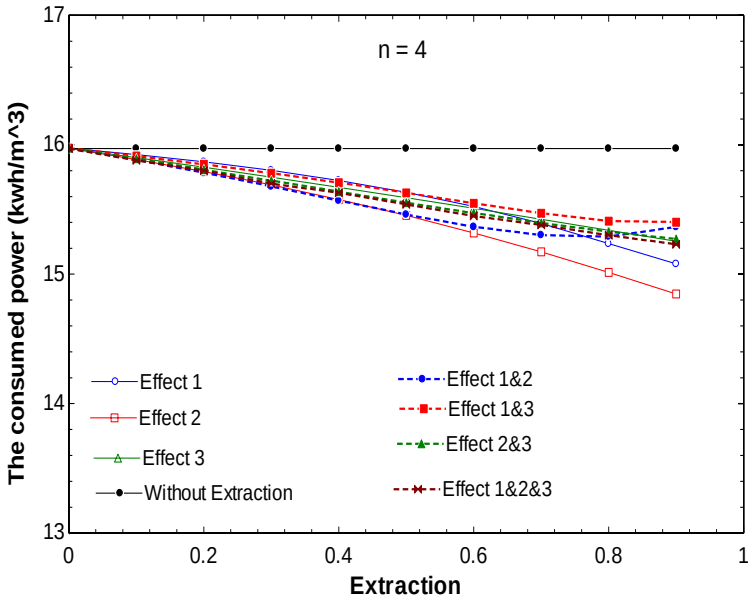

Figure 3.11 Comparisons between MED-MVC Forward Feed with addition of more compressors

CHAPTER 4

Parallel feed Multi-Effect Distillation with Mechanical Vapor Compression

In this Chapter, a modification to the original (conventional) layout of the parallel feed MED system is investigated. It includes adding a smaller compressor that extracts a portion of the vapor from one of the effects, compresses it to the state of the vapor entering to the first effect. Then this vapor is mixed with the vapor compressed in the main compressor before it enters to the first effect tube side to condense and hence enhance the heat transfer (and accordingly, evaporation rate of sprayed seawater) in the first effect.

4.1 Parallel feed Multi-Effect Distillation with two Mechanical Vapor Compressors

MED-MVC parallel Feed is a thermal desalination process (Fig 4.1); the saline water (Feed water) is sprinkled or otherwise spread onto the surface area of the effect (Evaporator) surface (Ordinarily horizontal tubes). The tubes in the evaporator of the first effect are heated by steam compressed in the mechanical vapor compressor. The vapor produced at the first effect is condensed in the tubes of the second effect, where again vapor is created. The other effects are heated by vapor created in each previous effect. Each effect has a lower temperature and pressure compared to the previous one. The vapor created in the last effect is compressed in the mechanical vapor compressor to superheated condition before it enters to the tubes of the first effect as the heating fluid.

Fig 4.2 shows the modified Multi Effect Desalination system with mechanical vapor compression system (MED-MVC) for parallel feed arrangement with additional secondary compressor. The secondary compressor receives a portion of the vapor formed in one of the other effects (1 to n-1) and compresses it to the same condition of the vapor leaving the main compressor. Both vapor streams are mixed together before they flow to the tubes of the first effect to preheat the sprayed seawater on the outer surface of the tubes and evaporate some of it. Although the layout shown in Fig. 4.2 illustrates connection of the secondary compressor to the exit of the first effect, we will study the effect of changing its location.

In the parallel cross system arrangement, the vapor formed in effects 2 to n is generated by boiling over the heat transfer surfaces and by flashing or free boiling within the liquid bulk. The temperature of the vapor formed by flashing is less than the effect boiling temperature by the boiling point elevation and the non-equilibrium allowance. Another small quantity of vapor is formed in the flashing box due to the flashing of distillate condensed in effect i. The flashed off vapor is produced at a temperature lower than the distillate condensation temperature by the non-equilibrium allowance. The flashing boxes offer a means for recovering heat from condensed fresh water. The boiling point elevation and temperature depression corresponding to pressure loss in the demister, transmission lines and during the condensation process reduces the available driving force for heat transfer in the evaporators and the preheaters.

The effects numbers start from (1 to n) and the direction of the vapor flow from are from left to right. An effect constitutes a heat transfer surface area (tubes), a vapor space, a demister and a brine pool to collect the un-evaporated brine.

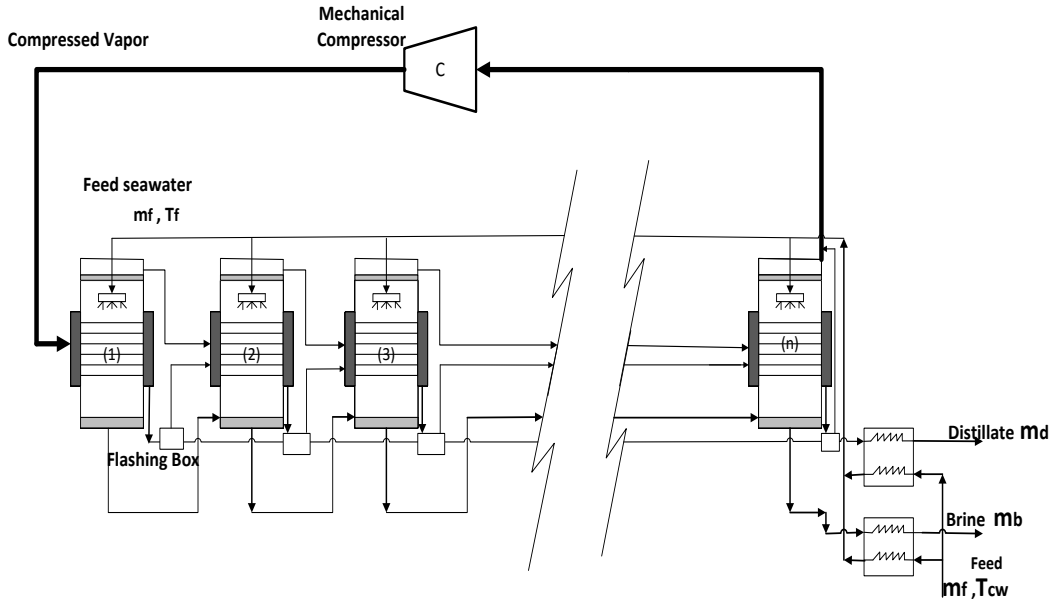

Figure 4.1 Parallel feed MED-Mechanical vapor compression.

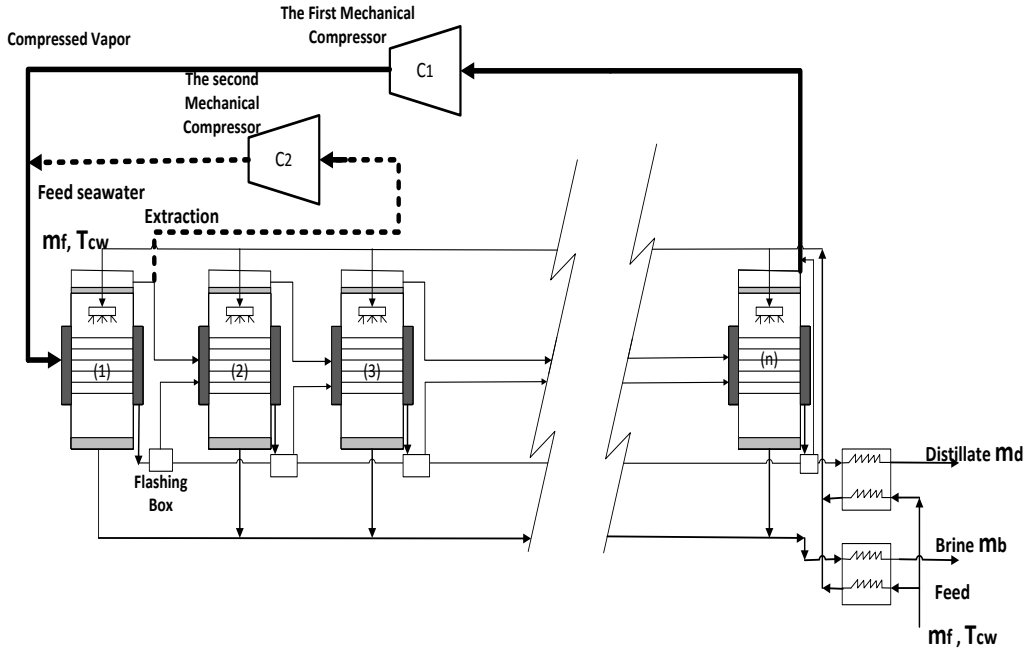

Figure 4.2 Parallel feed MED with Two Mechanical vapor compressors.

4.2 Mathematical model of MED-MVC for Parallel feed

The mathematical model for equations for effect (i) include mass and energy balance equations in addition to the calculation of the required heat transfer area. Then second law analysis is carried out.

Data generated are related to:

- Distillate flow rate ($\dot{m}_d$).
- Brine flow rate ($\dot{B}_n$).
- Heat transfer (H.T) area.
- Temperatures of streams entering and leaving each effect.

Material and heat balances for flash boxes and the two preheaters are also included in this model.

Model assumptions

- Specific heat at constant pressure, C_p for the seawater is calculated as a function of both temperature and salinity.
- Model variations in the thermodynamic losses (BPE, non-equilibrium allowance inside the evaporators and the flashing boxes, temperature depression corresponding to the pressure drop in the demister) from one effect to another.
- Variable physical properties of water.
- The heat transfer equations model the heat transfer area in each evaporator as the sum of the area for brine heating and the area for evaporation.

The number of mass, energy and material balance equations, which can be written for any effect, is three (mass balance equation, energy equation and the salt balance equation).

There is an equation for Heat transfer rate in any effect. It relates the thermal load to the overall coefficient of heat transfer, the area, and temperature (driving force for heat transfer).

Brine Flow rate, $\dot{B}_1, \dot{B}_2, \ldots, \dot{B}_{n-1}, \dot{B}_n$ (n unknowns)

Distillate flow rate, $\dot{D}_1, \dot{D}_2, \ldots, \dot{D}_{n-1}, \dot{D}_n$ (n unknowns)

Effect temperature, $T_1, T_2, \ldots, T_{n-1}$ (n-1 unknowns)

Heat transfer (H.T) area (1 unknown)

Flow rate of steam (1 unknown)

Total = (4n) unknowns

Parameters to be specified before solution:

- Heating steam temperature, T_s.
- Temperature in the last effect (n), T_n.
- Salt concentration leaving last effect (n),X_n.
- Distillate flow rate ($\dot{m}_d$).
- Salt concentration of feed (X_f).

4.2.1 Model equations

Mass balance: $B_i = F_i - \dot{D}_i$ (1)

Salt concentration balance:

$$X_{B_i} * \dot{B}_i = X_{F_i} * F_i \quad (2)$$

From equation (1) & (2) we get:

$$\dot{B}_i = \left(\frac{X_{F_i}}{X_{B_i} - X_{F_i}}\right) * \dot{D}_i \quad (3)$$

Energy Balance:

The energy balance is given by (This equation applies for effects 2 to n):

$$\dot{D}_{i-1} h_{fg,v(i-1)} + \dot{D}_{f(i-1)} h_{fv(i-1)} = F_i C_{pi} (T_i - T_f) + \dot{D}_i h_{fg,vi} \quad (4)$$

Flow rate of vapor flashed off in the distillate flashing boxes

$$\dot{D}_{fi} = \dot{D}_{i-1} * C_{p(i-1)} * \frac{\Delta T}{h_{fg,v(i-1)}} \quad (5)$$

For first effect:

$$\dot{D}_1 * h_{fg,v1} = \dot{m}_s * h_{fg,s} \quad (6)$$

$$\dot{D}_1 = xx * m_{v1} + m_{vn}$$

Note that, although the vapor leaves both compressors at a slightly superheated state, heat losses in the pipes results in losing its superheat such that it enters to the first effect as saturated vapor. It can also be assumed that the vapor leaving the compressors is in saturation condition and the losses in the pipes are neglected such that the vapor enters to the first effect in the same state.

Mass of vapor at first effect (m_{v1}):

$$\dot{D}_1 h_{fg,v1} = F_2 C_{p2}(T_2 - T_f) + m_{v1} * h_{fg,vi} \quad (7)$$

In this equation, the secondary compressor is placed at the exit of the first effect (Fig. 4.1) such that the vapor leaving the first effect would be splitted into two streams.

Distillate flow rate at second effect with extraction (xx) after first effect:

$$\dot{D}_2 = (1 - xx) * m_{v1}$$

Where:

m_{v1} = mass of the vapor formed in the first effect.

For effects i:

$$A_i * U_i * \Delta T_{loss} = \dot{D}_i * h_{fg,vi} + F_i C_{pi}(T_i - T_f) \quad (8)$$

Total Temperature drop:

$$\Delta T = T_s - T_n \quad (9)$$

This drop is equal for each effect;

$$\Delta T = \Delta T_1 + \Delta T_2 + \cdots + \Delta T_{n-1} + \Delta T_n \quad (10)$$

From above equations Find:

$$\Delta T_1 = \frac{\Delta T_t}{U_1 \sum_{i=1}^{n} \frac{1}{U_i}} \quad (11)$$

Actual Temperature profile:

For first effect:

$$T_1 = T_s - \Delta T_1 \quad (12)$$

For effects 2 to n:

$$T_i = T_{i-1} - \Delta T_1 \frac{U_1}{U_i} \quad (13)$$

Distillate flow rate:

$$\dot{m}_d = \dot{D}_1 + \dot{D}_2 + \cdots + \dot{D}_{n-1} + \dot{D}_n \quad (14)$$

Flow rate of brine in first effect:

$$\dot{B}_1 = \dot{m}_f - \dot{D}_1 \quad (15)$$

$$\dot{B}_i = \dot{B}_{i-1} - \dot{D}_i \quad (\text{i= 2… n}) \quad (16)$$

$$X_1 = X_f * (\dot{m}_f / \dot{B}_1) \quad (17)$$

$$X_i = X_{i-1} * (\dot{B}_{i-1} / \dot{B}_i) \quad (18)$$

Heat Transfer Area:

In First effect:

$$A_1 = \left(F_1 C_{p1}(T_1 \dot{-} T_f) + D_1 * h_{fg,v1}\right) / \left(U_1(T_s - T_1)\right) \quad (19)$$

Specific heat transfer area (sA):

$$sA = \frac{\sum_{i=1}^{n} A_i}{\dot{m}_d} \quad (20)$$

Heat exchangers (preheaters) thermal load $\dot{Q}_h$:

$$\dot{Q}_h = \dot{m}_d * c_p * (T_d - T_o) + \dot{B}_n * c_p * (T_b - T_o) \quad (21)$$

Where:

$$T_o = (T_{cw} - T_f) + \left(\frac{X_f}{X_b}\right) * T_b + \left(\frac{X_b - X_f}{X_b}\right) * T_d$$

The specific power consumption:

Total power consumption (w)

$$w = w_k + w_s \quad (22)$$

The consumed power of the first compressor w_s

$$w_s = m_{vn} \frac{\gamma}{\eta(\gamma-1)} P_{vn} v_{vn} \left[\left(\frac{P_s}{P_{vn}}\right)^{\frac{\gamma-1}{\gamma}} - 1\right] \quad (23)$$

The consumed power of the second compressor w_k

$$w_k = (xx * m_{v1}) \frac{\gamma}{\eta(\gamma-1)} P_{v1} v_{v1} \left[\left(\frac{P_s}{P_{v1}}\right)^{\frac{\gamma-1}{\gamma}} - 1\right] \quad (24)$$

The Entropy Generation

In general the entropy generation,

$$S_{gen} = \sum \dot{m}_e s_e - \sum \dot{m}_i s_i \quad (25)$$

The entropy generation for first compressor, $S_{gen.c1}$:

$$S_{gen.c1} = xx * m_{v1} * (s_{T_s} - s_{T_{v1}}) \quad (26)$$

The entropy generation for first compressor, $S_{gen.c2}$:

$$S_{gen.c2} = m_{vn} * (s_{T_s} - s_{T_{vn}}) \quad (27)$$

Where:

$s_{T_{vn}}$ = The specific entropy at, T_{vn}.

For first effect:

$$S_{gen.1} = \left[m_{v1} * s_{T_{v1}} + \dot{D}_1 * s_{T_1} + \dot{B}_1 * s_{T_1}\right] - [\,(xx * m_{v1} + m_{vn}) * s_{T_s} + F_1 * s_{T_{f1}}] \quad (28)$$

Second Effect:

$$S_{gen.2} = \left[\dot{D}_3 * s_{T_{v2}} + \dot{D}_2 * s_{T_2} + \dot{B}_2 * s_{T_2}\right] - \left[\dot{D}_2 * s_{T_{v1}} + F_2 * s_{T_{f1}}\right] \quad (29)$$

For effects 3 to (n-1):

$$S_{gen.i} = \left[\dot{D}_{i+1} * s_{T_{vi}} + \dot{D}_i * s_{T_i} + \dot{B}_i * s_{T_i}\right] - \left[F_i * s_{T_{f1}} + \dot{D}_i * s_{T_{v(i-1)}}\right] \quad (30)$$

For the last Effect:

$$S_{gen.n} = \left[m_{vn} * s_{T_{vn}} + \dot{D}_n * s_{T_n} + \dot{B}_n * s_{T_n}\right] - \left[F_1 * s_{T_{f1}} + \dot{D}_n * s_{T_{v(n-1)}}\right] \quad (31)$$

Where:

Then the total entropy generation $S_{gen.total}$:

$$S_{gen.total} = S_{gen.c1} + S_{gen.c1} + \sum_{i=1}^{n} S_{gen.i} \quad (32)$$

Where:

$S_{gen.i}$= the entropy generation at effect i. (i= 1….n)

Exergy Efficiency

Exergy Efficiency is a measure of the performance of the system that shows the components of the system where more losses are associated. It gives an indication to system designers of the locations that require further enhancements for better system performance. The exergy balance of the vapor compressor is developed as follows:

The exergy efficiency η_{II}

$$\eta_{II} = \frac{\dot{E}_{vapor,out} - \dot{E}_{vapor,in}}{w_{rev}} \quad (33)$$

$\dot{E}_{vapor,out} = \dot{m}_v(h_v - h_o - T_o(s_v - s_o))$

The exergy efficiency η_{II} first (main) compressor w_k

$$\eta_{II,n} = \frac{\dot{m}_{vn}(h_{g,n} - h_{g,s} - T_o(s_{g,n} - s_{g,s}))}{w_{rev}}$$

The exergy efficiency η_{II} second compressor w_k

$$\eta_{II,1} = \frac{\dot{m}_{v1}(h_{g,1} - h_{g,s} - T_o(s_{g,1} - s_{g,s}))}{w_{rev}}$$

The exergy efficiency

$$\eta_{II} = \frac{\dot{m}_{vn}\left(h_{g,n} - h_{g,s} - T_o\left(s_{g,n} - s_{g,s}\right)\right) + \dot{m}_{v1}\left(h_{g,1} - h_{g,s} - T_o\left(s_{g,1} - s_{g,s}\right)\right)}{w_{rev}}$$

Conditions

- Numbers of effects (n) are 4 and 6, 8.
- The salinity of seawater X_{cm}, and the temperature T_{cw}, are 42000 ppm and 25^{o}C.
- The salinity of rejected brine, X_b= 72000 ppm.
- The temperature of steam, T_s= 60^{o} C.
- The feed water temperature, T_f = 35^{o} C.
- The temperature in the final effect, T_n= 40^{o}C.
- The flow rate of distillate, m_d = 1 kg/s.
- The compressor efficiency, η = 76 %.

4.3 Validation of MED parallel feed

The results are compared with the case presented by Darwish and Abdulrahim [39] for parallel feed multi effect distillation system subject to the following condition:

- Numbers of effects (nn) = 4.
- The salinity of seawater X_{cm}, and the temperature T_{cw}, are 46 g/l and 28^{o} C.
- The salinity of rejected brine, X_b = 69 g/l.
- Top Boiling Temperature, T_1 = 64^{o} C.
- The feed water temperature, T_f = 32.3 ^{o} C.
- The temperature in the final effect, T_n = 36 ^{o} C.
- The flow rate of distillate, m_d = 52.616 kg/s.

  The results of the comparison are shown in Table 4.1 for conventional multi effect desalination with mechanical vapor compression in Parallel feed arrangement (MED-

MVC-PF) with one major compressor (original case). The table shows that the maximum deviation in the results does not exceed 0.22%.

Table 4.1 Validation of the MED-MVC-PF model with Darwish and Abdelrahim [39].

Effect	T		Error %	F		Error %	D		Error %
	[39]	Model		[39]	Model		[39]	model	
1	64	64	-	40.96	40.9	0.1465	13.65	13.64	0.0733
2	54.7	54.67	-	38.033	38	0.0868	12.68	12.67	0.0789
3	45.3	45.3	-	38.013	38.02	0.018	12.67	12.67	0
4	36	36	-	40.845	40.91	0.159	13.61	13.64	0.22

4.4 Results and Discussion

4.4.1 Specific power consumption

The specific power consumption in MED-MVC-PF depends on the rate of extracted vapor leaving any effect to enter the secondary compressor as well as the steam entering to the first effect, the compression ratio (since its temperature increases as a result of the change in its pressure) , and the number of effects.

Figs. 4.3 (a), (b), (c) show the variation of the specific power of the system with the extracted vapor entering the secondary compressor compared with the original case of no secondary compressor (original case) for systems of 4 effects (Fig. 4.3 a), 6 effects (Fig. 4.3 b) and 8 effects (Fig. 4.3 c). As depicted, in Fig 4.3 the specific power decreases with the increase in extraction rate because of the increase in the rate of steam that enters the first effect as a result of combined flow rates from both compressors. This, in turn, results

in an increased rate of evaporation of sprayed seawater in the first effect and results in more formed vapor in all effects and accordingly higher productivity or in other words, less power to produce a unit desalinated water flow rate. The decrease in the vapor specific volume at higher operating temperature also contributes to reduction in the specific power for vapor compression.

Comparing the specific power in Figures 4.3 (a), (b), (c), we notice that the increase in the specific power consumption corresponds to systems of lower number of effects. Thus, a general observation is made here that lower values of the specific power is at a higher value of Extraction occurs in the effect (n/2). Figure 4.4 (a), (b), (c) show the variation of the work ratio (w_k/w_s) of the system with the extraction.

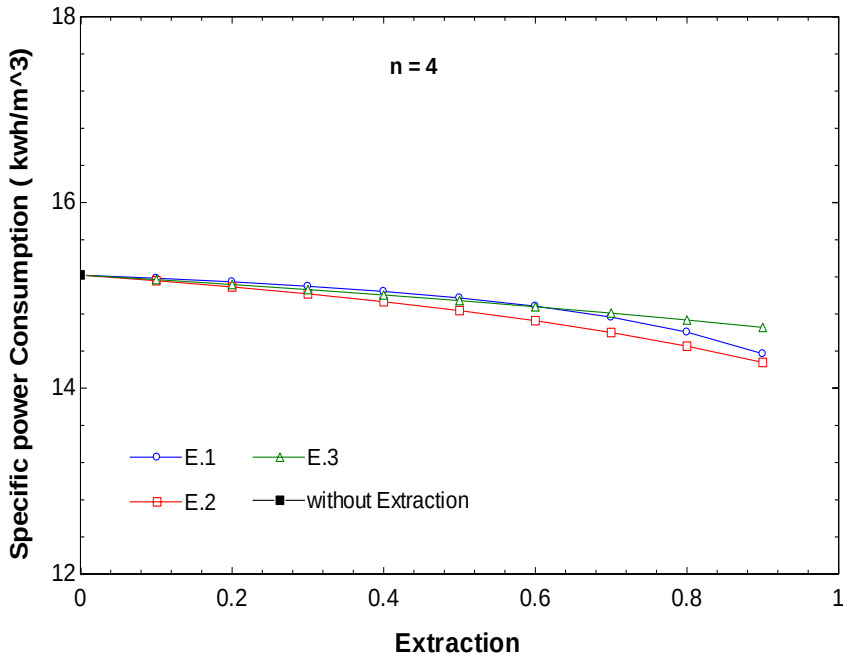

(a)

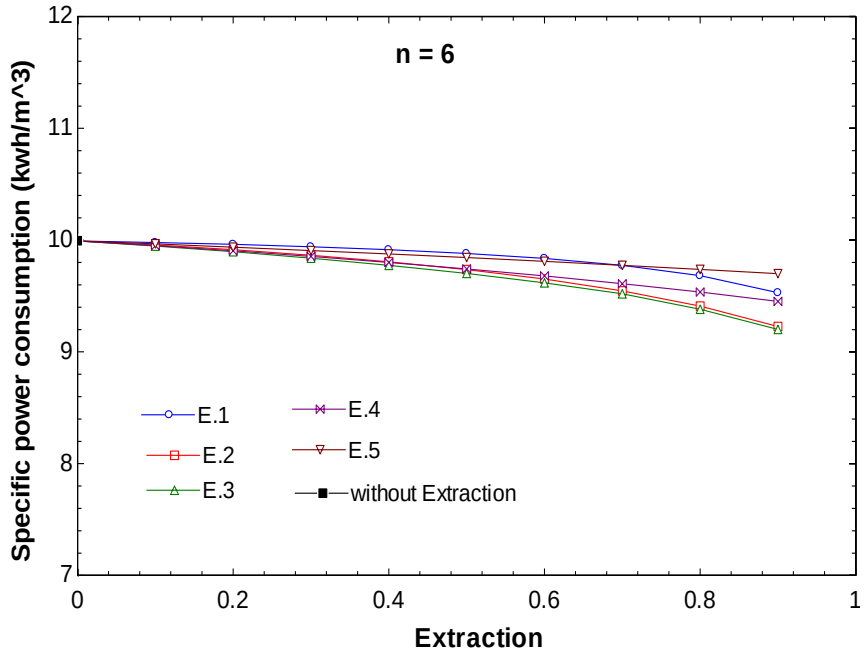

(b)

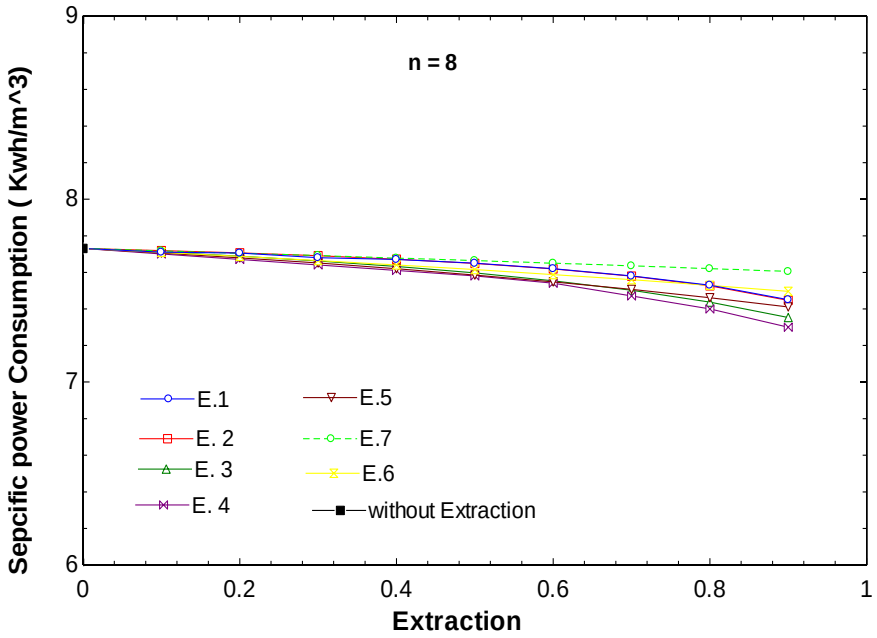

(c)

Figure 4.3 change in the consumed power for the parallel feed (MED-MVC) with Extraction for (a) n = 4 effects (b) n = 6 effects (c) n = 8 effects.

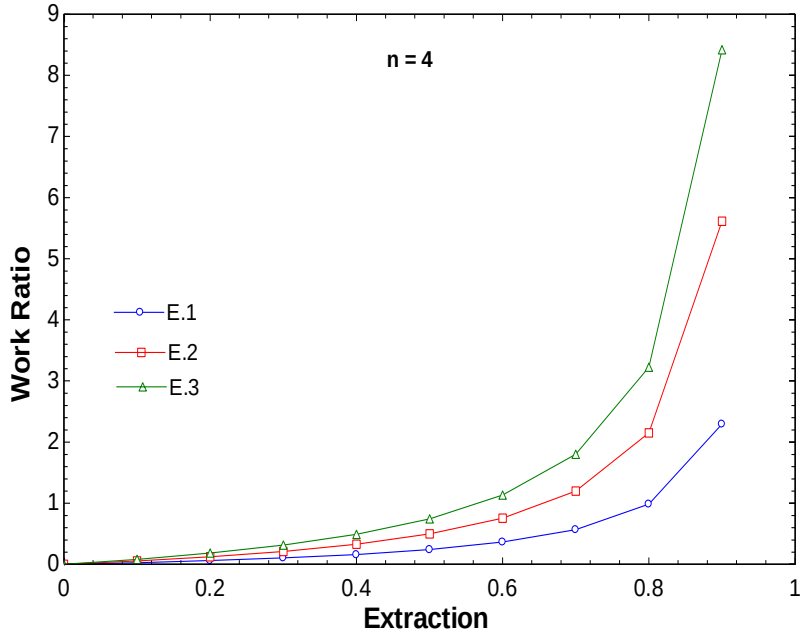
n = 4
Work Ratio
Extraction
E.1
E.2
E.3
0
1
2
3
4
5
6
7
8
9
0
0.2
0.4
0.6
0.8
1

(a)

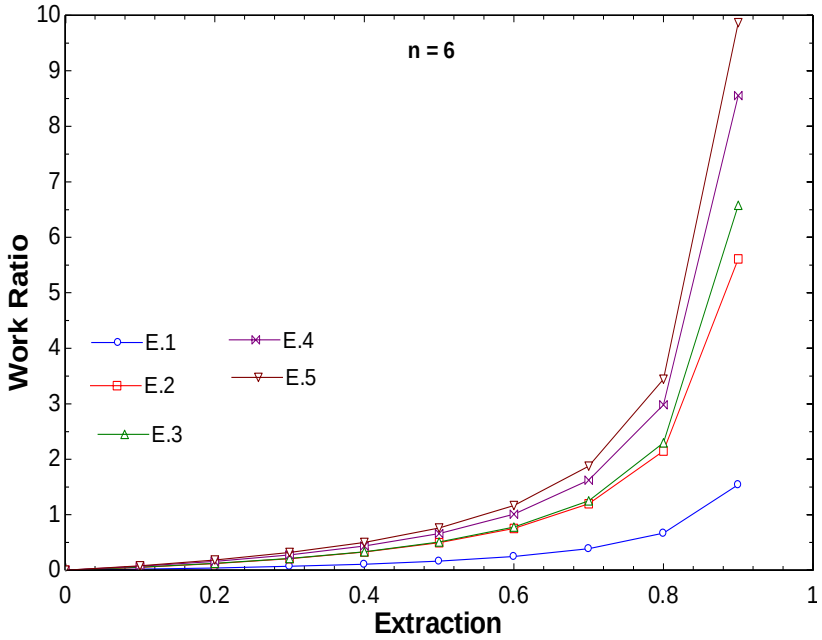
n = 6
Work Ratio
Extraction
E.1
E.2
E.3
E.4
E.5
0
1
2
3
4
5
6
7
8
9
10
0
0.2
0.4
0.6
0.8
1

(b)

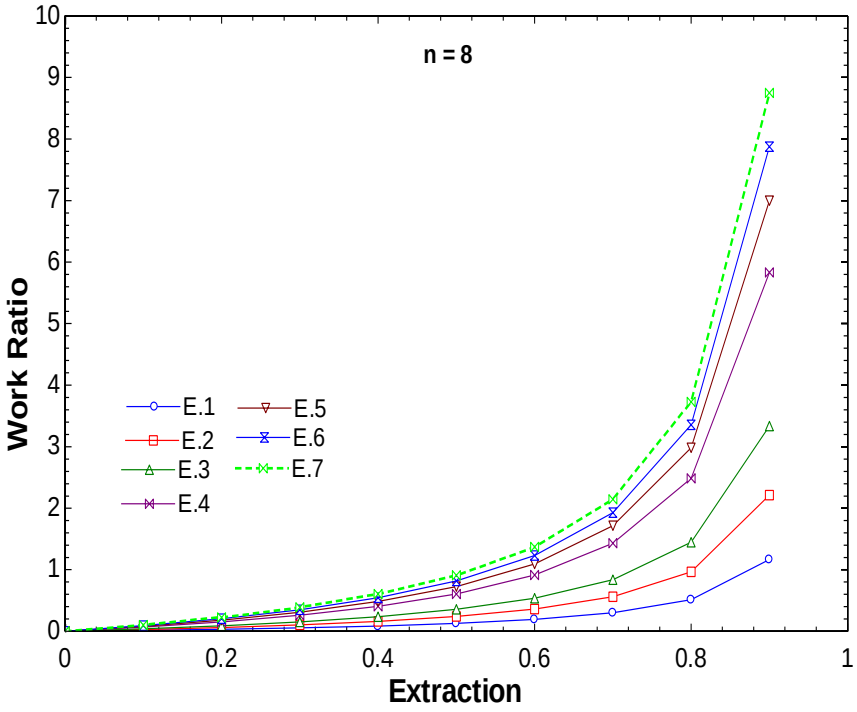

(c)

Figure 4.4 Change in the work ratio of the parallel feed MED-MVC with Extraction for (a) n = 4 Effects (b) n = 6 Effects (c) n = 8 Effects

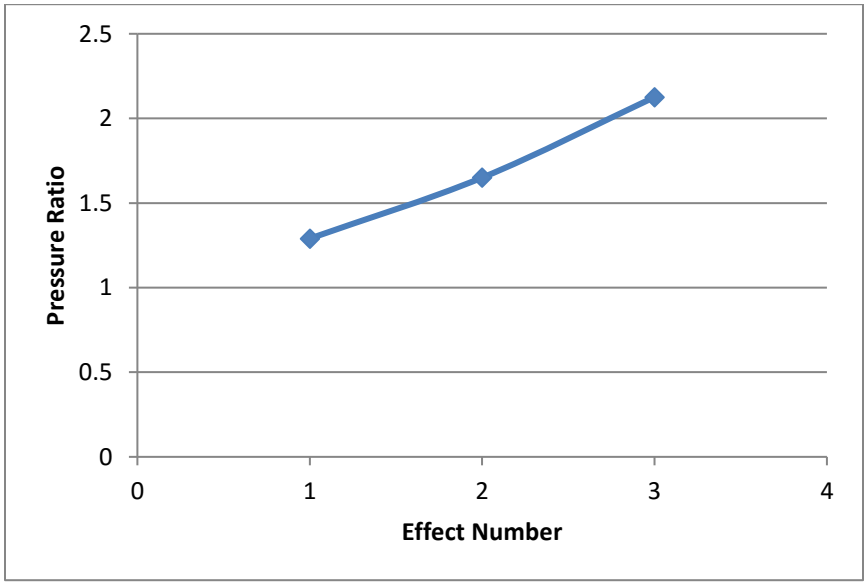

Figure 4.5 change of the pressure ratio for secondary compressor for n = 4 effects

Figure 4.5 shows the increase in the pressure ration that corresponds to the relocation of the secondary compressor to receive formed vapor from effects 1, 2 and 3 for a 4-effect system. The pressure ration increases as the extraction point is delayed to later effects due to the monotonic decrease in pressure as the vapor flows from on effect to the other to maintain evaporation in all effects while the first effect is at the maximum pressure and temperature. This trend is similar to the Forward feed case qualitatively.

4.4.2 Specific heat transfer area

Specific heat transfer area is the sum of the total area of the system per distillate flow rate. The specific heat transfer area in MED-MVC parallel Feed is dependent on distillate rate per effect as well as the latent heat of condensation at the temperature at which the vapor leaves the effect as well as Feed water per effect and the number of effects.

Figs 4.6 (a), (b), (c) show the variation of the specific heat transfer area of the system with the extracted vapor entering the secondary compressor compared with the original case of no secondary compressor for systems of 4 effects (Fig. 4.6 a), 6 effects (Fig. 4.6 b) and 8 effects (Fig. 4.6 c). The figures show that the specific heat transfer area (sA) to be constant with extraction rate. When the extraction of formed vapor to the secondary compressors occurs at any effect, the specific heat transfer area is constant due to the low latent heat (corresponding to maximum temperature) as well as the decrease of the distillate flow rate and Feed water rate that flows to the next effects. Generally, it is observed in Figs. 4.6 (a), (b), (c) that the heat transfer area decreases as the extraction increases. It obvious that the specific heat transfer area for the effect is higher than its previous effect at the same extraction because of the decrease in the temperature of the vapor formed in the effect where extraction of vapor occurs.

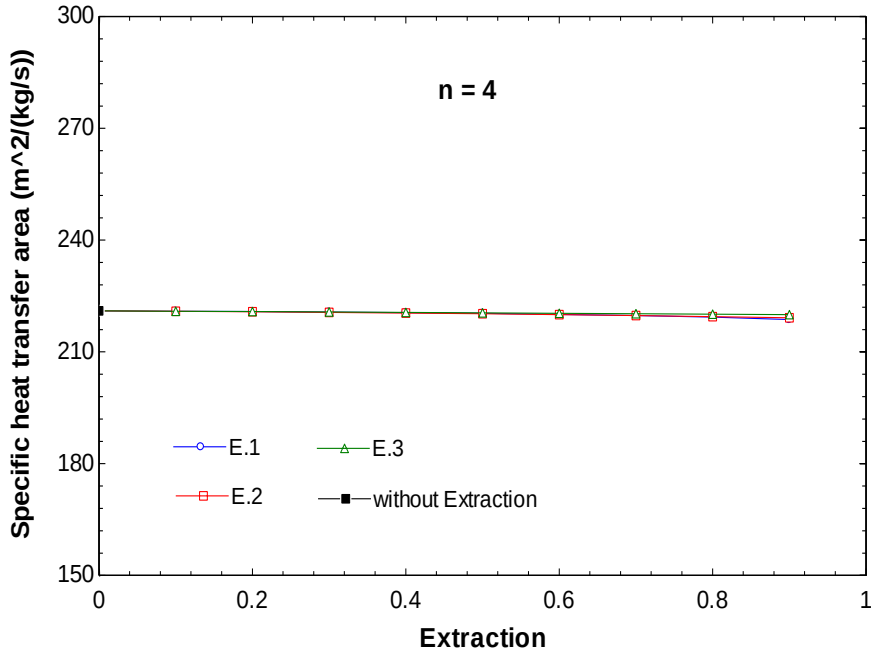
n = 4
Specific heat transfer area (m^2/(kg/s))
Extraction
E.1
E.2
E.3
without Extraction
300
270
240
210
180
150
0
0.2
0.4
0.6
0.8
1

(a)

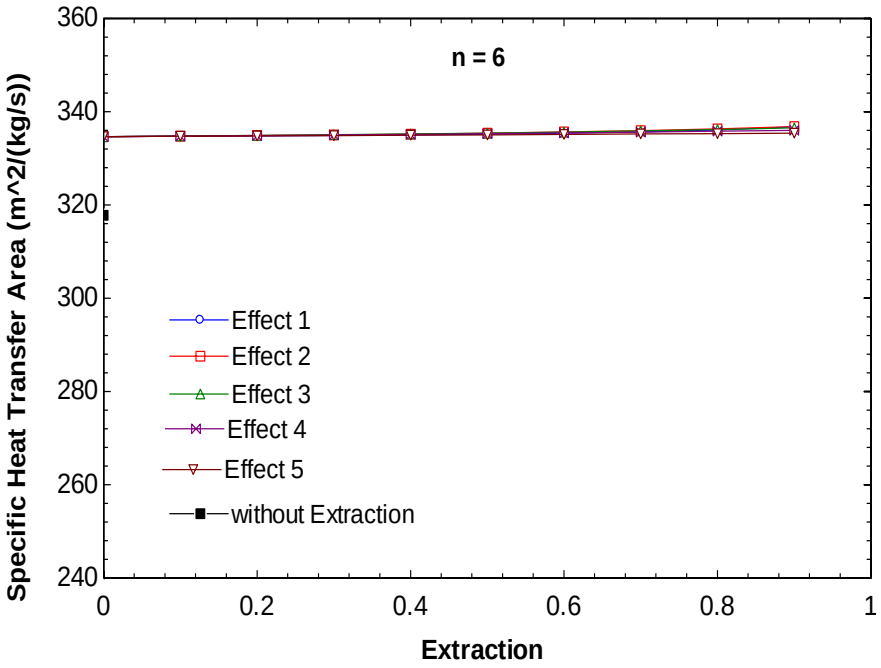
n = 6
Specific Heat Transfer Area (m^2/(kg/s))
Extraction
Effect 1
Effect 2
Effect 3
Effect 4
Effect 5
without Extraction
360
340
320
300
280
260
240
0
0.2
0.4
0.6
0.8
1

(b)

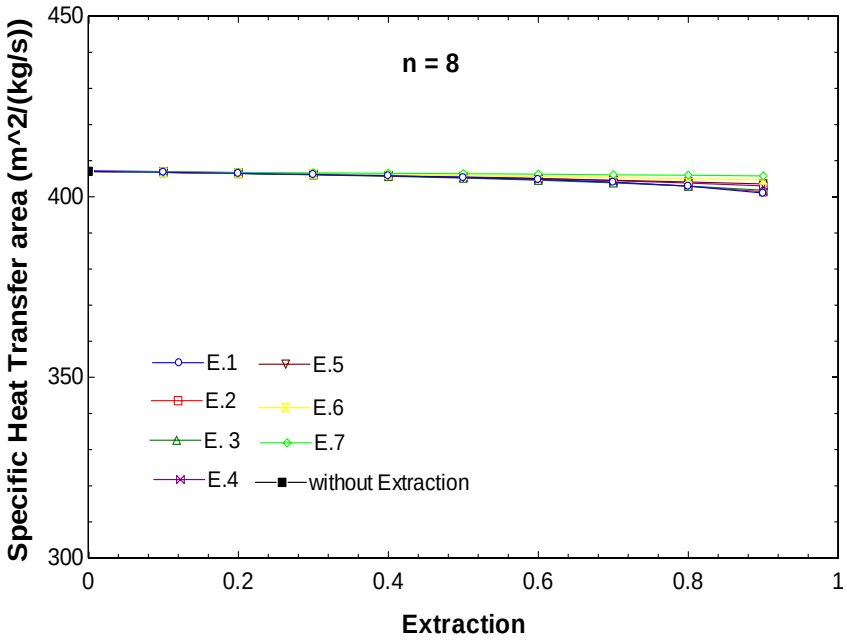

(C)

Figure 4.6 Specific heat transfer area of the parallel feed MED-MVC with Extraction for (a) n = 4 Effects (b) n = 6 Effects (c) n = 8 Effects.

4.4.3 Entropy generation

Entropy generation (S_{gen}) is a measure of the performance of the system that shows the components of the system where more losses are associated. Entropy is an extensive property created through the process. It gives an indication to system designers of the locations that require further enhancements for better system performance. The net entropy change of the effects and the entropy change of the compressors are balanced by the Entropy generation. The entropy change for the effects depends on the Extraction, the flow rate and the temperature of the distillate, the temperature of the brine, the flow rate and the temperature of the Feed water, the vapor temperature of the effect, and the number of effects.

Fig 4.7 (a), (b), (c) show the total entropy generation with the rate of extraction. Entropy generation of the compression increases due to the addition of a secondary compressor. In addition the entropy generation increases with the Extraction due to increased flow to the secondary compressor. Figures 4.7 shows that the Total entropy generation increases with the increase in the number of effects due to the increase in the entropy generation in each effect.

The entropy generation at Fig 4.7 (a), (b), (c) increases with the decrease the consumed power. (S_{gen}) increases gradually with the Extraction due to increase the entropy change of a closed system.

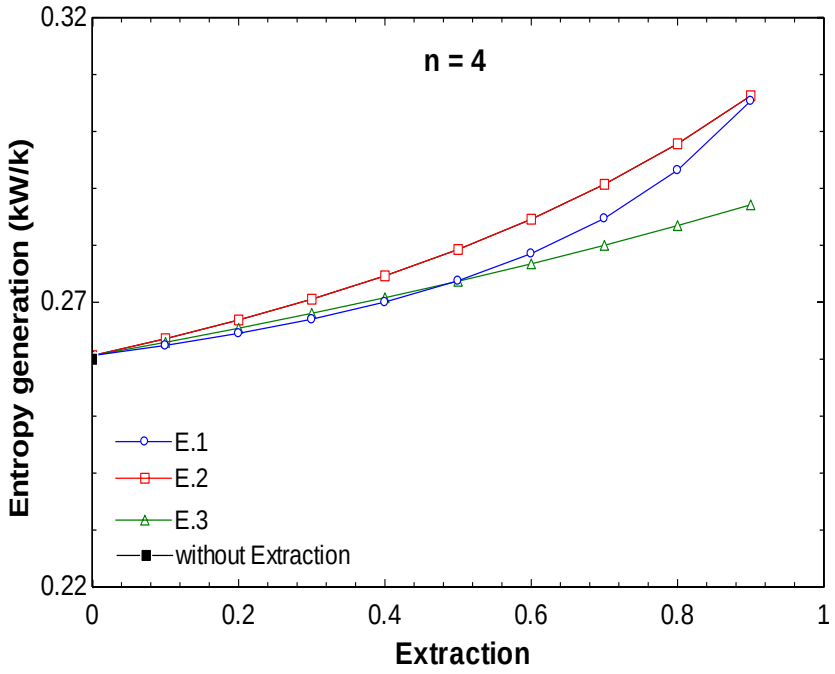

(a)

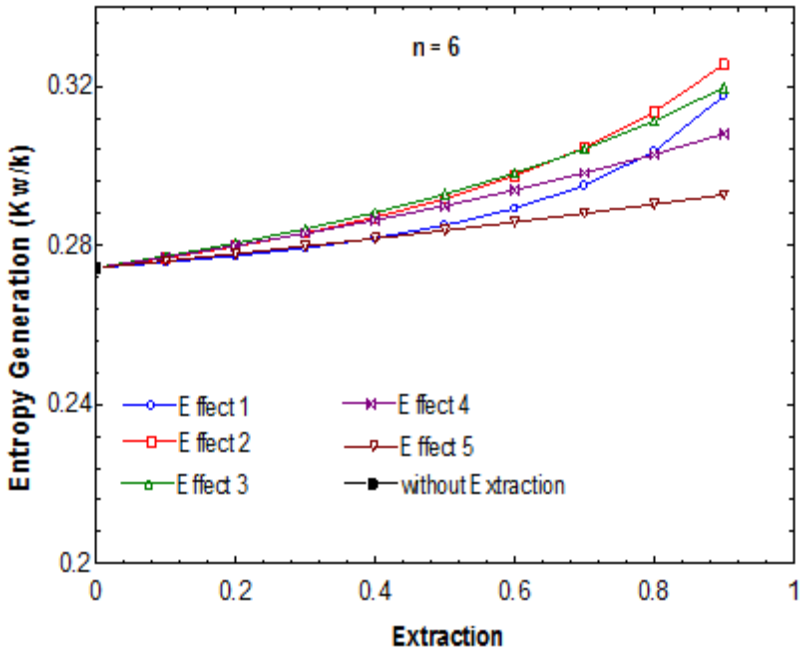

(b)

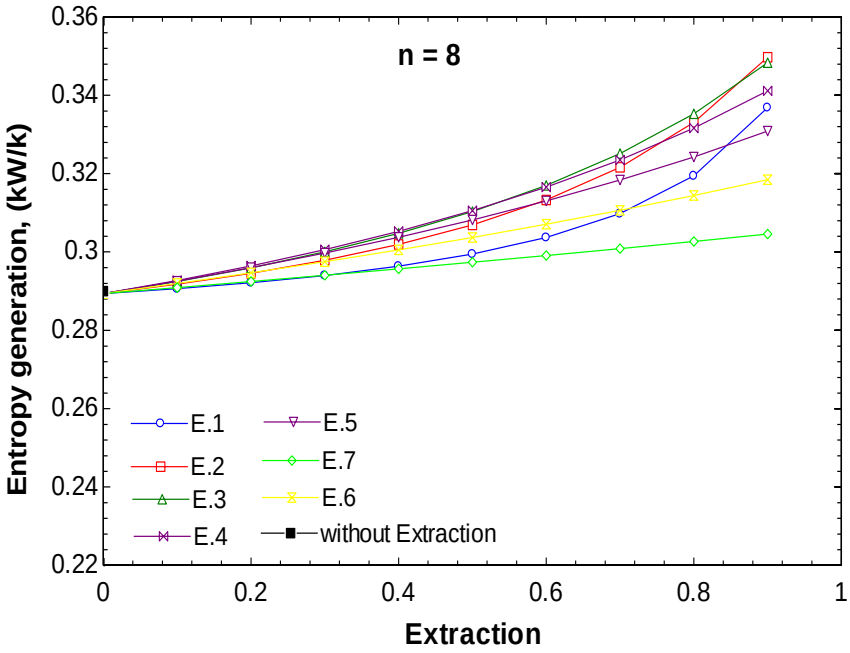

(c)

Figure 4.7 Entropy generation of the parallel feed MED-MVC with Extraction for (a) n = 4 Effects (b) n = 6 Effects (c) n = 8 Effects.

4.4.4 Exergy Efficiency

The exergy efficiency result is similar to the forward feed MED-MVC the exergy efficiency change with the rate of extraction. Fig 4.8 show the variation of the exergy efficiency of the system with the extracted vapor, the exergy efficiency increases with the increase in extraction rate due to decrease the total specific power consumption.

Fig 4.8 (a) shows that the exergy efficiency increases with increased extraction percentage. Furthermore, it is obvious that the relation between the exergy efficiency with the change in the point of extraction. It can be noticed that higher exergy efficiency occurs when vapor is extracted at the middle location of the extraction (n = 2).

Fig 4.8 (b), (c) shows similar trend of exergy efficiency dependence on the system with the percentage of vapor extracted and the location where the secondary flow (extracted vapor) takes place. It is also shown that extracting the vapor at effect (3), (4) resulted in the highest exergy efficiency, and hence better system performance.

Thus, a general observation is made here that higher values of the exergy efficiency correspond to a higher value of extraction that occurs in the effect (n/2).

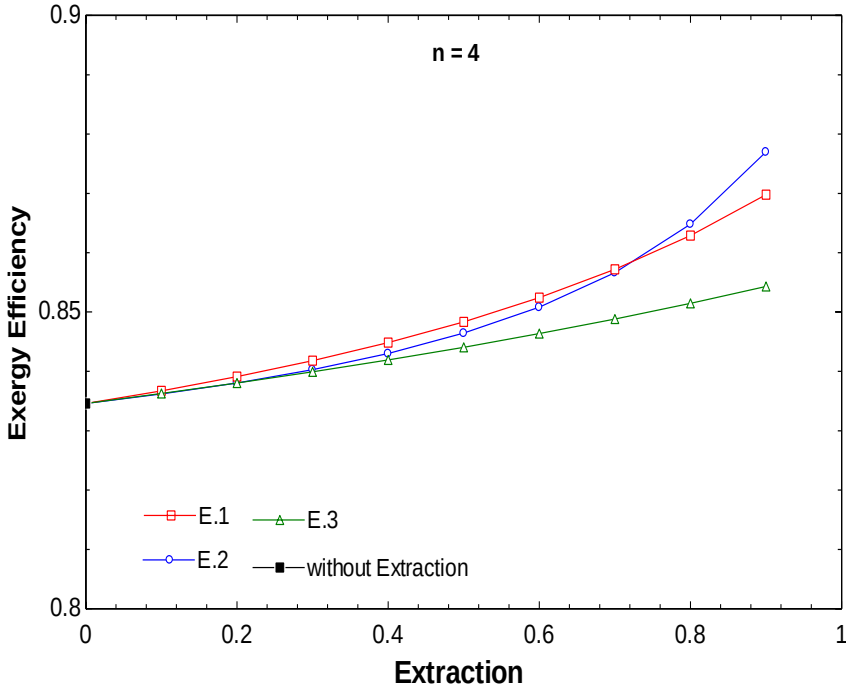
n = 4
Exergy Efficiency
Extraction
0.9
0.85
0.8
0
0.2
0.4
0.6
0.8
1
E.1
E.3
E.2
without Extraction

(a)

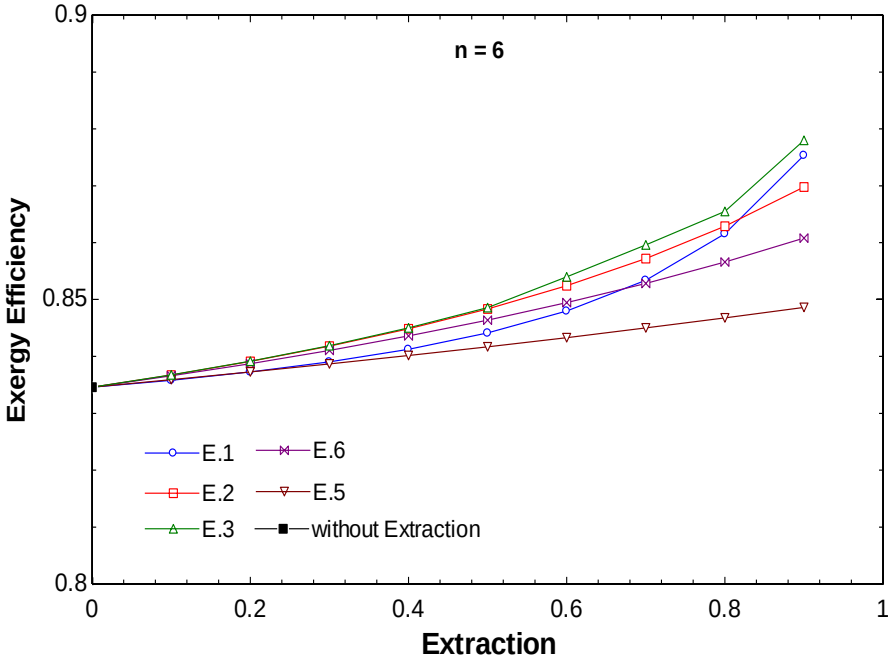
n = 6
Exergy Efficiency
Extraction
0.9
0.85
0.8
0
0.2
0.4
0.6
0.8
1
E.1
E.6
E.2
E.5
E.3
without Extraction

(b)

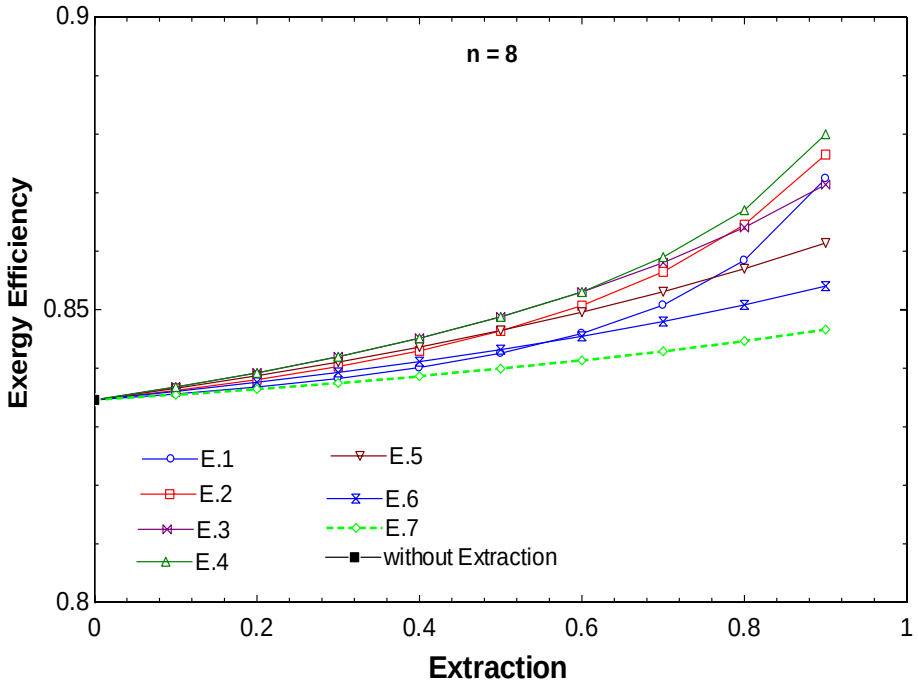

(c)

Figure 4.8 change in the exergy efficiency of the parallel feed MED-MVC with Extraction for (a) n = 4 Effects (b) n = 6 Effects (c) n = 8 Effects.

CHAPTER 5

Parallel Cross feed Multi-Effect Distillation with Mechanical Vapor Compression

In this Chapter, the Multi effect desalination system with Parallel Cross feed arrangement operated mechanically though a compressor (MED-PC–MVC) is analyzed. It is similar to the previous case (PF-MED-MVC), except that the brine leaving an effect is admitted to the brine pool of the next effect where it flashes due to pressure difference and hence produces some more vapor. This vapor increases the total vapor formed in each effect and hence improved the unit productivity for the same energy input. A secondary compressor is used and the effect of adding it on the performance and surface area is investigated.

5.1 Parallel Cross feed Multi-Effect Distillation with two Mechanical Vapor Compressors

Parallel Cross Feed MED-MVC is a thermal desalination process (Fig. 5.1) where the Feed-water is sprinkled or otherwise spread onto the surface of the horizontal evaporator tubes in an effect. Fig 5.2 shows a MED-MVC parallel cross feed with two mechanical vapor compressors similar to Parallel Cross Feed MED-MVC shown in Fig. 1 with the exception of adding another (secondary) compressor. The MED-MVC-PC system uses heat exchangers since the vapor leaving the last effect is forwarded to the suction side of the main compressor. Therefore, no condensers are needed for this arrangement too. The vapor formed in the last effect that is fed into the suction side of the compressor where it

is compressed to the desirable super-heated state identified by a preset temperature and pressure. Another stream of formed vapor is extracted from one of the other effects where it is compressed to the same state before mixing with the feed steam leaving the main compressor. Then, both are admitted to the tube side of the first effect as the system source of energy to raise the temperature of the feed seawater to the saturation state and eventually evaporate some of it in the first effect. The formed vapor from the first effect condenses inside the tubes of the second effect and thus releasing heat that is used to sensibly heat the sprayed seawater in this effect to saturation condition and evaporating some of it. This process is repeated till the last effect.

The direction of the vapor flow in all the effects started from 1 to n and the usually from left to right. Any effect constitutes a vapor space, heat transfer area, demister and a brine pool to collect un-evaporated seawater.

The principle of operation is similar to the previous systems. The inlet seawater ($\dot{m}_{cw}$) is passed through two preheaters where it's heated by transferring heat from the distillate ($\dot{m}_d$) and brine ($\dot{m}_b$) stream, respectively. This process of heat exchange improves thermal efficiency since it represents another form of energy recovery. Brine, that do not evaporate in the effect is collected in the brine pool at the bottom of the effect. Then it is forwarded to the bottom of the next effect that is essentially at a lower pressure (and temperature) where some of it flashes as its temperature reduces to the new effect state. The flashed vapor rises to join the formed vapor of the sprayed seawater on the evaporator tunes. This vapor mixture leaves the effect to enter into the tube side of the next effect where is condenses, releasing heat to sensibly heat and evaporate another portion of the seawater. The process continues in all other effects.

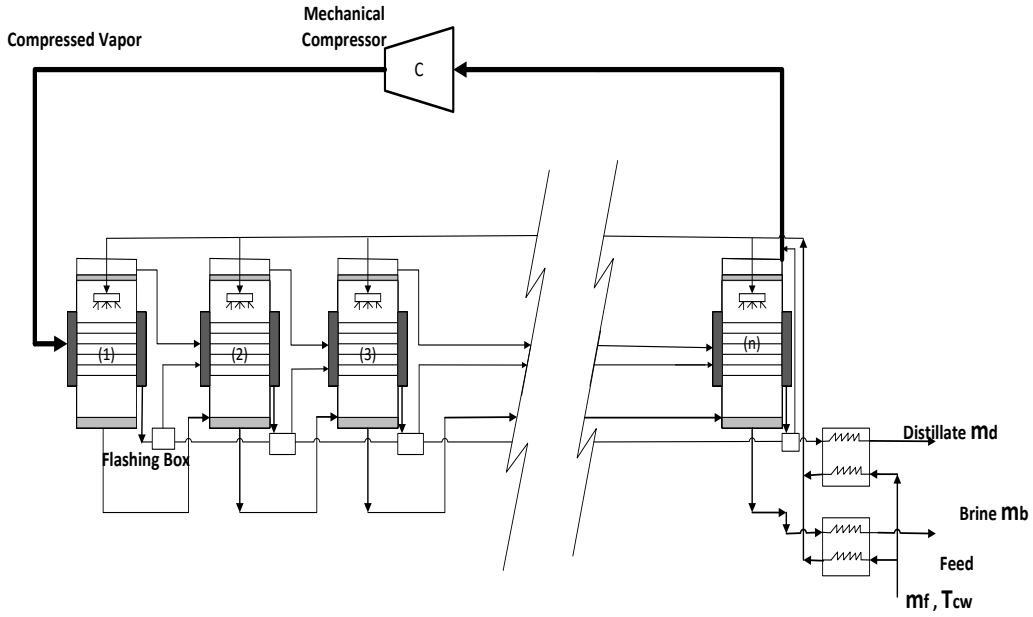

Figure 5.1 Parallel cross feed MED with Mechanical vapor compression

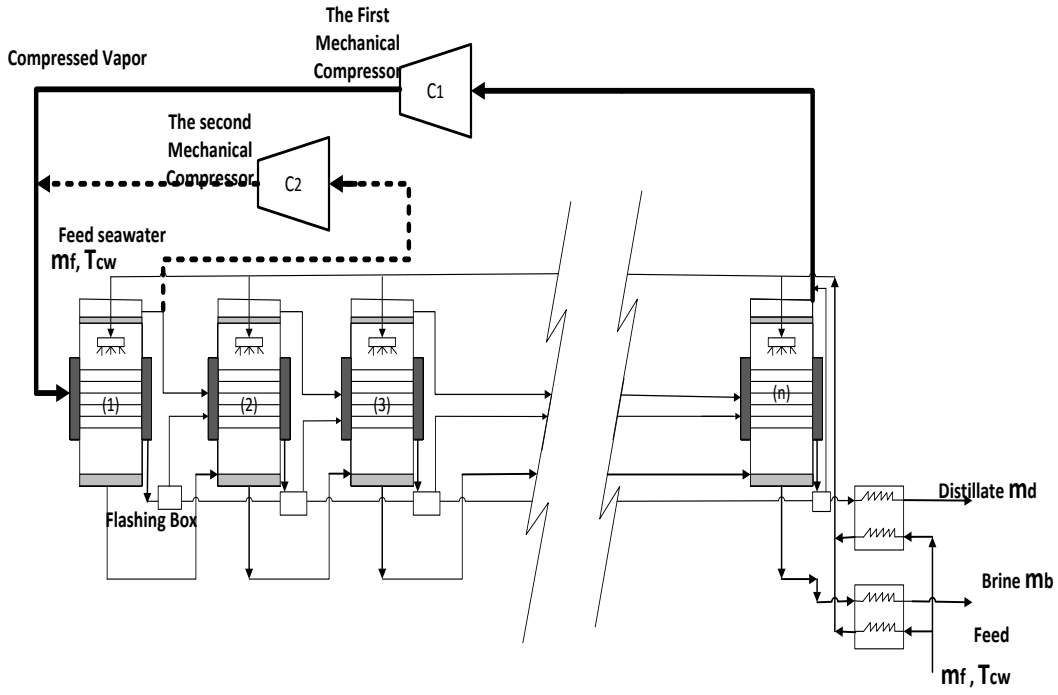

Figure 5.2 Parallel cross feed MED with Two Mechanical vapor compression.

5.2 Mathematical model of MED-MVC for Parallel Cross feed

The mathematical model for an effect (i), includes the mass, energy and material balances equation for the effect in addition to the heat transfer (H.T) equation that is used to calculate the surface area for the evaporator tubes in the effect.

Results are expressed in terms of:

- Distillate flow rate ($\dot{m}_d$).
- Concentration of the brine.
- Brine flow rate ($\dot{B}_n$).
- Heat transfer (H.T) area.

Material and heat balances for flash boxes and preheaters are also included in this model.

Assumption

- Specific heat at constant pressure, C_p for the seawater is calculated as a function of both temperature and salinity.
- Model variations in the thermodynamic losses (BPE, non-equilibrium allowance inside the evaporators and the flashing boxes, temperature depression corresponding to the pressure drop in the demister) from one effect to another.
- Variable physical properties of water.
- The heat transfer equations model the heat transfer area in each evaporator as the sum of the area for brine heating and the area for evaporation.

The number of mass, energy and material balance equations, which can be written for any effect, is three (Seawater mixture between salt water and fresh).

There are (n) equations for H.T rate in any effect, which relates the effect thermal load to the overall coefficient of heat transfer, the area, and temperature as a driving force.

Brine Flow rate, $\dot{B}_1, \dot{B}_2, \dots, \dot{B}_{n-1}, \dot{B}_n$ (n unknown)

Distillate flow rate, $\dot{D}_1, \dot{D}_2, \dots, \dot{D}_{n-1}, \dot{D}_n$ (n unknown)

Effect temperature, $T_1, T_2, \dots, T_{n-1}$ (n-1 unknown)

Heat transfer (H.T) area (1 unknown)

Flow rate of steam (1 unknown)

Total = (4n) unknowns

Parameters to be specified before solution

- Steam temperature, T_s.
- Temperature in the last effect (n), T_n.
- Salt concentration leaving last effect (n),X_n.
- Distillate flow rate ($\dot{m}_d$).
- Salt concentration of the feed stream (X_f).

5.2.1 Model equations

Mass balance: $$B_i - B_{i-1} = F_i - \dot{D}_i \quad (1)$$

Salt concentration balance:

$$X_{B_i} * \dot{B}_i = X_{F_i} * F_i + X_{B_{i-1}} * \dot{B}_{i-1} \quad (2)$$

Total Temperature drop:

$$\Delta T = T_s - T_n \tag{3}$$

This drop is equal for each effect;

$$\Delta T = \Delta T_1 + \Delta T_2 + \cdots + \Delta T_{n-1} + \Delta T_n \tag{4}$$

From above equations Find:

$$\Delta T_1 = \frac{\Delta T_t}{U_1 \sum_{i=1}^{n} \frac{1}{U_i}} \tag{5}$$

Temperature profile:

For first effect:

$$T_1 = T_s - \Delta T_1 \tag{6}$$

For effects 2 to n:

$$T_i = T_{i-1} - \Delta T_1 \frac{U_1}{U_i} \tag{7}$$

The thermal load, thus

$$\dot{D}_{i-1} h_{fg,v(i-1)} + \dot{D}_{f(i-1)} h_{fv(i-1)} + \dot{D}_{n(i-1)} h_{nv(i-1)} = F_i C_{pi} (T_i - T_f) + \dot{D}_i h_{fg,vi} \tag{8}$$

$$\dot{D}_{fi} = \dot{D}_{i-1} * C_{p(i-1)} * \frac{\Delta T}{h_{fg,v(i-1)}} \tag{9}$$

$$\dot{D}_{n(i-1)} = \dot{B}_{i-1} * C_{p(i-1)} * \frac{\Delta T}{h_{fg,v(i-1)}}$$

This is equation for 2 to n effects.

For first effect:

$$\dot{D}_1 * \ h_{fg,v1} = \dot{m}_s * h_{fg,s} \quad (10)$$

$$\dot{D}_1 = xx * m_{v1} + m_{vn}$$

Mass vapor at first effect (m_{v1}):

$$\dot{D}_1 h_{fg,v1} = F_2 C_{p2}(T_2 - T_f) + m_{v1} * h_{fg,v2} \quad (11)$$

Distillate flow rate at second effect with extraction (xx) after first effect:

$$\dot{D}_2 = (1 - xx) * m_{v1}$$

Where:

m_{v1} = mass vapor for the first effect.

For effects i:

$$A_i * U_i * \Delta T_{loss} = \ \dot{D}_i * \ h_{fg,vi} + \ F_i C_{pi}(T_i - T_f) \quad (12)$$

Distillate flow rate:

$$\dot{m}_d = \ \dot{D}_1 + \dot{D}_2 \ + \cdots + \dot{D}_{n-1} \ + \ \dot{D}_n \quad (13)$$

Flow rate of brine in first effect:

$$\dot{B}_1 = \ F_1 - \ \dot{D}_1 \quad (14)$$

$$\dot{B}_i + \ \dot{D}_1 = \ \dot{B}_{i-1} + F_i \quad (\text{i= 2… n}) \quad (15)$$

Salt concentration balance:

$$X_1 = X_f * (\dot{m}_f / \dot{B}_1) \quad (16)$$

$$X_F = (X_{B_i} * \dot{B}_i + X_{B_{i-1}} * \dot{B}_{i-1}) / F_i \quad (17)$$

Heat Transfer Area in First effect:

$$A_1 = \left(F_1 C_{p1} (T_1 \dot{-} T_f) + D_1 * h_{fg,v1}\right) / (U_1 (T_s - T_1)) \quad (18)$$

Steam flow rates ($\dot{m}_s$):

$$\dot{m}_s = (\dot{D}_1 * h_{fg,v1}) / h_{fg,vs} \quad (19)$$

Specific heat transfer area (sA):

$$sA = \frac{\sum_{i=1}^{n} A_i}{\dot{m}_d} \quad (20)$$

Heat exchangers thermal load $\dot{Q}_h$:

$$\dot{Q}_h = \dot{m}_d * c_p * (T_d - T_o) + \dot{B}_n * c_p * (T_b - T_o) \quad (21)$$

Where:

$$T_o = \left(T_{cw} - T_f\right) + \left(\frac{X_f}{X_b}\right) * T_b + \left(\frac{X_b - X_f}{X_b}\right) * T_d$$

c_p = the specific heat at constant pressure.

The specific power consumption:

Total power consumption (w):

$$w = w_k + w_s$$

The consumed power of the first compressor w_s

$$w_s = m_{vn}\ \frac{\gamma}{\eta(\gamma-1)}\ P_{vn}v_{vn}\ \left[\left(\frac{P_s}{P_{vn}}\right)^{\frac{\gamma-1}{\gamma}} - 1\right] \tag{22}$$

The consumed power of the second compressor w_k

$$w_k = (xx * m_{v1})\ \frac{\gamma}{\eta(\gamma-1)}\ P_{v1}v_{v1}\ \left[\left(\frac{P_s}{P_{v1}}\right)^{\frac{\gamma-1}{\gamma}} - 1\right] \tag{23}$$

It is important to state that the previous equations are adjusted whenever the extraction point changes in a similar manner. Therefore, there is no need to repeat writing the balance equations here for different points of extraction and it is taken care of in the written code.

Entropy Generation:

In general the entropy generation,

$$S_{gen} = \sum \dot{m}_e s_e - \sum \dot{m}_i s_i \tag{24}$$

The entropy generation for first compressor, $S_{gen.c1}$:

$$S_{gen.c2} = m_{vn} * (s_{T_s} - s_{T_{vn}}) \tag{25}$$

The entropy generation for second compressor, $S_{gen.c2}$:

$$S_{gen.c2} = xx * m_{v1} * (s_{T_s} - s_{T_{v1}}) \tag{26}$$

For first effect:

$$S_{gen.1} = \left[m_{v1} * s_{T_{v1}} + \dot{D}_1 * \ s_{T_1} + \dot{B}_1 * s_{T_1} \right] - [(xx * \ m_{v1} + m_{vn}) * s_{T_s} + \ F_1 * s_{T_{f1}}] \quad (27)$$

Second Effect:

$$S_{gen.2} = \left[\dot{D}_3 * s_{T_{v2}} + \dot{D}_2 * \ s_{T_2} + \dot{B}_2 * s_{T_2} \right] - \left[\dot{D}_2 * s_{T_{v1}} + F_2 * s_{T_{f1}} \quad + \dot{B}_1 * s_{T_1} \right] \quad (28)$$

For effects i= 3 to (n-1):

$$S_{gen.i} = \left[\dot{D}_{i+1} * s_{T_{vi}} + \dot{D}_i * \ s_{T_i} + \dot{B}_i * s_{T_i} \right] - \left[F_i * s_{T_{f1}} + \ \dot{D}_i * s_{T_{v(i-1)}} + \dot{B}_{i-1} * s_{T_{i-1}} \right]$$

(29)

For the last Effect:

$$S_{gen.n} = \left[\ m_{vn} * s_{T_{vn}} + \dot{D}_n * \ s_{T_n} + \dot{B}_n * s_{T_n} \right] - \left[F_1 * s_{T_{f1}} + \ \dot{D}_n * s_{T_{v(n-1)}} + \dot{B}_{n-1} * s_{T_{n-1}} \right]$$

(30)

Then the total entropy generation $S_{gen.total}$:

$$S_{gen.total} = S_{gen.c1} + \ S_{gen.c1} + \sum_{i=1}^{n} S_{gen.i} \quad (31)$$

Exergy Efficiency

Exergy Efficiency is a measure of the performance of the system that shows the components of the system where more losses are associated. It gives an indication to system designers of the locations that require further enhancements for better system performance. The exergy balance of the vapor compressor is developed as follows:

The exergy efficiency η_{II}

$$\eta_{II} = \frac{\dot{E}_{vapor\,,out} - \dot{E}_{vapor\,,in}}{w_{rev}} \quad (32)$$

$\dot{E}_{vapor\,,out} = \dot{m}_v(h_v - h_o - T_o(s_v - s_o))$

The exergy efficiency η_{II} first (main) compressor w_k

$$\eta_{II,n} = \frac{\dot{m}_{vn}(h_{g,n} - h_{g,s} - T_o(s_{g,n} - s_{g,s}))}{w_{rev}}$$

The exergy efficiency η_{II} second compressor w_k

$$\eta_{II,1} = \frac{\dot{m}_{v1}(h_{g,1} - h_{g,s} - T_o(s_{g,1} - s_{g,s}))}{w_{rev}}$$

The exergy efficiency

$$\eta_{II} =$$

$$\frac{\dot{m}_{vn}\left(h_{g,n} - h_{g,s} - T_o\left(s_{g,n} - s_{g,s}\right)\right) + \dot{m}_{v1}\left(h_{g,1} - h_{g,s} - T_o\left(s_{g,1} - s_{g,s}\right)\right)}{w_{rev}}$$

Conditions

- Numbers of effects (n) are 4 and 6, 8.
- The salinity of seawater X_{cm}, and the temperature T_{cw}, are 42000 ppm and 25° C.
- The salinity of rejected brine, X_b = 72000 ppm.
- The temperature of steam, T_s = 60° C.
- The feed water temperature, T_f = 35° C.
- The temperature of the boiling in the final effect, T_n = 40° C.
- The flow rate of distillate, m_d = 1 kg/s.
- The compressor efficiency, η = 76 %.

5.3 Results and Discussion

5.3.1 The specific power consumption

The consumed specific power is power consumption required for separating saline water into a unit mass flow rate of pure water and concentrated brine. It is dependent on the salt content of the saline water. The consumed power MVC-PC changes with steam pressure, specific volume, vapor pressure, pressure ratio, Feed water per effect, and a number of effects.

Fig 5.3 (a), (b), (c) show the variation of the specific power of the system with the extracted vapor entering the secondary compressor compared with the original case of no secondary compressor for systems of 4 effects (Fig. 5.3 a), 6 effects (Fig. 5.3 b) and 8 effects (Fig. 5.3 c).

The specific power (MVC-PC) is always lower when extraction is made for the formed vapor in effect number one. This is believed to be a result of the changes in compression ratio of the secondary compressor and distillate rate per effect. Thus, a general observation is made here that lower values of the specific power is at a higher value of Extraction occurs in the effect (n/2). Figure 5.4 (a), (b), (c) show the variation of the work ratio (w_k/w_s) of the system with the extraction.

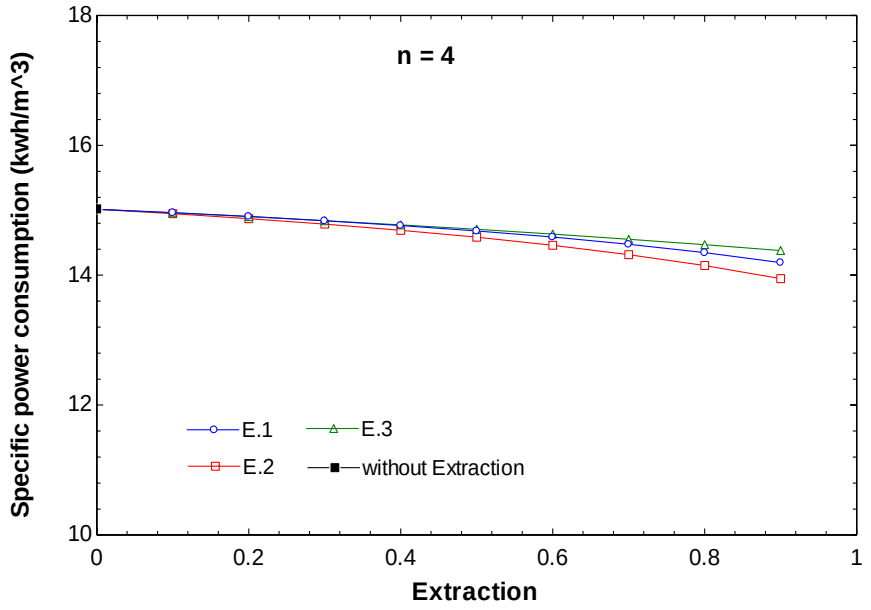
n = 4
Specific power consumption (kwh/m^3)
Extraction
E.1
E.3
E.2
without Extraction

(a)

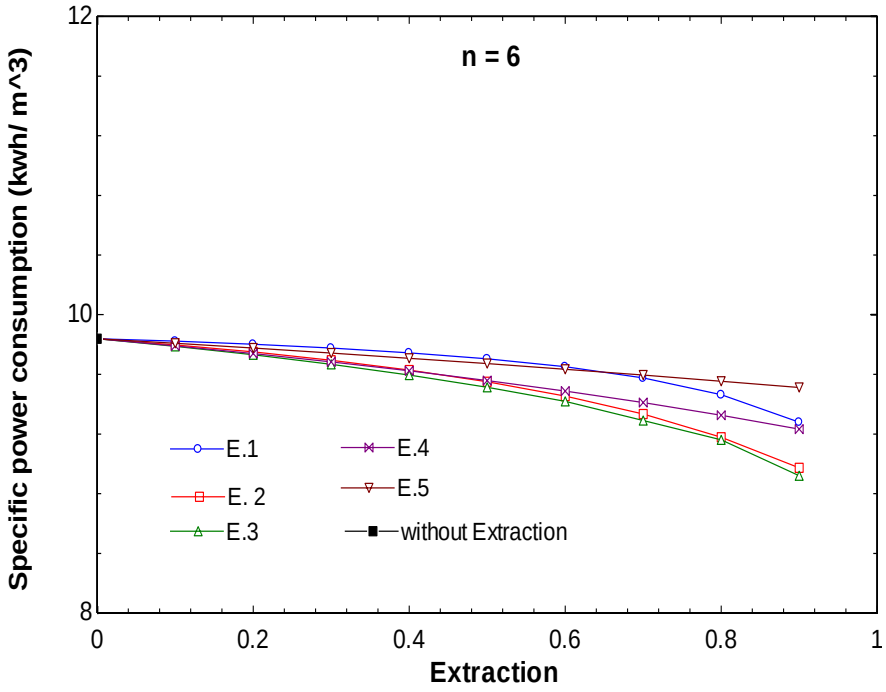
n = 6
Specific power consumption (kwh/ m^3)
Extraction
E.1
E.4
E. 2
E.5
E.3
without Extraction

(b)

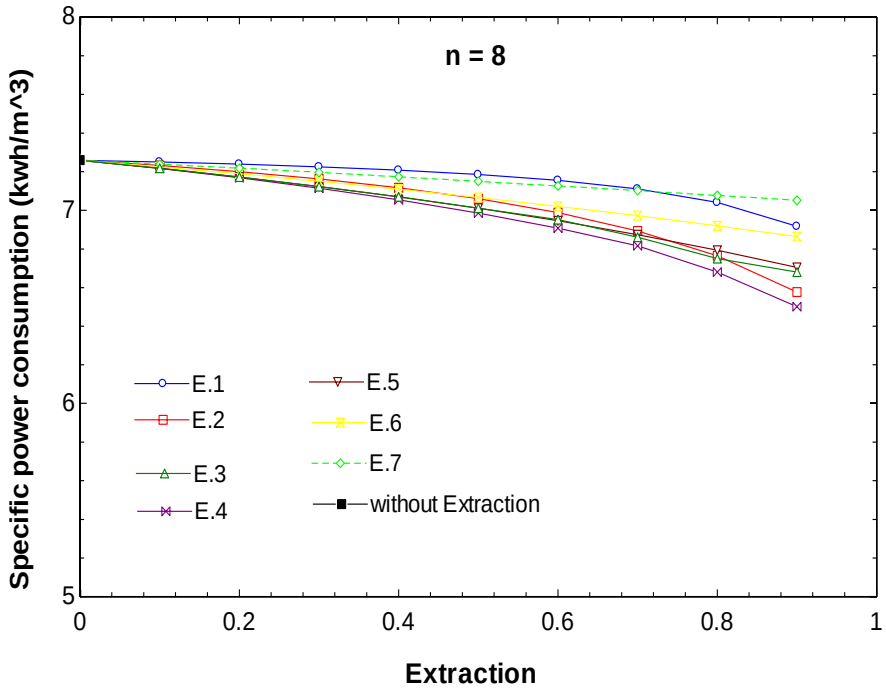

(c)

Figure 5.3 Change in the consumed power for the parallel cross feed (MED-MVC) with Extraction for (a) n = 4 Effects (b) n = 6 Effects (c) n = 8 Effects.

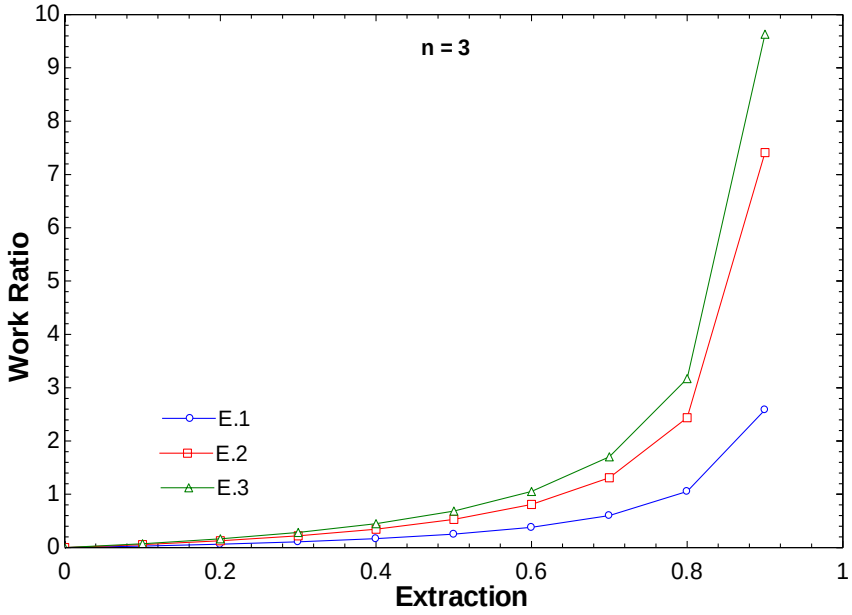

(a)

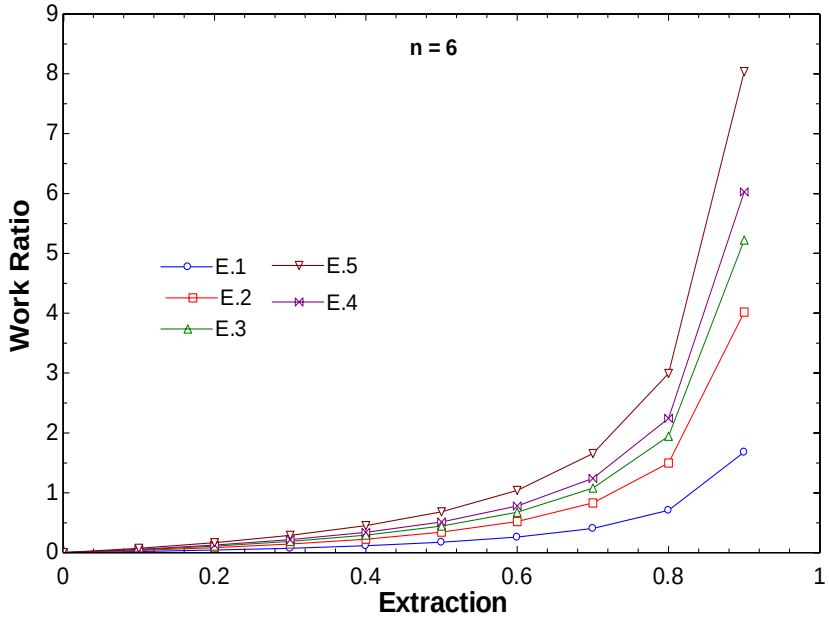

(b)

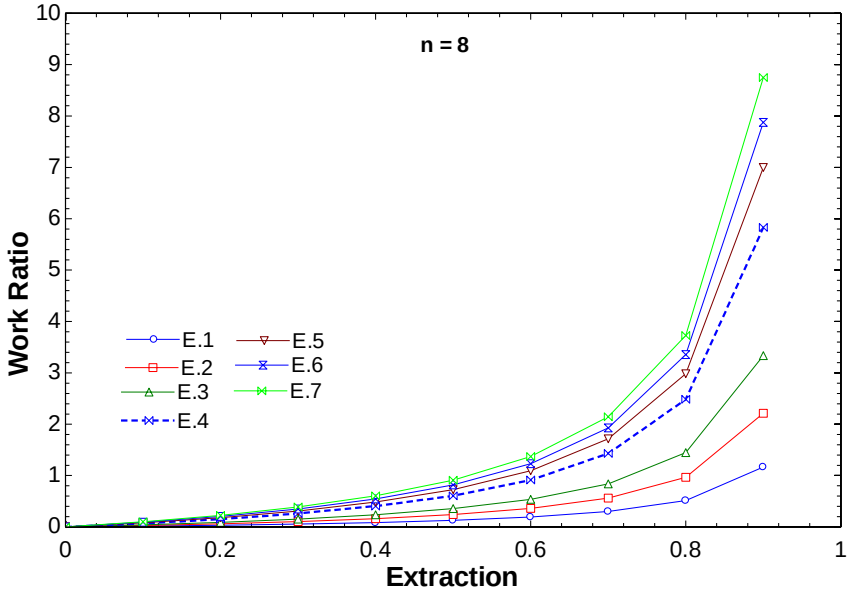

(c)

Figure 5.4 change in the work ratio of the parallel feed MED-MVC with Extraction for (a) n = 4 Effects (b) n = 6 Effects.

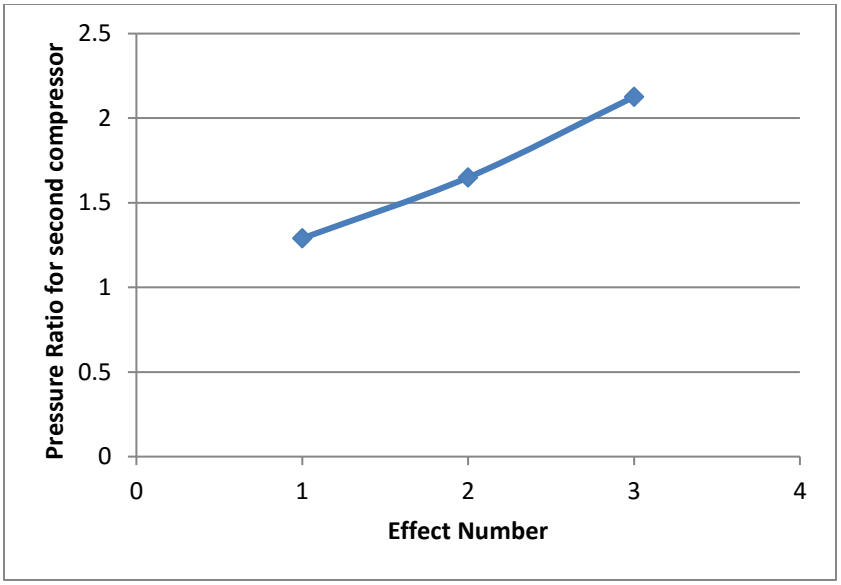

Figure 5.5 Change of the pressure ratio for secondary compressor for n = 4 effects.

Figure 5.5 The pressure ration increases as the extraction point is delayed to later effects due to the monotonic decrease in pressure as the vapor flows from on effect to the other to maintain evaporation in all effects while the first effect is at the maximum pressure and temperature. Figure 5.6 vapor flow rate entering the second compressor is the highest with the extraction percentage.

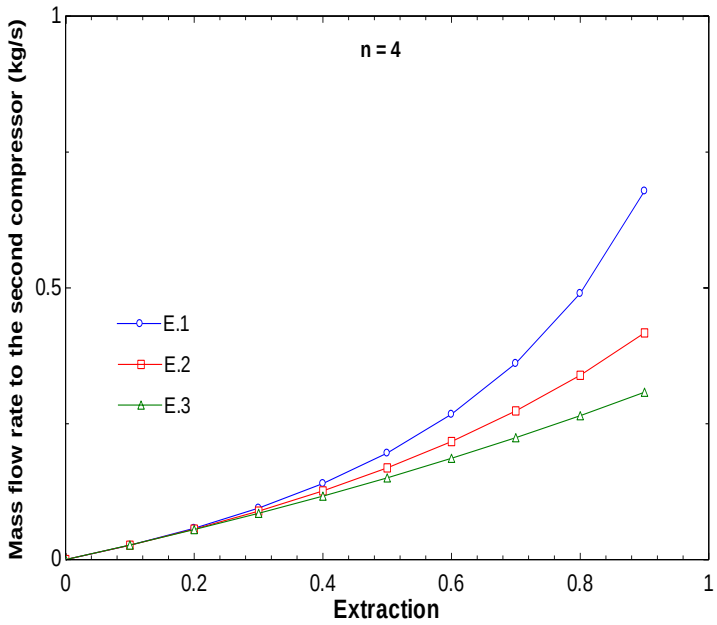

Figure 5.6 Change the mass flow rate enter the second compressor with Extraction for n =4 effects.

5.3.2 Specific heat transfer area

Specific heat transfer area is the sum of the total area of the system per distillate flow rate. The specific heat transfer area in MED-MVC parallel cross Feed is dependent on distillate rate per effect as well as the latent heat of condensation at the temperature at which the vapor leaves the effect as well as Feed water per effect and the number of effects.

Fig 5.7 (a), (b), (c) show the variation of the specific heat transfer area of the system (MED-MVC) parallel cross Feed with the extracted vapor entering the secondary compressor compared with the original case of no secondary compressor for systems of 4 effects (Fig. 5.7 a), 6 effects (Fig. 5.7 b) and 8 effects (Fig. 5.7 c). Show the specific heat transfer (sA) remains constant with the increase the extraction.

When the extraction of formed vapor to the secondary compressors occurs at any effect, the specific heat transfer area is constant due to the low latent heat (corresponding to maximum temperature) as well as the decrease of the distillate flow rate and Feed water rate that flows to the next effects. Generally, it is observed in Figs. 5.7 (a), (b), (c) that the heat transfer area decreases as the extraction increases. It obvious that the specific heat transfer area for the effect is higher than its previous effect at the same extraction because of the decrease in the temperature of the vapor formed in the effect where extraction of vapor occurs.

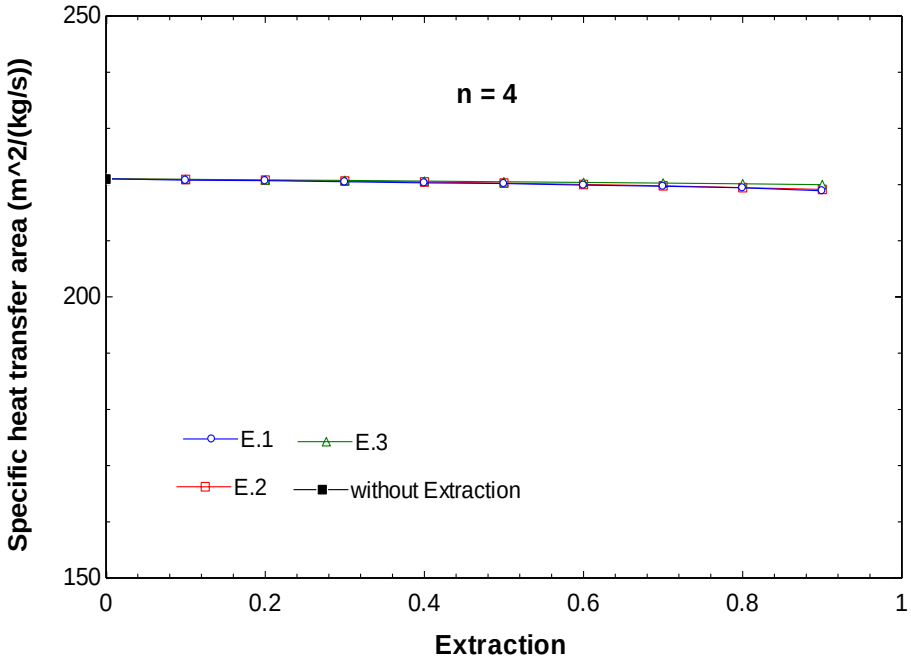

(a)

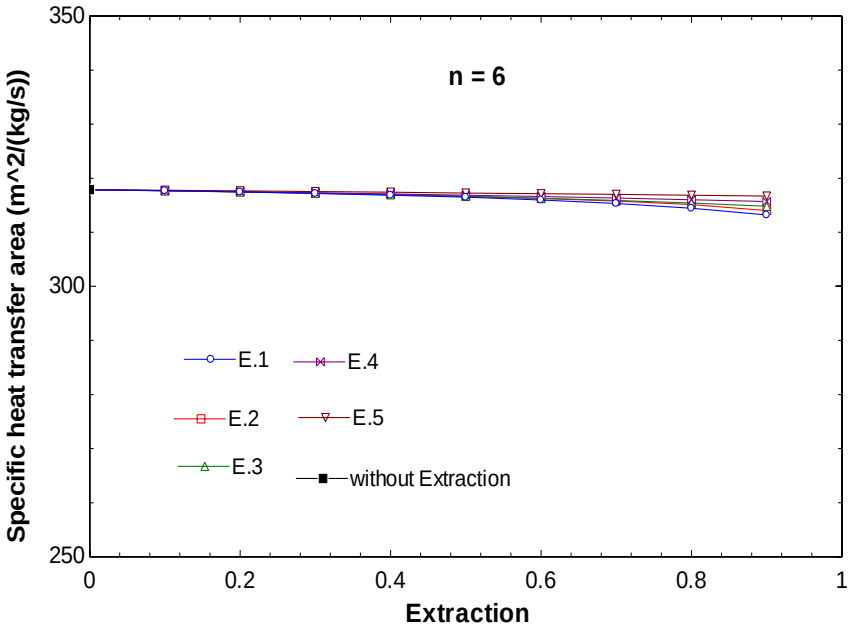

(b)

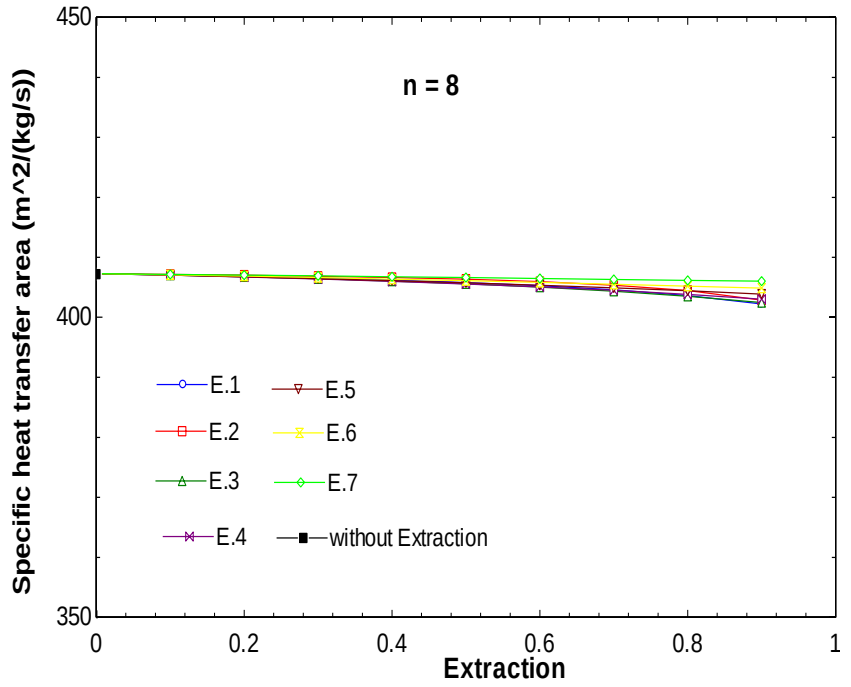

(C)

Figure 5.7 Heat transfer area of the parallel cross feed MED-MVC with Extraction for (a) n = 4 Effects (b) n = 6 Effects (c) n = 8 Effects.

5.3.3 Entropy generation

Entropy generation is a measure of the performance of the system that shows the components of the system where more losses are associated. It gives an indication to system designers of the locations that require further enhancements for better system performance. The net entropy change of the effects and the entropy change of the compressors are balanced by the Entropy generation. The entropy change for the effects depends on the extraction rate, the flow rate and the temperature of the distillate, the temperature of the brine, the vapor temperature of the effect, and the number of effects.

Fig 5.8 (a), (b), (c) show the total entropy generation with the rate of extraction. Entropy generation of the compression increases due to the addition of a secondary compressor. Also show that the entropy generation increases with the extraction due to increased flow to the secondary compressor. The entropy generation shown in Fig 5.8 (a), (b), (c) increases with the decrease the consumed power.

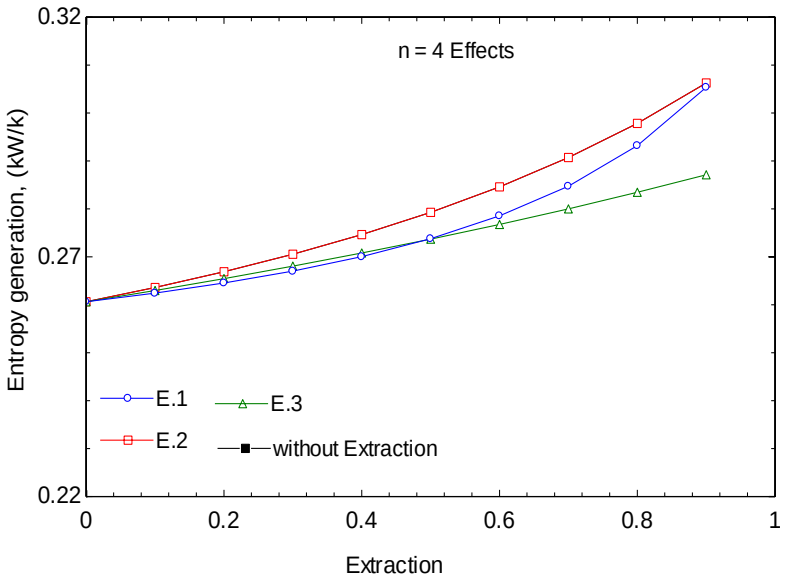

(a)

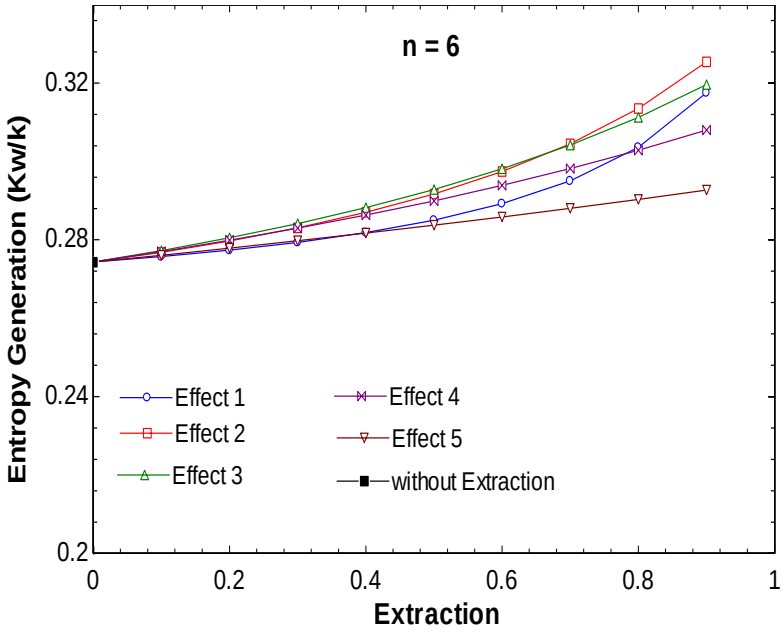

(b)

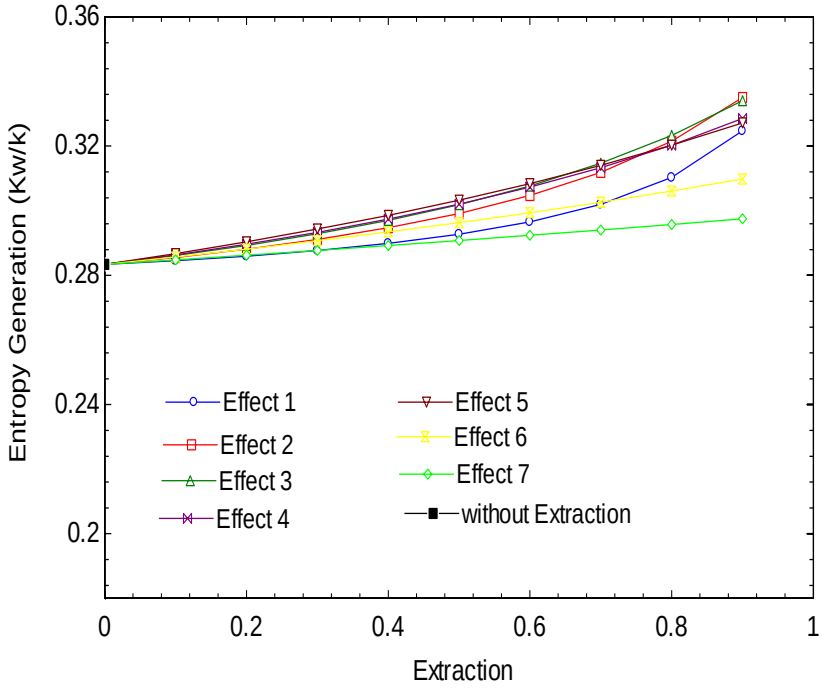

(c)

Figure 5.8 Entropy generation of the parallel cross feed MED-MVC with Extraction for (a) n = 4 Effects (b) n = 6 Effects (c) n = 8 Effects.

5.3.4 Exergy Efficiency

Exergy efficiency is a measure of the performance of the system. Figs. 5.9 (a), (b), (c) show the variation of the exergy efficiency of the system with the extracted vapor entering the secondary compressor compared with the original case of no secondary compressor for systems of 4 effects (Fig. 5.9 a), 6 effects (Fig. 5.9 b) and 8 effects (Fig. 5.9 c). The exergy efficiency increases with the increase in extraction rate.

The exergy efficiency at Fig 5.9 (a), (b), (c) increases with the decrease the consumed power. (η_{II}) increases with the Extraction due to decrease the total specific power consumption. Thus, a general observation is made here that higher values of the exergy efficiency correspond to a higher value of extraction that occurs in the effect (n/2).

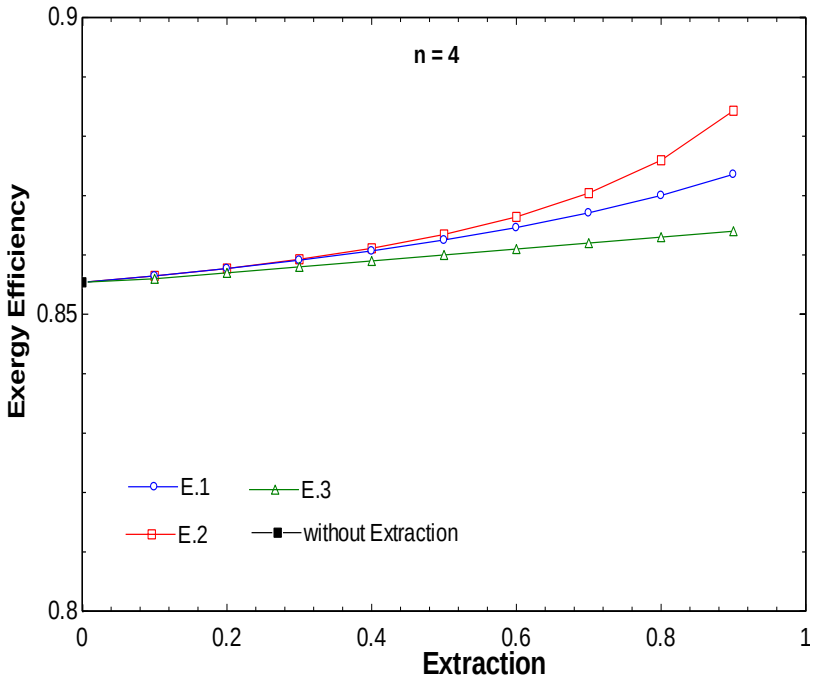

(a)

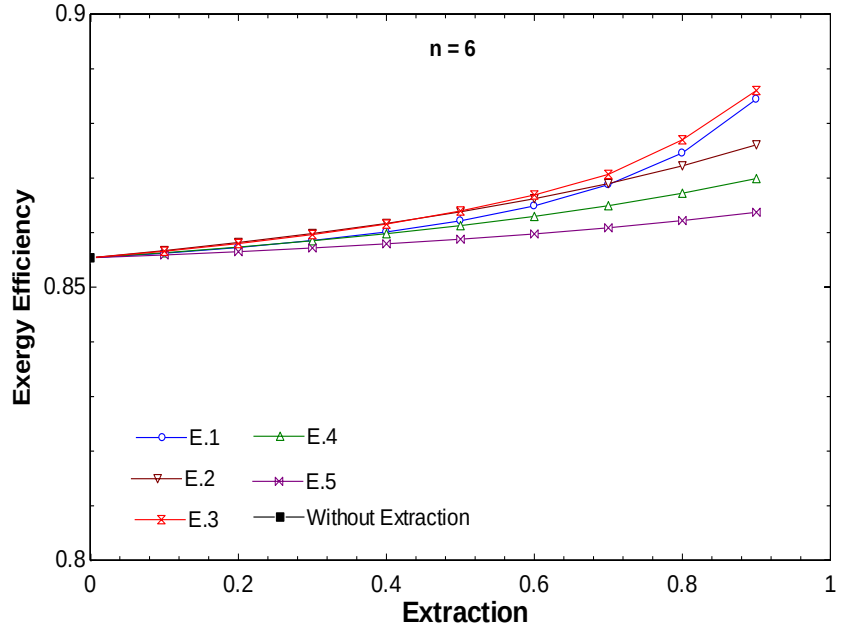

(b)

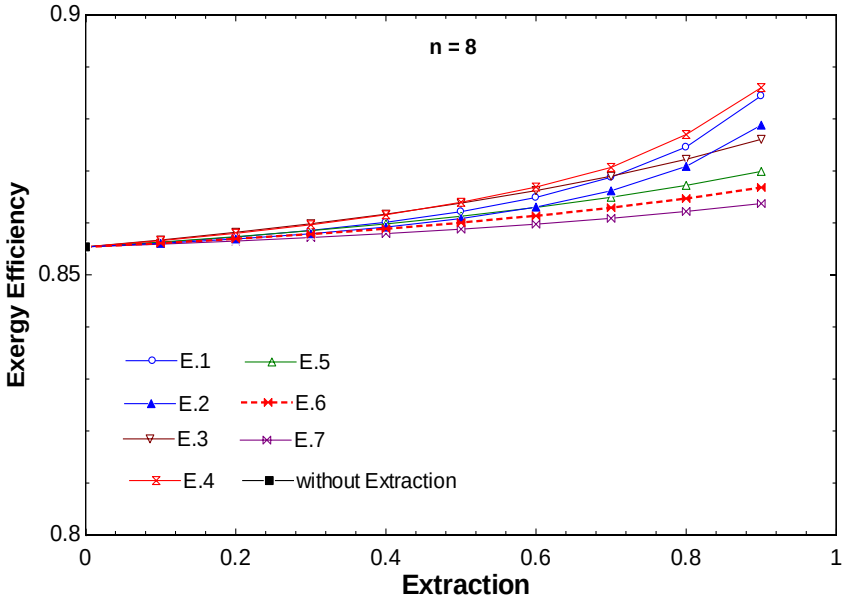

(c)

Figure 5.9 change in the exergy efficiency of the parallel feed MED-MVC with Extraction for (a) n = 4 Effects (b) n = 6 Effects (c) n = 8 Effects.

CHAPTER 6

Economic Study

The economic analysis is implemented to show the cost of water production and to determine the unit product cost as well as to point out the unit which needs more improvement. Thermo economic analysis requires solving energy, cost balance equations of the considered desalination plant.

The capital investment and operating and maintenance are calculated using the illustrated relations in Table 6.1.

Table 6.1 Cost data of the process units

Unit	Equation	Reference
Effect, $	Z = 430*0.582*$U_i * A_i * \Delta P_i^{-0.01} * \Delta P_s^{-0.1}$ U, kW/m^2 k ; ΔP, kPa ; A, m^2	El-Sayed [40]
Pump, $	1000*32*0.000435*$\dot{m}_f{}^{0.55}$*$\Delta P^{0.55}$ * $\left(\frac{\eta_p}{1-\eta_p}\right)^{1.05}$ η_p, Pump efficiency	El-Sayed [40]
Heat exchanger, $	1000*(12.86+A$^{0.8}$) A, m^2	El-Mudir [41]
Compressor, $	7364* $\dot{m}_{vapor} * \left(\frac{P_o}{P_i}\right) * (\frac{\eta}{1-\eta})^{0.7}$	El-Sayed [40]

6.1 case 1: MED-MVC-FF with 4 effects

6.1.1 Original layout (4 effects - No Extraction)

Cost data includes the following:

Direct capital cost (DC) = $142269.04

Plant capacity (m) = 86.4 m^3/day

Specific consumption of electric power (w) = 15.97 kWh/m^3

Specific chemicals cost (k) = $0.025/$m^3$ [4]

i= interest rate (5%)

c= Electric cost ($0.05/$m^3$) [4]

w= specific power consumption

f= Plant availability (0.9) [4]

£ = specific cost of operating labor ($0.1/$m^3$) [4]

The calculations proceed as follows:

- Amortization factor

$$a = \frac{i*(1+i)^n}{(1+i)^n-1} = \frac{0.05*(1+0.05)^{30}}{(1+0.05)^{30}-1} = 0.065051 \text{ /yr}$$

-Annual fixed charges

A_1= (a) (DC) = (0.065051) (142269.04) = $9254 /yr

-Annual electric power cost

A_3 = (c) (w) (f) (m) (365) = (0.05) (15.97) (0.9) (86.4) (365) = $22663 /yr

-Annual chemicals cost

A_4 = (k) (f) (m) (365) = (0.025) (0.9) (86.4) (365) = $709.6 /yr

- Annual labor cost

A_5 = (£) (f) (m) (365) = (0.1) (0.9) (86.4) (365) = $2838.24 /yr

- Total annual cost

$A_t = A_1 + A_3 + A_4 + A_5$ = $ 35465.5 /yr

- Unit product cost

$A_s = A_t/((f)(m)(365))$ = $ 1.25 /m^3

6.1.2 A system of 4 effects with two mechanical compressors

Cost data includes the following:

Direct capital cost (DC) = $149072.04

Plant capacity (m) = 86.4 m^3/d

Specific consumption of electric power (w) = 14.85 kWh/m^3

Specific chemicals cost (k) = $0.025/$m^3$

i= interest rate (5%)

c= Electric cost ($0.05/$m^3$)

w= specific power consumption

f= Plant availability (0.9)

£ = specific cost of operating labor ($0.1/m^3)

The calculations proceed as follows:

- Amortization factor

$a = \frac{i*(1+i)^n}{(1+i)^n-1} = \frac{0.05*(1+0.05)^{30}}{(1+0.05)^{30}-1}$ = 0.065051 /yr

-Annual fixed charges

A_1= (a) (DC) = (0.065051) (149072.04) = $ 9697.2 /yr

-Annual electric power cost

A_3 = (c) (w) (f) (m) (365) = (0.05) (14.85) (0.9) (86.4) (365) = $21073.9 /yr

-Annual chemicals cost

A_4 = (k) (f) (m) (365) = (0.025) (0.9) (86.4) (365) = $709.6 /yr

- Annual labor cost

A_5 = (£) (f) (m) (365) = (0.1) (0.9) (86.4) (365) = $2838.24 /yr

- Total annual cost

$A_t = A_1 + A_3 + A_4 + A_5$ = $ 34319 /yr

- Unit product cost

$A_s = A_t/((f)(m)(365)) = \$\ 1.2\ /m^3$

6.2 Case 2: MED-MVC-FF system with 6-Effects

6.2.1 Original case (6 effects -no extraction)

Cost data includes the following:

Direct capital cost (DC) = $ 225816.9

Plant capacity (m) = 86.4 m^3/d

Specific consumption of electric power (w) = 11.41 kWh/m^3

Specific chemicals cost (k) = $0.025/$m^3$

i= interest rate (5%)

c= Electric cost ($0.05/$m^3$)

f= Plant availability (0.9)

£ = specific cost of operating labor ($0.1/$m^3$)

The calculations proceed as follows:

- Amortization factor

$$a = \frac{i*(1+i)^n}{(1+i)^n-1} = \frac{0.05*(1+0.05)^{30}}{(1+0.05)^{30}-1} = 0.065051\ /yr$$

- Annual fixed charges

A_1= (a) (DC) = (0.065051) (225816.9) = $ 14689.6 /yr

- Annual electric power cost

A_3 = (c) (w) (f) (m) (365) = (0.05) (11.41) (0.9) (86.4) (365) = $16192.15 /yr

- Annual chemicals cost

A_4 = (k) (f) (m) (365) = (0.025) (0.9) (86.4) (365) = $709.6 /yr

- Annual labor cost

A_5 = (£) (f) (m) (365) = (0.1) (0.9) (86.4) (365) = $2838.24 /yr

- Total annual cost

$A_t = A_1 + A_3 + A_4 + A_5$ = $ 34429.6 /yr

- Unit product cost

$A_s = A_t/((f)(m)(365))$ = $ 1.21 /m^3

6.2.2 A system of 6 effects with two mechanical compressors

Cost data includes the following:

Direct capital cost (DC) = $ 237384

Plant capacity (m) = 86.4 m^3/d

Specific consumption of electric power (w) = 9.844 kWh/m^3

Specific chemicals cost (k) = $0.025/$m^3$

i= interest rate (5%)

c= Electric cost ($0.05/$m^3$)

w= specific power consumption

f= Plant availability (0.9)

£ = specific cost of operating labor ($0.1/m^3)

The calculations proceed as follows:

- Amortization factor

$a = \frac{i*(1+i)^n}{(1+i)^n-1} = \frac{0.05*(1+0.05)^{30}}{(1+0.05)^{30}-1}$ = 0.065051 /yr

- Annual fixed charges

A_1= (a) (DC) = (0.065051) (237384) = $ 15442.06 /yr

- Annual electric power cost

A_3 = (c) (w) (f) (m) (365) = (0.05) (9.844) (0.9) (86.4) (365) = $13969.8 /yr

- Annual chemicals cost

A_4 = (k) (f) (m) (365) = (0.025) (0.9) (86.4) (365) = $709.6 /yr

- Annual labor cost

A_5 = (£) (f) (m) (365) = (0.1) (0.9) (86.4) (365) = $2838.24 /yr

- Total annual cost

$A_t = A_1 + A_3 + A_4 + A_5$ = $ 32959.7 /yr

- Unit product cost

$A_s = A_t/((f)(m)(365)) = \$\ 1.16\ /m^3$

6.3 Case 3: MED-MVC-FF system with 8-Effects

6.3.1 Original case (8 effects - no extraction)

Cost data includes the following:

Direct capital cost (DC) = $ 378777.5

Plant capacity (m) = 86.4 m^3/d

Specific consumption of electric power (w) = 7.994 kWh/m^3

Specific chemicals cost (k) = $0.025/$m^3$

i= interest rate (5%)

c= Electric cost ($0.05/$m^3$)

f= Plant availability (0.9)

£ = specific cost of operating labor ($0.1/$m^3$)

The calculations proceed as follows:

- Amortization factor

$$a = \frac{i*(1+i)^n}{(1+i)^n-1} = \frac{0.05*(1+0.05)^{30}}{(1+0.05)^{30}-1} = 0.065051\ /yr$$

- Annual fixed charges

A_1= (a) (DC) = (0.065051) (378777.5) = $ 24639.8 /yr

- Annual electric power cost

A_3 = (c) (w) (f) (m) (365) = (0.05) (7.994) (0.9) (86.4) (365) = $10099.8 /yr

- Annual chemicals cost

A_4 = (k) (f) (m) (365) = (0.025) (0.9) (86.4) (365) = $709.6 /yr

- Annual labor cost

A_5 = (£) (f) (m) (365) = (0.1) (0.9) (86.4) (365) = $2838.24 /yr

- Total annual cost8A_t = A_1 + A_3 + A_4 + A_5 = $ 38287.4 /yr
- Unit product cost

A_s = A_t/((f)(m)(365)) = $ 1.35 /m^3

6.3.2 A system of 8 effects with two mechanical compressors

Cost data includes the following:

Direct capital cost (DC) = $ 315339.6

Plant capacity (m) = 86.4 m^3/d

Specific consumption of electric power (w) = 7.117 kWh/m^3

Specific chemicals cost (k) = $0.025/$m^3$

i= interest rate (5%)

c= Electric cost ($0.05/$m^3$)

w= specific power consumption

f= Plant availability (0.9)

£ = specific cost of operating labor ($0.1/m^3)

The calculations proceed as follows:

- Amortization factor

$a = \frac{i*(1+i)^n}{(1+i)^n-1} = \frac{0.05*(1+0.05)^{30}}{(1+0.05)^{30}-1}$ = 0.065051 /yr

- Annual fixed charges

A_1= (a) (DC) = (0.065051) (315339.6) = $ 22149.4 /yr

- Annual electric power cost

A_3 = (c) (w) (f) (m) (365) = (0.05) (7.117) (0.9) (86.4) (365) = $11344.44 /yr

- Annual chemicals cost

A_4 = (k) (f) (m) (365) = (0.025) (0.9) (86.4) (365) = $709.6 /yr

- Annual labor cost

A_5 = (£) (f) (m) (365) = (0.1) (0.9) (86.4) (365) = $2838.24 /yr

- Total annual cost

$A_t = A_1 + A_3 + A_4 + A_5$ = $ 37041.6 /yr

- Unit product cost

$A_s = A_t/((f)(m)(365)) = \$\ 1.31\ /m^3$

The results of the economic analysis are summarized in Table 6.2.

Table 6.2: Summary of the economic analysis for MED-MVC-FF systems with and without the addition of a second compressor at effect n/2

Number of Effects	4 effects		6 effects		8 effects	
	Without Extraction	With Extraction At middle	Without Extraction	With Extraction At middle	Without Extraction	With Extraction At middle
Specific Power consumption (Kwh/m^3)	15.97	14.85	11.41	9.844	7.994	7.117
Unit product cost($\$/m^3$)	1.25	1.2	1.21	1.16	1.35	1.31

The economic analysis shows that adding a secondary compressor is already paid back in terms of increasing the productivity and hence it leads to lower water production price. Moreover, a system of 6 effects shows better water price compared to the other two systems of 4 and 8 effects. Decreasing in the capital cost also reduces the unit product cost.

CHAPTER 7

Conclusion

In this study, multi effect desalination with Mechanical vapor compression have been investigated. Three layouts are considered; forward feed arrangement MED-MVC-FF, parallel feed MED-MVC-PF and parallel cross feed MED-MVC-PC. A modification was studied to enhance the performance of the system by adding a secondary compressor where a portion of the vapor is extracted from one of the effects, compressed in the secondary compressor to the state of the vapor that enters the tube side of the first effect. Both vapor streams are mixed to increase the heat transfer rate and hence the evaporation rate in the first effect and accordingly increases the system productivity. The following conclusions can be drawn for each arrangement.

7.1 MED-MVC-FF arrangement

- Performance improvement of the MED-MVC-FF desalination system has been realized through the addition of a secondary compressor to the system. This addition results in an increase in the formed vapor that is admitted to the first effect to condense and hence, produce additional formed vapor. That main performance criteria used is the specific power that represents the total compressors power per unit flow rate of desalinated water (specific power).

- Forward feed-multi effect desalination system with mechanical vapor compression, using a secondary compressor that draws formed vapor from a middle effect (n/2) results in a best scenario for the system performance. When the extraction after the first effect the pressure ratio is lower and extraction percentage higher and the extraction after the effect (n-1) the pressure ratio is higher and extraction percentage lower the after that the optimum location at effect (n/2).
- The exergy efficiency increases with the extraction rate to increased flow to the secondary compressor.
- Results show that the utilization of a secondary compressor at the exit of the second effect of a 4-effect system to get a portion of the form vapor at the suction side of the compressor results in best performance of the unit. Howe ever, this improvement comes on the expense of additional surface area.

7.2 MED-MVC-PF arrangement

- Performance improvement of the MED-MVC-PF desalination system has been realized through the addition of a secondary compressor to the system. The decrease in the vapor specific volume at higher operating temperature also contributes to reduction in the specific power for vapor compression. Parallel feed-multi effect desalination system with mechanical vapor compression, using a secondary compressor that draws formed vapor from a middle effect (n/2) results in a best for the system performance. The vapor extracted after the first effect has the lowest pressure ratio whereas its mass vapor entering the second compressor is the highest with the extraction percentage, and the vapor extracted after effect (n-1) has the

highest pressure ratio whereas its mass vapor is the lowest. Therefore, the optimal case is to extract the vapor after the effect (n/2).

- The Extraction rate has insignificant effect on the specific heat transfer area, and the exergy efficiency increases with the extraction rate to increased flow to the secondary compressor.

7.3 MED-MVC-PC arrangement

- Parallel Cross feed-multi effect desalination system with mechanical vapor compression, using a secondary compressor that draws formed vapor from a middle effect (n/2) results in a best for the system performance. The Extraction rate has insignificant effect on the specific heat transfer area.
- The exergy efficiency increases with the extraction rate to increased flow to the secondary compressor.
- Parallel Cross feed is recommended as the most suitable layout for lower specific power consumption as shown in Figure 7.1.

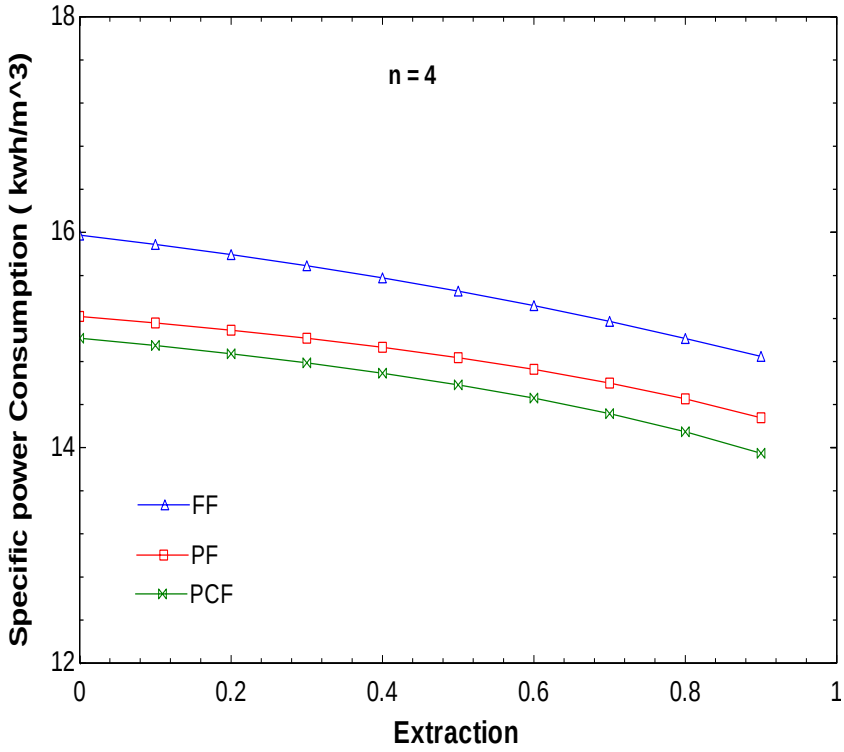

Fig. 7.1 Comparison between FF, PF and PCF for MED-MVC

References

[1] Meyers, S, " Develpoments in aquatic microbiology, " Int. Microbiol, 3, pp. 203-211, 2000.

[2] Mohsen, M. S. and 0. R. Al-Jayyousi, "Brackish water desalination: an Alternative for water supply enhancement in Jordan, "Desalination. 124: 163-174, 1999.

[3] Noble, R. D. and S. A. Stern (Ed), " Membrane separations technology: Principle and applications, "Elsevier Science B.V. Amsterdam, The Netherlands, 1995.

[4] Hisham T. El-Dessouky and Hisham M. Ettouney, "Fundamentals of Salt Water Desalination, " Elsevier Science B.V. Amsterdam, The Netherlands, 2002.

[5] Ahmed Al-Zuhairi," A Novel Manipulated Osmosis Desalination Process, ", Guildford, UK , 2008.

[6] Hamed, O. A., Zamamiri, A.M , Aly, S and Lior, N, "The thermal performance and exergy Analysis of thermal vapor compression desalination system," Energy convers. and Management, vol. 37, No.4, pp.379–387, 1996.

[7] Faisal Al-Juwayhel, Hisham El-Dessouky, Hisham Ettouney, "Analysis of single evaporator desalination systems combined with vapor compression heat pumps," *Desalination*, vol. 114, pp. 253–275, 1997.

[8] Hikmet S. Aybar, "Analysis of a mechanical vapor compression desalination system," Desalination, vol. 142, pp. 143–150, 2002.

[9] N. H. Aly and A. K. El-fiqi, "Mechanical vapor compression desalination systems - a case study," Desalination, vol. 158, pp. 143–150, 2003.

[10] K. M. El-Khatib, a. S. Abd El-Hamid, a. H. Eissa, and M. a. Khedr, "Transient model, simulation and control of a single-effect mechanical vapor compression (SEMVC) desalination system," *Desalination*, vol. 166, no. 1–3, pp. 157–165, 2004.

[11] H. Ettouney, “Design of single-effect mechanical vapor compression,” *Desalination*, vol. 190, no. 1–3, pp. 1–15, 2006.

[12] S. Mussati, N. Scenna, E. Tarifa, S. Franco, and J. a. Hernandez, “Optimization of the mechanical vapor compression (MVC) desalination process using mathematical programming,” *Desalin. Water Treat.*, vol. 5, no. 1–3, pp. 124–131, 2009.

[13] M. G. Marcovecchio, “Modelado de procesos y Métodos de optimización global aplicados a la síntesis de procesos de desalinización”, Thesis doctoral, Facultad de Ingeniería y Ciencias Hídricas. Universidad Nacional del Litoral, Santa Fe, 2007.

[14] M. Marcovecchio, P. Aguirre, N. Scenna, and S. Mussati, *Global Optimal Design of Mechanical Vapor Compression (MVC) Desalination Process*, vol. 28, no. Mvc. Elsevier B.V., 2010.

[15] Fuad N. Alasfour, Hassan K. Abdulrahim, “The effect of stage temperature drop on MVC thermal performance,” Deaslination, vol. 265, pp. 213–221, 2011.

[16] D. Han, W. F. He, C. Yue, and W. H. Pu, “Study on desalination of zero-emission system based on mechanical vapor compression,” *Appl. Energy*, 2016.

[17] A.A. MADANl, “Economics of Desalination for Three Plant Sizes, Desalination” pp. 187–200, 1990.

[18] H. T. EL·DFSSOUKY, H. M. ETTOUNEY and F. AL·JUWA YHEL, “MULTIPLE EFFECT EVAPORATION-VAPORCOMPRESSION DESALINATION PROCESSES,” Trans IChemE. Vol 78, Part A. May 2000.

[19] Gustavo Kronenberg, Fredi Lokiec, “Low-temperature distillation processes in single-and dual-purposa plants,” Desalination, vol. 136, pp. 189–197, 2001.

[20] R. Bahar, M. N. a. Hawlader, and L. S. Woei, “Performance evaluation of a mechanical vapor compression desalination system,” Desalination, vol. 166, pp. 123–127, 2004.

[21] Mohammad Al-Sahali, Hisham Ettouney, "Developments in thermal desalination process: Design, energy, and costing aspects," *Desalination,* vol. 214, pp. 227 - 240, 2007.

[22] A. Ophir, A. Gendel, "Steam driven large multi effect MVC (SD MVC) desalination process for lower energy consumption and desalination costs," *Desalination.* vol. 205, pp. 224–230, 2007.

[23] E. Cardona, A. Piacentino, F. Marchese, "Performance evaluation of CHP hybrid seawater desalination plants," Desalination 205, pp. 1–14, 2007.

[24] A.A. Mabrouk, A.S. Nafey, H.E.S. Fath, "Analysis of a new design of a multi-stage flash–mechanical vapor compression desalination process," Desalination 204, pp.482–50, 2007.

[25] J.R. Lara, G. Noyes, M.T. Holtzapple, "An investigation of high operating temperatures in mechanical vapor-compression desalination,"Desalination, vol. 227, pp. 217–232, 2008.

[26] A.S. Nafey, H.E.S. Fath, A.A. Mabrouk, "Thermo-economic design of a multi-effect evaporation mechanical vapor compression(MEE–MVC) desalination process, "Desalination 230,pp. 1- 15, 2008.

[27] M.A. Sharaf , A.S. Nafey, Lourdes García-Rodríguez," Thermo-economic analysis of solar thermal power cycles assisted MED-VC (multi effect distillation-vapor compression) desalination processes, " Energy. 36: 2753-2764, 2011.

[28] M. N. Labib, S. S. Kim, D. Choi, T. Utomo, H. Chung, and H. Jeong, "Numerical investigation of the effect of inlet skew angle on the performance of mechanical vapor compressor," *Desalination,* vol. 284, pp. 66–76, 2012.

[29] H. Wu, Y. Li, and J. Chen, "Analysis of an evaporator-condenser-separated mechanical vapor compression system," *J. Therm. Sci.*, vol. 22, no. 2, pp. 152–158, 2013.

[30] Karan H. Mistry, Mohamed A. Antar, John H. Lienhard, “An improved model for multiple effect distillation, “desalination and Water Treatment 51, no. 4–6, pp. 807 – 821, 2013.

[31] J. Shen, Z. Xing, X. Wang, and Z. He, “Analysis of a single-effect mechanical vapor compression desalination system using water injected twin screw compressors,” *Desalination*, vol. 333, no. 1, pp. 146–153, 2014.

[32] J. Shen, Z. Xing, K. Zhang, Z. He, and X. Wang, “Development of a water-injected twin-screw compressor for mechanical vapor compression desalination systems,” *Appl. Therm. Eng.*, vol. 95, pp. 125–135, 2016.

[33] Aly Karameldin, A. Lotfy, S. Melchemar, “The Red Sea area wind-driven mechanical vapor compression desalination system,” Desalination, vol. 153, pp. 47–53, 2002.

[34] Lourdes Garcia-Rodriguez, “Seawater desalination driven by renewable energies: a review,” *Desalination*, pp. 103–113, 2002.

[35] Lourdes Garcıa-Rodrıguez, “Renewable energy applications in desalination: state of the art,” *Desalination*, vol. 75, pp.381–393, 2003.

[36] Markus Forstmeier, Fredrik Mannerheim, Fernando D’Amato, Minesh Shah, Yan Liu Michael Baldea, Albert Stella, “Feasibility study on wind-powered desalination,” *Desalination*, 203, pp. 463–470, 2007.

[37] C. Fernández-López, a. Viedma, R. Herrero, and a. S. Kaiser, “Seawater integrated desalination plant without brine discharge and powered by renewable energy systems,” *Desalination*, vol. 235, no. 1–3, pp. 179–198, 2009.

[38] Driss Zejli , Ahmed Ouammi, Roberto Sacile, Hanane Dagdougui, Azzeddine Elmidaoui, “An investigation of high operating temperatures in mechanical vapor-compression desalination, ”Desalination, vol. 227, pp. 217–232, 2008.

[39] M.A. Darwish, Hassan K. Abdulrahim, “Feed water arrangements in a multi-effect desalting system, ”Desalination, vol. 228, pp. 30–54, 2008.

[40] Y.M. E1-Sayed, “Designing desalination systems for higher productivity” Elsevier, Desalination. 134: 129-158, 1999.

[41] W. El-Mudir, M, El-Bousifi and S. Al-Hengari, Performance evaluation of a small size TVC desalination plant. Desalination, 165: 269-279, 2004.

Vitae

Name	: Saddam Eltayib Ajib Jaber
Nationality	: Sudanese
Date of Birth	: 01/11/1991
Email	: Saddam085@hotmail.com
Address	: House no. 271 street no. 5 Khartoum North - Sudan
Academic Background	: Master of Science (MSc.) Mechanical Engineering (Thermo-fluids) King Fahd University of Petroleum & Minerals Dhahran, Saudi Arabia. Bachelor of Science in Mechanical Engineering University of Khartoum.